AD-755 820

EFFECTS OF HIGH POWER LASERS

Informatics, Incorporated

Prepared for:

Air Force Office of Scientific Research

12 January 1973

DOCUMENT CONTROL DATA - R & D

(Security classification of title, body of abstract and indexing annotation must be entered when the overall report is classified)

1. ORIGINATING ACTIVITY (Corporate author)	2a. REPORT SECURITY CLASSIFICATION
Informatics Inc. 6000 Executive Boulevard Rockville, Maryland 20852	UNCLASSIFIED
	2b. GROUP

3. REPORT TITLE

Effects of High Power Lasers, No. 2, July 1971 -- December 1972

4. DESCRIPTIVE NOTES (Type of report and inclusive dates)

Scientific . . . Interim

5. AUTHOR(S) (First name, middle initial, last name)

Stuart G. Hibben

6. REPORT DATE	7a. TOTAL NO. OF PAGES	7b. NO. OF REFS
January 12, 1973	130	- - -

8a. CONTRACT OR GRANT NO	9a. ORIGINATOR'S REPORT NUMBER(S)
F44620-72-C-0053	
b. PROJECT NO 1622-3	
c. 62701D	9b. OTHER REPORT NO(S) (Any other numbers that may be assigned this report) AFOSR - TR - 73 - 0269
d.	

10. DISTRIBUTION STATEMENT

Approved for public release; distribution unlimited.

11. SUPPLEMENTARY NOTES	12. SPONSORING MILITARY ACTIVITY
Tech. Other	Air Force Office of Scientific Research 1400 Wilson Boulevard Arlington, Virginia 22209

13. ABSTRACT

This report is a compilation of all abstracts dealing with Soviet high-power laser technology that were published in 1972 in the monthly series on Selected Material from Soviet Technical Literature. The material covers source acquisitions from late 1971 through late 1972, and thus serves to update the first report on Effects of High Power Lasers, December 1971.

Articles were selected as the most pertinent of a total of 272 bibliographic entries on powerful laser effects recorded in this interval. For consistency the structure of the 1971 report has again been used; within each category the abstracts are grouped alphabetically by author.

A first-author index and an index of source abbreviations are appended.

13H

EFFECTS OF

HIGH POWER LASERS,

NO. 2

July 1971 - December 1972

Sponsored by

Advanced Research Projects Agency

ARPA Order No. 1622-3

January 12, 1973

Approved for public release; distribution unlimited

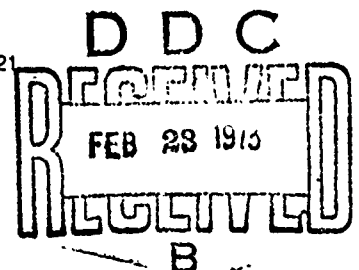**Informatics inc**

Systems and Services Company
6000 Executive Boulevard
Rockville, Maryland 20852
(301) 770-3000 Telex: 89-521

DDC

RECEIVED
FEB 28 1973

B

INTRODUCTION

This report is a compilation of all abstracts dealing with Soviet high-power laser technology that were published in 1972 in the monthly series on Selected Material from Soviet Technical Literature. The material covers source acquisitions from late 1971 through late 1972, and thus serves to update the first report on Effects of High Power Lasers, December 1971.

Articles were selected as the most pertinent of a total of 272 bibliographic entries on powerful laser effects recorded in this interval. For consistency the structure of the 1971 report has again been used; within each category the abstracts are grouped alphabetically by author.

A first-author index and an index of source abbreviations are appended.

TABLE OF CONTENTS

1. Laser Breakdown of Gas

Alkhimov, A. P., V. F. Klimkin, A. I.
Ponomarenko, and R. I. Soloukhin. On
the development of a discharge initiated
by a laser spark. 10th Int. Conf. Phenomena
Ioniz. Gases, Oxford, 1971. Oxford,
1971, 227 (RZh Mekh, 8/72, no. 8 B196)
(Translation)

A study is made of the initial stages of the formation of
a laser-initiated discharge in air at atmospheric pressures (Al electrodes
10 cm in diameter, gap 15 mm, voltage - about 35 kv). The time relation-
ships of the radiation intensity of a Nd laser (pulse~30 nanosec, power ~
20 Mw) and the discharge current are registered; in addition a study is made,
by means of an electronicoptical converter under conditions of scanning
and frame photography, of the pattern of discharge development over
nanosecond intervals. The discharge commences with the formation of a
plasmoid in the cathode region independently of the point of laser-beam
focusing with progressive development of a streamer moving toward the anode
(rate of motion ~10^9 cm/sec) and closure of the gap. An examination is made
of the qualitative pattern of the physical processes taking place during this
time.

Arifov, U. A., M. R. Bedilov, T. G. Tsoy,
D. Kuramatov, and A. Ibragimov. Interaction
of a laser plasma with air. DAN UzSSR, no. 5,
1972, 19-21. (RZhF, 10/72, no. 10D1006)
(Translation)

A study is reported on the interaction of a plasma jet, generated by focused laser radiation on Al, W, Ta and Ni targets, with neutral air molecules at 10^{-6} and 760 torr. Peak laser power in a Q-switched mode attained 10^{11} w/cm^2. Kinetics and emission spectrum of the plasma were studied in the visible (400-600 nm) and ultraviolet (220-400 nm) ranges, as well as propagation of the plasma from the target face to a collector, with no applied external electric field. At 10^{-6} torr, electron and ion currents up to 10^{13} particles were registered, at velocities of 10^7 cm/sec. It was established that at 760 torr ambient, the charged particles are fully recombined in travelling the 5 cm from target to collector.

Kantorovich, I. I. Frequency dependence
of optical breakdown in gases. ZhPS, v. 16,
no. 4, 1972, 605-610.

An analysis is given of the contribution of atomic excitation processes, particularly avalanche ionization, to optical breakdown in gas. The study is generally limited to the area around breakdown threshold, $\sim 10^6$ v/cm, with argon and xenon used as hypothetical media. Expressions are derived for the probability $f(\omega)$ of continuous ionization of Ar and Xe, and these results are plotted in Fig. 1.
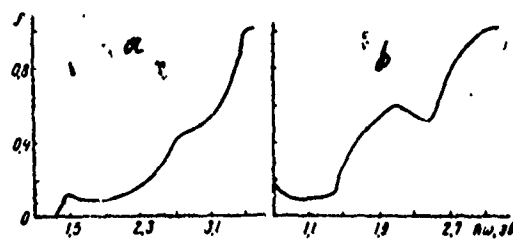
Fig. 1. Frequency dependence of ionization probability for Ar (a) and Xe (b). ω = optical frequency.
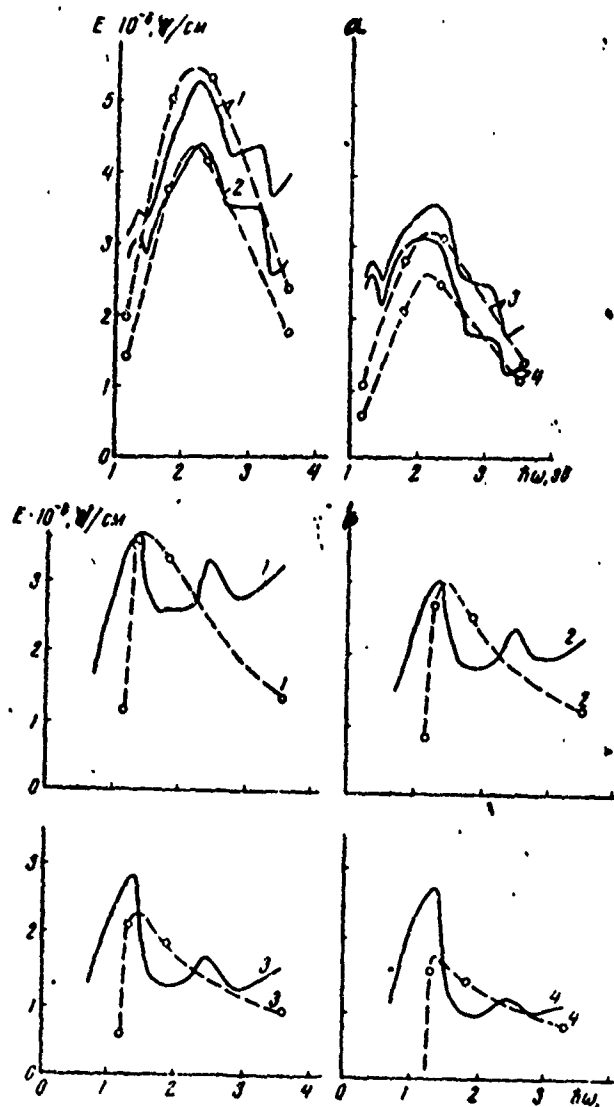

Fig. 2. Frequency dependence of breakdown threshold in Ar (a) and Xe (b) at pressures of 1000 (1); 2000 (2); 4000 (3) and 8000 torr (4). Solid line - theory; dashed - experiment.

Breakdown threshold vs. beam frequency is shown in Fig. 2, which compares theory with earlier experimental results. The divergence seen at lower frequencies and higher pressures is ascribed to increased .multiphoton ionization probabilities owing to local nonuniformity.

Krasyuk, I. K., and P. P. Pashinin. Breakdown in argon and nitrogen from a picosecond laser pulse at 0.35 micron wavelength. ZhETF P, v. 15, no. 8, 1972, 471-473.

Optical breakdown triggered in Ar and N_2 by the second harmonic emission from a ruby laser was studied to ascertain the breakdown mechanism from 30-50 psec. pulses at 0.35μ wavelength. Breakdown threshold I_{th} was measured in the gases at a pressure in the 400-4500 torr range in an experimental arrangement analogous to one described by the authors and A. M. Prokhorov (ZhETF P, v. 9, 1969, 581). The power of the filtered second harmonic emission was measured with a resolution equal to or better than 20 psec. The emission peak corresponding to the limit of visibility was assumed to be I_{th}. The experimental plots (Fig. 1) indicate that breakdown is triggered by multi-photon ionization of gas atoms or molecules. This mechanism is confirmed by experimental data obtained by the authors and A. M. Prokhorov (ZhETF, v. 58, 1970, 1606) at 0.69μ wavelength. Analysis of the cited data and that of other authors reveals that the quasiclassic formula derived by Keldysh adequately describes the relative decrease in I_{th}, i.e., the increased probability of photoionization, with the increases in frequency of optical emission. In contrast, no theory exists to explain the fact that I_{th} in Ar and Xe also decreases when the breakdown is triggered by a 20 nsec laser pulse at the 0.35μ wavelength; accepted avalanching theory predicts instead a monotonic rise in I_{th} with laser frequency in the nanosecond case. Hence different breakdown mechanisms must be considered in the picosecond and nanosecond pulse cases.
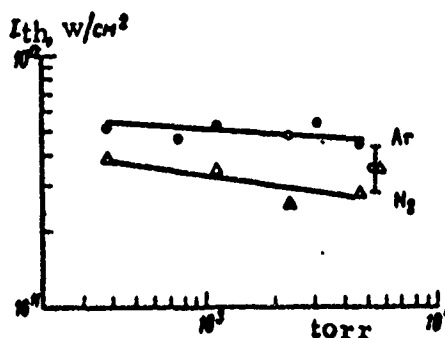

Fig. 1. Experimental plots of I_{th} vs. pressure: o- in argon, Δ - in nitrogen

Letokhov, V. S., Ye. A. Ryabov, and O. A. Tumanov. Luminescence and optical breakdown in gas under a CO_2 laser pulse. The Sixth All-Union Conference on Nonlinear Optics, Minsk, July 1972 (Preprint).

Powerful lasers in the i-r range have opened the possibility of studying resonance impact of strong fields on molecular systems. Borde (?) and others have observed the visible luminescence of ammonia exposed to continuous powerful CO_2 laser radiation whose frequency coincided with the line of ammonia absorption; this phenomenon was attributed to heating NH_3 to a high temperature. The present paper is also devoted to an analysis of the effects of powerful CO_2 laser radiation on ammonia. It was discovered that at a definite threshold intensity P_{th-lum} visible luminescence occurred, growing in intensity with the increase of radiation strength until at a second threshold $p_{th} > P_{th-lum}$, optical breakdown took place. The main purpose of the experiment was the investigation of the mechanism of the first threshold luminescence generation. Initially it was beli-ved that this effect could perhaps be explained by oscillatory heating of NH_3 molecules with subsequent dissociation and luminescence of dissociation products. However, a study of luminescence time characteristics has shown that the mechanism of oscillatory heating is too inertial and could not be used to explain a luminescence pulse of $\sim 2 \times 10^{-7}$ sec duration, occurring without delay with respect to a laser pulse of $\sim (2 \div 5) \times 10^{-7}$ sec. Ultraviolet radiation with an intensity of $p > P_{th-lum}$ was detected, which could be explained by high-level electron states of the NH_3 molecule. This also excludes the mechanism of oscillatory heating of NH_3 molecule by laser radiation. The paper reviews possible mechanisms of threshold visible and ultraviolet luminescence of gas at intensities lower than the optical breakdown threshold.

Malyshev, G. M., G. T. Razdobarin,
and V. V. Semenov. Scattering method
for determining the plasma parameters
of a laser spark in air. ZhTF, no. 7,
1972, 1429-1431.

A method is described for determining plasma parameters
of interest in a laser spark in air which eliminates the usual requirement
for high spectral resolution. It is shown that electron density n_e,
temperature T_e and the parameter α can be found from the measured
differential to the satellite peak, λ_m, together with the ratio of integral
intensity of electron peaks to Rayleigh scattering in air, J_e/J_p. Formulas
defining these relations are given, showing that the desired unknowns can
be determined without any stipulation as to mean ion charge or the ratio
of electron to ion temperature. Experimental verification was obtained
using two synchronized lasers and a scattering radiation registry
system, described earlier by the authors (Diagnostika plazmy, vyp. 3.
Moskva, Atomizdat, 1972). Fig. 1 gives a comparison of test vs. theoretical
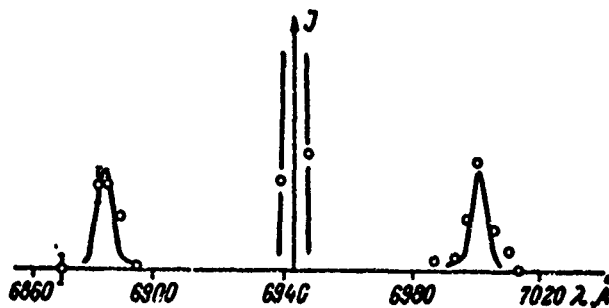data, showing qualitative agreement; the data points shown are averaged

Fig. 1. Scattering radiation spectrum

for several readings. As seen from the figure, the separation of main and satellite peaks λ_m = 58 ± 2Å. The cited data refer to the first 11 microseconds of the spark life, at a laser energy of approximately 1 joule. For these conditions the following were calculated: $n_e \cong 1.2 \times 10^{17}/cm^3$; $T_e \cong 1.4 \times 10^4$ deg K; and $\alpha \cong 3.3$. When beam energy was reduced to 0.6-- 0.8 j, these values were essentially unchanged, within limits of experimental accuracy, indicating the relatively weak correlation of laser energy to spark spectral parameters.

Mitsuk, V. E., R. M. Savvina, and V. A. Chornikov. Optical breakdown in gas mixtures. 10th Int'l Conference on Phenomena of Ionized Gases, Oxford, 1971, 233. (RZhMekh, 8/72, no. 8B201)(Translation)

'Studies were made on lowering the breakdown threshold of gas mixtures irradiated by a Q-switched Nd glass laser. The mixtures tested were Hg + Ar, Hg + Kr, Hg + He, He + Ar, He + Kr and He + Xe. Test results with all mixtures agreed well with the theory of simple avalanche ionization of gas by electrons, and indicated that atom-atom collisions are not a significant factor in the breakdown process.

Norinskiy, L. V. Initiation of a controlled breakdown in gas by third-harmonic emission from a neodymium laser. IN: Kvantovaya elektronika. Sbornik. Moskva, Izd-vo Sovetskoye radio, no. 5, 1971, 108-109.

An experiment is described which was an extension of work by Akmanov et al (ZhETF P, v. 8, no. 8, 1968, 417), in which a directional breakdown in gas was triggered by u-v laser radiation at 4.7 ev photon

energy and 300 Mw/cm^2 density. The present author has duplicated the effect in atmospheric air, obtaining a controlled breakdown from the third harmonic of an Nd glass laser at 3.5 ev. A collimated 3rd harmonic beam was passed through slotted high-voltage electrodes which were 1 cm apart, to obtain the controlled breakdown effect. Power density in the gap was about 3Gw/cm^2, or two orders less than natural optical breakdown. Attempts to repeat the effect at the fundamental and second harmonic were unsuccessful since breakdown threshold was first exceeded in both cases. The results confirm the inability of the fundamental (1.17 ev) and second harmonic (2.34 ev) to generate the controlled breakdown condition owing to their insufficient photoionization levels. Norinskiy emphasizes that his results were obtained with a multimode laser, and should be repeated with a single-mode regime for better clarification of this phenomenon.

2. Laser Interaction with Plasma

Afanas'yev, A. A., V. S. Burakov, V. V. Zheludok, and
S. V. Nechayev. Nonlinear interaction between laser
radiation and an alkali metal plasma. DAN BSSR, nc. 10,
1971, 889-891.

Nonlinear optical effects are described on passing a laser beam
through sodium and potassium plasma. Dye lasers including rhodamine 6G
were used, developing up to 10 Mw and 250j at pulse widths of 25-30 nsec;
beam divergence was limited to 10^{-2} -- 10^{-3} rad. In the potassium experiment
nitrobenzol was used, with a spectrum covering the $4S_{\frac{1}{2}}$ - $4P_{\frac{1}{2}}$ and $4S_{\frac{1}{2}}$ - $4P_{3/2}$
absorption lines; for Na, rhodamine - 6G was used, excited by ruby second
harmonic, and giving a spectral range fully covering the yellow doublet $3S_{\frac{1}{2}}$ - $3P$
and $3S_{\frac{1}{2}}$ - $3P_{3/2}$. The nonlinear response was generally seen in the 10^4 - 10^6
w/cm^2 intensity range, where beam spectral spread near the resonant absorpti
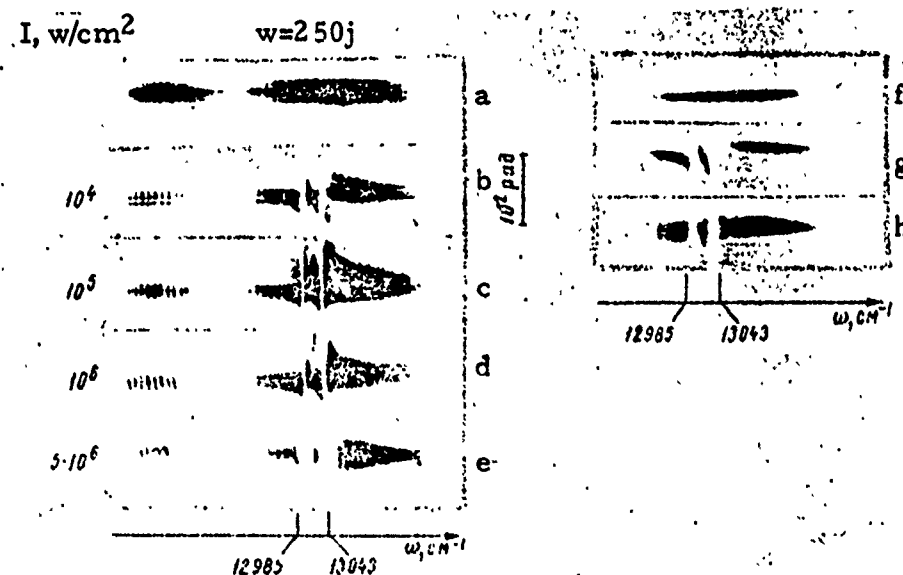
Fig. 1. Spectral response of a dye
laser beam passed through potassium plasma.

lines was found to be a function of beam intensity. This is seen in Fig. 1
for potassium, with the non-excited spectrum included for comparison.
A strong dependence of spectral characteristic on plasma density was also
found; this is seen in comparing Fig. 1g (60j) with 1h (250j), both at
10^5 w/cm^2. Response to the first Stokes component from Raman scattering
in the nitrobenzol was also observed, and showed an asymmetric broadening,
with the longer-wave portion more heavily absorbed by K lines. Results
for K and Na were qualitatively the same.

Afanas'yev, Yu. V., and V. B. Rozanov.
Spectrum of multiply-charged ions in a laser
plasma. ZhETF, v. 62, no. 1, 1972, 247-252.

A physical model is proposed for the energy spectral form of multiply ionized atoms in a laser plasma. Based on certain assumptions regarding plasma diffusion, the model permits the development of an analytical expression which describes the desired ion energy distribution. The analysis demonstrates that a principal factor governing the energy spectrum for a range of Z-charged ions is the recombination process during the diffusion period following termination of the laser pulse. It is furthermore shown that the set of Z present at the end of the pulse does not necessarily contain all Z values present following this time. For simplicity a spherically symmetrical plasma flare is assumed to exist at pulse termination, expanding into a vacuum according to a self-similar law. The energy spectrum is then derived as a function of initial flare density N_0 and time. Assuming values of $N_0 = 10^{20}/cm^3$, temperature $T = 100$ ev and $Z \cong 20$, the authors find a characteristic photorecombination time $\tau_{pr} \cong 3 \times 10^{-10}$ sec, which is less than plasma diffusion time, hence the recombination effect can be appreciable. Analogous experimental work of Bykovskiy et al is cited (ZhTF, 1970, 2578, and ZhETF, v. 60, 1971, 1306), but lack of complete data from the latter preclude a useful comparison of theory with experiment. A more recent similar work of Mattioli is also cited (Plasma Physics, v. 13, 1971, 19) in which decay of an LiH plasma was calculated from ionization and recombination processes

Anisimov, S. I., and V. I. Fisher. Ionization
relaxation and light absorption behind a strong
shock wave in hydrogen. ZhTF, no. 12, 1971,
2571-2576.

A simplified analysis is presented which describes the effect of ionization kinetics behind a shock wave on e-m radiation absorption in this region. The model assumes a plane stationary shock wave, and limits the consideration to hydrogen, since this avoids the complications of multiple ionization. The ionization relaxation zone in the shock wave wake is divided for analytical purposes into two regions with differing mechanisms of free electron formation: (1) a region of "seed electron" formation from atom-atom collisions; and (2) an electron avalanche region, with electrons freed predominantly by electron-atom collisions. Most of the optical absorption, as well as the significant change in gas state, occurs in region (2), which is therefore the region mainly treated in the paper. Equations for incident flux density and degree of ionization are numerically integrated, together with equations for one-dimensional stationary flow of the gas. The calculated results of density and temperature profile, together with ionization characteristics, are shown to have a definite correlation with incident flux density. The authors emphasize that the characteristics of hydrodynamic variables in such a shock wave, i.e. one absorbing an intense optical flux, will differ from the corresponding parameters in the usual detonation wave, owing to the ionization relaxation region which will exist in the former case. Some graphical solutions of the results are included.

Data are presented on plasma behaviour in magnetic traps
of two different configurations, referred to as "plug-type" and "antiplug-
type". Experiments have shown that magnetic traps with "anti-plug"
geometry are far more effective in capturing and retaining bunches of
dense laser-produced plasma than the plug-type traps (probkotrons).
A ruby laser, 150 x 12 mm at an energy of 0.15 joule and 50 nsec pulse
duration, was focused on a flat titanium target surface in a vacuum chamber
at 3×10^{-6} torr. A plasma bunch front of $n > 10^{13}$ cm^{-3} density moved along
the trap axis at a velocity $v = (4-5) \cdot 10^{6}$ cm/sec. The total number of
particles in the plasma bunch was determined from the mean energy of the
bunch, target mass measurements, and chamber pulse pressure variations.
In all three cases the total was determined to be $N = 3 \times 10^{16}$ particles. An
SHF generator ($\lambda = 0.8$ cm) was used to measure laser plasma physical
characteristics. The SHF cutoff of the freely expanding plasma bunch
5 cm from the target was $\tau = 1.2$--1.4 μsec. This value increased sharply
with an increase in magnetic field intensity in the trap. Results are:
in antiplug traps $\tau = 160 \mu$sec at an intensity of H = 6 koe; in plug-type traps
τ was 25 μsec at 7-8 koe. The injected plasma in the trap was photographed
during the trapping process and two different patterns were again observed
as a function of trap geometry. In the antiplug traps, the plasma bunch
moving along the magnetic field filled the trap; as revealed by the photo-
graphs, part of the bunch was disk-shaped and remained stable longer.
Increases of τ were accompanied by increased flow energy q moving through th
trap equatorial slot. It was observed that for the plug-type traps, although
an increase of field resulted in a specific increase in time during which the
plasma remained in the trap, this dependence is rather weak; with increased
intensity, the plasma was also compressed into a narrow filament. The
authors suggest that the brevity of plasma entrapment may be due to the
nonuniformity of trap filling.

The authors note some limitations to neutron production from
laser heating of a target for fusion purposes. Specifically, the effect of an
increasingly powerful focused laser becomes offset by diffusion of the high
temperature region owing to thermoconductive and gasdynamic energy loss.
An alternative approach suggested recently by Basov et al is to heat a
spherical target simultaneously with multiple beams; in the present case
this was done with a deuterated polyethylene target exposed to nine equal
beams, as indicated in Fig. 1, using an Nd glass laser in the giant pulse
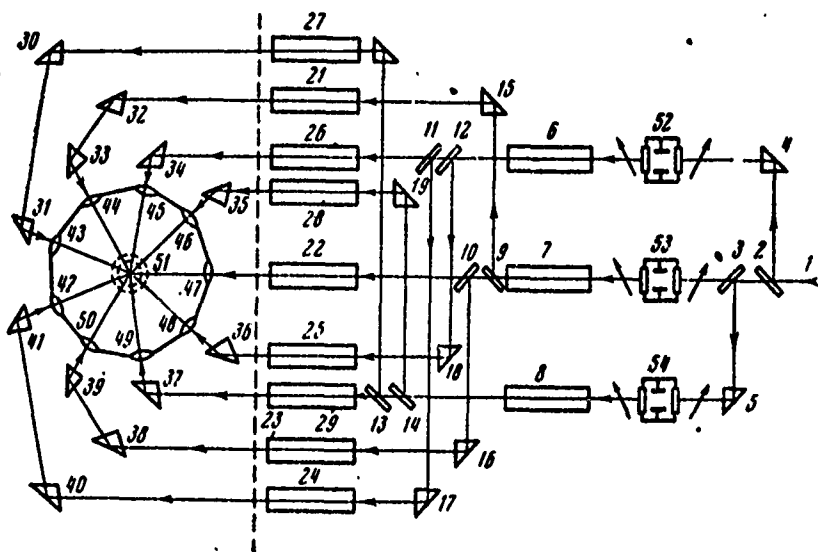
Fig. 1. Multibeam array for CTR target.
1- preamplified beam
6-8- second amplifier
21-29- third amplifier
42-50- focus lenses
Compensating delays for differing path lengths
not shown.

mode. This array attained a mean power density of 10^{16} w/cm^2 on the target
surface, at 2--16 ns duration. The focusing objectives were placed to obtain
a focal plane 200μ from the target, for minimum reflection and uniform
heating.

Some results are shown in Table I for various target sizes and
beam energies; the measured value was obtained from three scintillation
counters. The $n\tau$ values, calculated independently for thermoconductive
and gas dynamic regimes, were 2.4×10^{12} and 2×10^{11} respectively. The
effect of cumulation in the cited experiments is concluded to be a minor one.

Target radius, cm	Laser energy, j	Mean temp., ev	Neutron output per pulse	
			exp.	calc.
$2,50 \cdot 10^{-2}$	600	40	–	–
$1,25 \cdot 10^{-2}$	202	120	–	10^2
$5,50 \cdot 10^{-3}$	214	840	$3 \cdot 10^6$	$8 \cdot 10^7$
$3,00 \cdot 10^{-3}$	232	$4 \cdot 10^3$	–	$1 \cdot 10^{10}$

Table I. Neutron generation with multiple laser beam

Batanov, V. A., V. K. Goncharov, and L. Ya. Min'ko. Powerful optical erosion plasmatron. ZhPS, v. 16, no. 5, 1972, 931-934.

A versatile laser-driven plasmatron is described which may be compared to the one described previously by Goncharov et al in this report. In the present design the simple chamber shown in Fig. 1 was used to
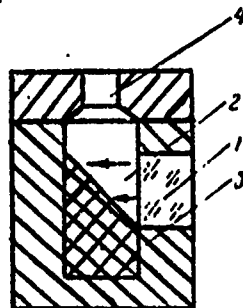
Fig. 1. Laser plasmatron

1- quartz window; 2- chamber;

3- target material; 4- exit nozzle

generate a plasma jet from any given target material, with the plasma driven out through the nozzle by generated pressure. By varying pulse parameters, chamber dimensions, fill gas, etc., a wide range of plasma jet characteristics can be obtained, ranging from subsonic to supersonic. The authors used an Nd glass laser at 0.8 millisecond pulses of 5 kj peak energy, in a quasi-cw regime, to develop target surface densities on the

order of 10^6 w/cm^2. Glass textolite was used as target material, and helium at pressures from 5×10^{-2}torr to several atmospheres served as the fill gas. The many possible variations in jet parameters are discussed and both high-speed and streak photos are given of jet propagation. Table I compares results of two modes. The results generally show the versatility of this type of low temperature plasmatron.

Jet type	E, joules	Nozzle dia., cm	Chamber pressure, atm	Exit velocity km/sec	Adiab. index, γ	Mach no.
With shock wave	3.0	0.9	11	3.1	1.67	——
With period-ic struc-ture	2.2	0.9	8	2.6	1.67	1.9

Table I. Comparative data on supersonic nondivergent plasma jets

Batanov, B. A., F. V. Bunkin, A. M. Prokhorov, and V. B. Fedorov. Self-focusing of light in plasma and a supersonic ionization wave in the laser beam. ZhETF P v. 16, no. 7, 1972, 378-382.

A plasma flare was generated, characterized by almost total absorption of internal laser radiation. The process occurred during progressive vaporization of a bismuth target in a helium atmosphere (pressure P_o = 2.5-5 atm) by a laser beam (λ = 1.06μ at an intensity of $I_o \approx 10^7$ w/cm^2 and 1 ms pulse width). A time scan of the bismuth plasma flare is presented containing a time stabilized flare cross-section which shows that as a result of flare expansion the internal pressure P

becomes equal to the external pressure P_o. The plasma is sustained by the beam in a slow burning mode. The condition for maintaining the plasma in the beam is expressed by $aI = Q$, where Q is the radiation recombination loss. The plasma temperature T and electron density n_e are calculated from the condition $P = P_o$ by the time and length averaged coefficient of inhibition $a \approx 0.4$ cm^{-1}. Self-focusing instability also develops in a plasma cloud at $P = P_o$. The laser beam, at a level $n_e \sim P_o/T \sim P_o/I$, generates a plasma cross-section profile $\epsilon = 1 - \text{const} \times n_c$, similar to the profile I, with a maximum on the beam axis. The plasma beam itself focuses on the profile ϵ, which is made possible by the plasma low thermal conductivity. As a result of self-focusing and an absorption burst, a plasma bunch is formed in cold vapor. The characteristics of this process are: 1) taking beam attenuatio into account, plasma lens focus intensity $I_{sf} \gtrsim 1.5 \times 10^7$ w/cm^2 is lower than the optical breakdown threshold; 2) the bunch is formed at the target and not in the plasma lens focus; and 3) the burst takes much longer to develop ($\sim 10^{-4} - 10^{-5}$ sec) than breakdown into avalanche ionization. The bunch movement toward the beam is in the form of a supersonic ionization wave along the cold vapor between the target and the drifting plasma; one-dimensional propagation of the wave proceeds through laser beam energy absorption in the wave. The velocity of the burst luminescence region exceeds that of the plasma cloud drifting away from the target. The bunch then overtakes the drifting plasma and the process repeats itself. Six cycles of instability self-focusing with increased periodicity were established.

Bessarab, Ya. Ya., Yu. B. Tkach, V. P. Zeydlits, N. P. Gadetskiy, and V. V. Dyatlova.
Study of collective processes in a plasma using light of stimulated emission. ZhETF, v. 62, no. 2, 1972, 569-572.

The use of coherent light emission to study the collective processes in a plasma-beam discharge is described. It is shown that an effective method of studying these processes is the direct observation of the form of oscillation in the intensity of spontaneous-emission spectral lines, with a subsequent application of Fourier analysis. Study of the oscillation spectrum was performed through investigation of the fluctuation intensity of coherent emission in the Ar II transitions $4p^2D^0_{5/2} \rightarrow 4s^2P_{3/2}$ at a wavelength of 4880 Å, and $4p^4D^0_{5/2} \rightarrow 4s^2P_{3/2}$ at a wavelength of 5145 Å. The maximum frequency excited in the plasma, which depends upon modulation of the

emission intensity, is determined by the relationship $\omega_{max}\tau \lesssim 1$ where τ is the lifetime at the upper level of the observed transition. In this study $\omega_{max} \approx 100\text{-}120$ MHz. In the case of coherent emission, the spectrum of the oscillation being investigated has a lower limit given by

$$\omega_{min} \approx \frac{2\varepsilon_0 E^2 c(1-R)}{(N_1 - N_2)\hbar\omega_{12}d},$$

where ε_0 is the dielectric permeability of the active medium, E is the field intensity of the light wave in the resonator, c is the speed of light, R is the reflection coefficient of the resonator mirrors, d is the distance between mirrors, $\hbar$ is Planck's constant, ω_{12} is the frequency of the observed transition and N_1 and N_2 the corresponding population densities of the upper and lower laser levels, respectively. Fig. 1 compares obtained spectra of coherent and spontaneous emission.
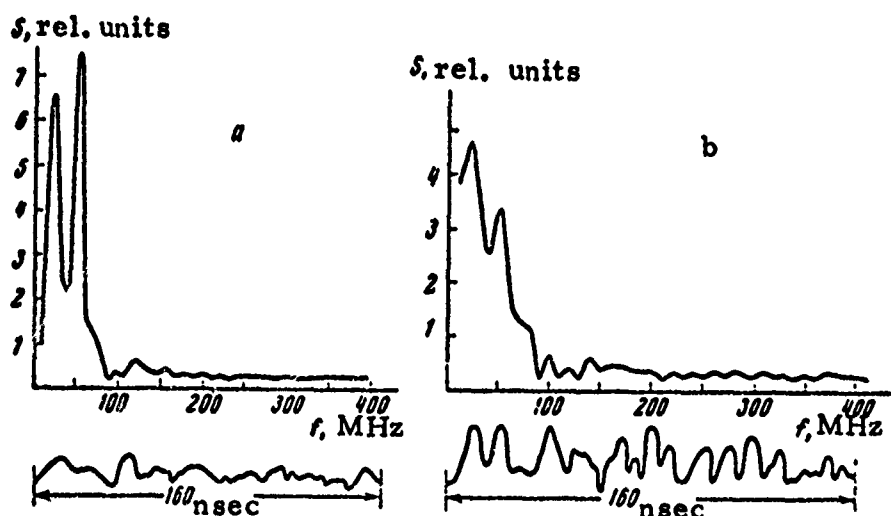

Fig. 1. Realization and type of spectrum obtained. a - by modulation of coherent emission, b - by modulation of spontaneous emission.

Bonch-Bruyevich, A. M., Ye. N. Kaliteyevskaya,
and T. K. Razumova. Effect of single-pulse ruby
laser radiation on a mercury arc plasma. OiS,
v. 32, no. 6, 1972, 1171-1175.

It was determined by the authors that, when the radiation of
a single-pulse ruby laser is focused into the region of a direct-current arc
discharge, the discharge radiation flux increases and the voltage at the
discharge gap drops. A superhigh-pressure mercury lamp was used in the
investigation; the interelectrode gap was 1.4 mm; the incandescent body
diameter was 0.9 mm; current was 6.3 a; and the discharge gap voltage was
43 v. The voltage drop is linked both to photoionization and, more significantly
to electron heating by laser radiation. Assuming that the electron concentration
value is linearly related to the decreasing laser radiation, an increase of the la
flux radiation in the background region proportional to the square of the number
of electrons will have a square-law relationship to the laser energy. The line
flux increment is apparently linked to a population density increase of the
corresponding states of HgI. The increase is also probably related to
population due to recombination during triple collision, stepwise electron
impact excitation and cascade transitions from the higher excited states populate
during ion recombination. An evaluation of the energy balance in the excited
plasma shows that the energy consumption for additional ionization and
excitation, heating the initial electrons and the new electrons and ions, and
for radiation comprised about 30% of the absorbed energy. This evaluation
was made under the assumption that the plasma was heated from 8000 to 8600 K,
the number of electrons was increased by 75%, and the radiation flux was
increased by 100%.

Borisov, V. V. Stable regime in the case of incidence
of an e-m signal of finite duration on an ionization front
moving at light velocity. IVUZ Radiofizika, no. 12,
1971, 1923-1924.

, A brief extension is given to an earlier paper by the author on the
same subject (Borisov, IVUZ Radiofizika, no. 1, 1971, 54). A rectangular
electromagnetic pulse is assumed to intersect an ionization front moving at
light velocity; electron velocity in the intersect region is taken to be well below
light velocity, and ion motion is neglected. Using this model the author derives
general expressions for the transverse electric and magnetic field vectors in
the impact region. Graphical results are included which compare the field
characteristics at short pulse widths ($\omega_0 T = 1$) to those at extended widths
($\omega_0 T = 40$). It is shown that at sufficiently great pulse widths the E vector
at intersection tends to zero, and practically all energy in the incident pulse
converts to a static magnetic field which is confined to a region determined by
the pulse width.

Bud'ko, N. I., V. I. Karpman, and D. R. Shklyar.
Stability of a plasma in the field of an axial monochromatic
wave. ZhETF, v. 61, no. 4, 1971, 1463-1476.

An extended analysis is given of the development of plasma excitation
from interaction of an axial monochromatic wave. The discussion is based on the
phenomenon reported by Wharton et al (Phys. Fl., 11, 1968, 1761), that for a
sufficiently intense wave, satellites are generated in the plasma whose frequencies
differ from the beam fundamental by a predictable amount. The present authors
interpret the satellite phenomenon as a result of instability, caused by a nonlinear
variation in the distribution function of the excitation wave in the plasma. The
amplitude characteristics of satellites near the instability point is accordingly
investigated; it is shown that for the experimental conditions of Wharton et al,
excitation of the satellites is caused by a non-parametric type of instability.
The results are compared with those of several other authors on the same pheno-
menon.

Burakov, V. S., P. A. Naumenkov, V. P. Ivanov, and G. A. Kolosovskiy. Study of the passage of powerful laser radiation through an optically dense plasma. ZhPS, v. 16, no. 2, 1972, 239-242.

Some nonlinear absorption characteristics of laser propagation through a plasma are described. The plasma used was optically dense (4--7/ cm) and at ~4ev in a textolite capillary 2.9 mm in diameter. Transmissibility was measured with a passively Q-switched ruby laser generating a 30 ns pulse at 10^6--10^8 w/cm^2. A pronounced bleaching peak was found at about 10^7 w/cm^2. as seen in Fig. 1. The left-most point of the extrapolated
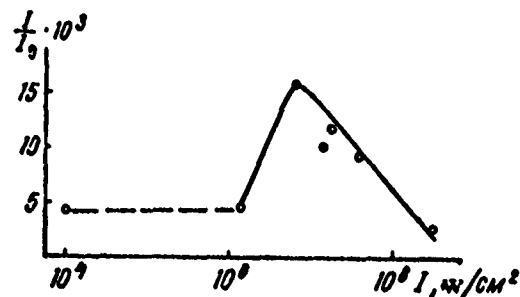

Fig. 1. Plasma transmissibility vs. laser intensity

portion was obtained with a free-running ruby; it was not possible to excite the plasma in the Q-switched mode below 10^6 w/cm^2. The absorption characteristic vs. temperature are given for the HI, CI, OI and CII components. Results indicate the ion and electron temperatures vary almost in synchronism. A general conclusion is that in a multicomponent, highly ionized plasma of the type tested, deviation from equilibrium concentration of electrons can be caused by individual hard-ionizing elements; in the present case this was due to the C II component. It follows that care must be taken to allow for nonlinear absorption when using a powerful laser for certain plasma diagnostics.

Burakov, V. S., P. A. Naumenkov, and G. A. Kolosovskiy. Using a tunable laser to determine absorption characteristics of a plasma. ZhPS, v. 16, no. 1, 1972, 54-57.

Tunable dye lasers using several active solutions were used for plasma diagnosis. Dye pumping was by neodymium, ruby, or xenon flashlamp; Fig. 1 shows the configuration for pumping with ruby second harmonic. By introducing dispersion elements into
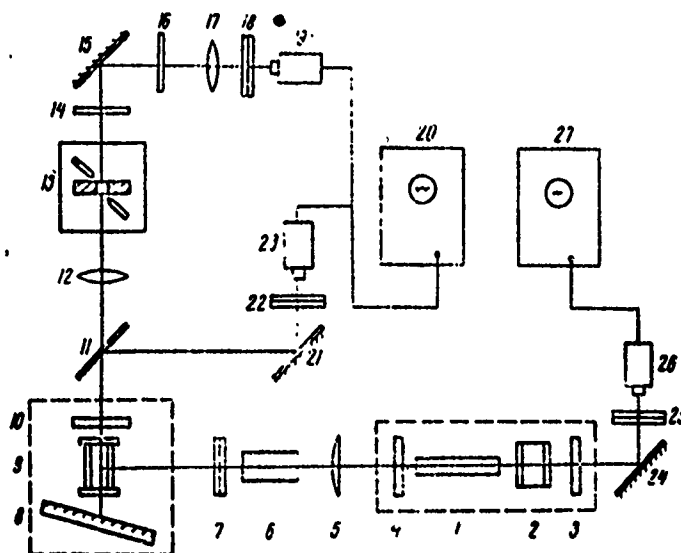
Fig. 1. Dye laser plasma probe
1-4 - ruby pump; 5- lens; 6- KDP doubler; 7, 8- diffraction grids; 9- active solution; 10- output mirror; 11, 14- semi-transparent glass; 12, 17- lenses; 13- plasma in capillary; 19, 23, 26- phototubes; 15, 21, 24- rotatable mirrors; 16, 22, 25- neutral filters; 18- interference filter; 20, 27-oscilloscopes.

the solution it was possible to vary generation over a range of 20-30 nm. The probe beam was focused to 1.5 mm diameter on a plasma formed by a high-current discharge through a 3 mm dia. textolite capillary. The 400 μs current pulse was rectangular at 7.5 ka; plasma temperature reached 40,000°K. The transmitted spectral response was recorded as indicated in the figure, for four different dye solutions whose parameters are given in Table I. A sample spectrogram is included, but the bulk of the article deals with the technique rather than its results.

Active element	1	2	3	4	5
Rhodamine 6G	603-575	599	4.5	589	7.0
		588	4.4	589	7.0
		578	4.0	573	7.5
Uranyl	570-545	558	2.8	558	6.0
1, 1, 4, 4-tetraphenyl-butadiene in cyclo-hexane	550-480	517	2.7	513	8.0
7-diethylamino-3, 4-dimethylcoumarin	490-457	468	2.3	473	9.0

Table I. Dye laser probe parameters.

1- lasing range, nm; 2- selected wave-lengths, nm; 3- plasma absorption co-efficient, cm^{-1}; 4- transmission peak of filter, nm; 5- filter bandpass, nm.

Fanchenko, S. D., and G. V. Sholin. Possible mechanisms of turbulent heating of a plasma by ultrashort laser pulses. DAN SSSR, v. 204, no. 5, 1972, 1090-1093.

The authors consider the initial ionization phenomena arising from interaction of a picosecond laser pulse with a very dense plasma. A feature of this case is that the optical field strength E is comparable to intra-atomic field E_a; this results in an ionization time τ_{ion} on the order of or less than electron-atom on electron-ion collision time, and possibly less than the laser wave period. The model used assumes a picosecond pulse with optical

frequency Ω falling on a condensed neutral target. During the first portion of the optical wave rise time, light penetrates the target virtually without ionization taking place; as the optical field approaches its peak of E, ionization begins but with an electron plasma frequency $\omega_{p\ell}$ still below Ω . As $E \rightarrow E_a$ the affected electrons proceed from bounded to unbounded motions in a time interval $\approx 10^{-16}$ sec. The authors then treat the two general intervals of collisionless plasma heating which ensue, namely when $\omega_{p\ell} < \Omega$ and $\omega_{p\ell} > \Omega$. Ionization parameters are obtained taking into account the magnetic piston effect exerted by the optical field when $\omega_{p\ell}$ overtakes Ω . Results show that at this point a beam of electrons forms in the focal region which may attain directional energies of 10^4 ev. Calculations based on a typical set of plasma parameters show that this current may exist for up to 10^{-12} sec. and reach densities above 10^{12} a/cm^2. It is emphasized that these deductions apply only to the initial one or two periods of laser pulse oscillation, applied to a neutral medium. Analogous effects from shock-wave and electron beam heating of a plasma are also noted.

Generalov, N. A., V. P. Zimakov, G. I. Kozlov, V. A. Masyukov, and Yu. P. Rayzer. Experimental investigation of a continuous hot optical discharge. ZhETF, v. 61, no. 4, 1971, 1434-1446.

Rayzer, Yu. P. Continuous sustaining of a plasma by laser radiation, and the optical plasmatron. VAN, no. 10, 1971, 28-32.

Rayzer, Y., G. Kozlov, and N. Generalov. Nonlinear absorption of intensive radiation in plasma. Soviet Science Review, v. 1, no. 1, 1970, 42-46.

These papers generally review and extend the experimental data already reported on the optical plasmatron (Rayzer, Generalov et al, Effects of High-Power Lasers, Dec. 1971, 17-21). The experiment uses a Q-switched CO_2 laser to ignite and sustain a suspended plasma in argon and xenon, over a variety of pressure and laser power levels. The general purpose here has been to define the limits to the critical parameters for plasma maintenance, and to observe the dynamics of plasma development. It is shown for example that there is a limited gas pressure range within which the plasma will subsist, for a given laser power; this is seen in Fig. 1 for Ar and Xe. It is evident from the curves

o - argon

• - xenon
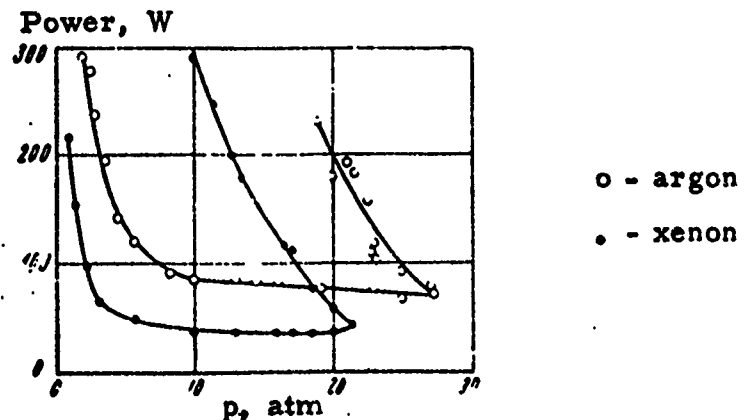
Fig. 1. Limits for optical plasmatron generation.

that over a range of some 10 to 25 atm, threshold power is practically independen of pressure. Other data given include beam transmissibility through the plasma and propagation behavior of the plasma; typical results show an initial velocity of 10 m/sec, decaying to zero at the stable configuration in the order of several hundred microseconds.

Golant, V. Ye. Wave penetration in plasma
at frequencies near the lower hybrid. ZhTF,
no. 12, 1971, 2492-2503.

Theoretical considerations are presented for optimizing the
introduction of e-m radiation into a magnetized plasma. It has been
shown that injection near the lower hybrid frequencies may be advantageous
since plasma opacity to the incident wave will be minimal here, to a wave
with correctly applied longitudinal delay. The author therefore investigates
the transformation region for frequencies near the lower hybrid, and
derives expressions for optimum energy transfer under these conditions.
It is assumed that the applied frequency lies well below electron cyclotron
resonance and well above ion cyclotron resonance. For the case of a
uniform applied magnetic field, expressions for optimal delay structure
parameters are obtained, assuming the idealized delay configuration
of Fig. 1. In some cases in a uniform field the requirements on delay
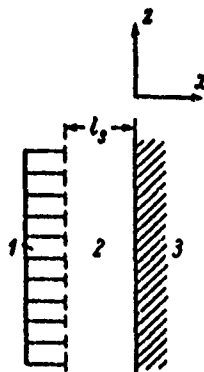

Figure 1. Delay geometry.
1 - delay element; 2 - vacuum;
3 - plasma.

parameters may become excessive; in that event a nonuniform external
field may be applied, resulting in two transformation regions and
simplifying the delay line operation.

Goncharov, V. K., A. N. Loparev, and L. Ya. Min'ko.
Self-igniting pulsed optical discharge in an erosive laser
plasma. ZhETF, v. 62, no. 6, 1972, 2111-2114.

A variant on the optical plasmatron is described in which a
self-igniting optical discharge is obtained from irradiation of a
target surface. The technique was to defocus the incident beam
such that the focal point was several millimeters above the target
surface; vapor products from the surface, traveling at about
100 m/sec, would ignite on reaching the focal point and
provide a "hanging" optical discharge for the remainder of the laser
pulse. The experiment cited used an Nd glass laser at 1.5 μs
pulsewidth and generating relatively low surface intensities on
the order of $10^6 w/cm^2$. Various metals and dielectrics were
tested as target materials, including ebonite, textolite, brass
and a type POS-40 alloy. Depending on the material, a stable
discharge was achieved in a 10 - 20 mm range above the target
surface; spectral studies show discharge temperatures $\simeq 22,000^{\circ}K$.
Streak photos of the discharge development are given; Fig. 1 shows
one form of the discharge.

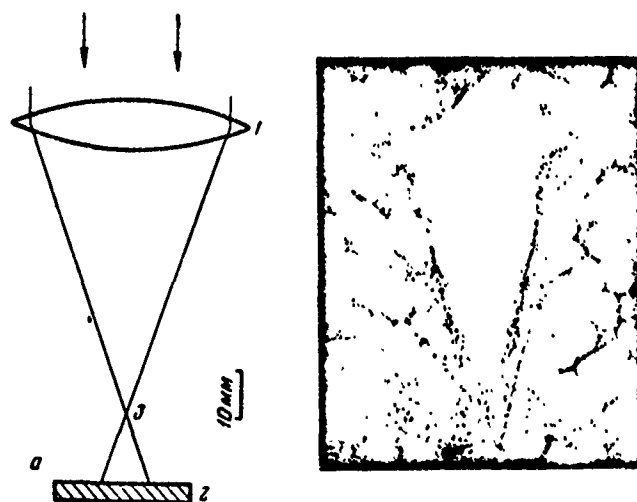
Fig. 1 . "Hanging"
optical discharge.

The authors suggest adapting the effect to a c-w discharge,
using a CO_2 laser for excitation. The effect is claimed as the
first of its kind obtained at atmospheric pressure.

Gusev, V. K., G. M. Malyshev, G. T. Razdobarin, and L. V. Sokolova. Measuring electron temperature and concentration from laser scattering by plasma in the Tuman-2. ZhTF, no. 2, 1972, 340-343.

A laser diagnostic technique for measuring plasma parameters in a Tuman-2 torus is described in detail. The method was based on recording scattered radiation from a current-heated plasma at an angle of 140°, as shown in Fig. 1. The ruby was Q-switched by a KDP cell
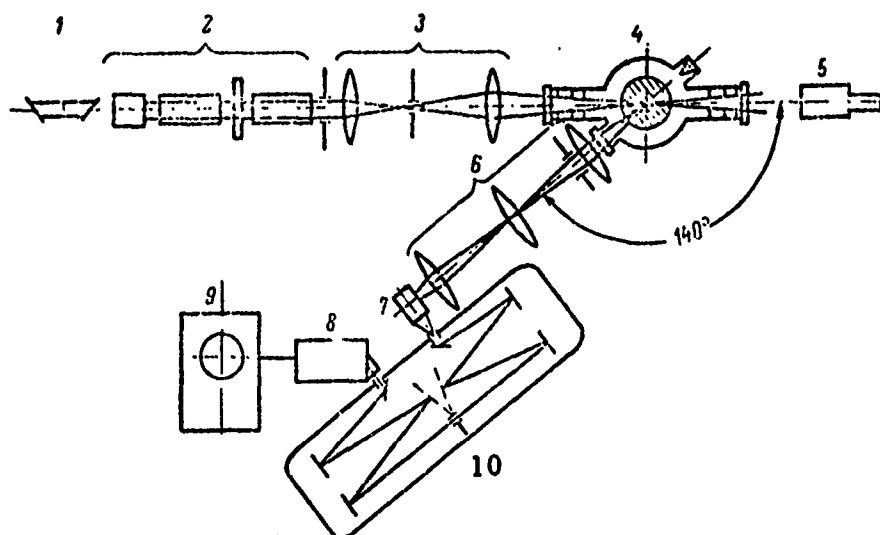
Fig. 1. Plasma diagnostic experiment
1- He-Ne alignment laser; 2- two stage ruby; 3- focus optics; 4- plasma chamber; 5- TB-3 theodolite; 6, 7- projection optics; 8- photomultiplier; 9- CRO; 10- DFS-12 dual monochromator.

to give 1.5j, 30 nsec pulses; an optical absorber was installed opposite the laser entrance port to minimize parasitic scatter effects. With this configuration the scattering spectra were registered for discharge pulses of 4.5 and 9 ka, as seen in Fig. 2. From this data the electron

Fig. 2. Laser scatter spectra
a- 4.5 ka;   b- 9 ka.

temperature and density at the center of the discharge was calculated
to be 10.5 ev and 3.3 x 10^{13}/cm^3 for the 4.5 ka discharge, while for the
9 ka pulse the figures were 6.2 ev and 4.4x10^{13}/cm^3. The lower
temperature in the latter case is attributed to increased losses, and to
the fact that in these cases the measurements were taken near the end
of the 1.6 μs current pulse. The data also show that the electron para-
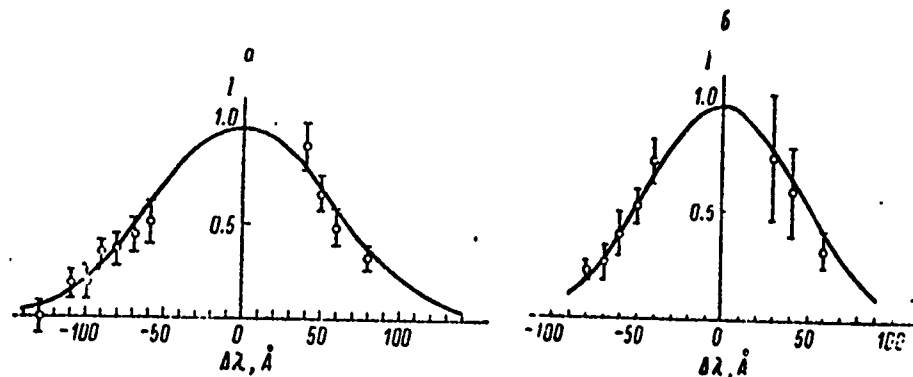meters at the center of the discharge column did not differ appreciably
from the mean values taken over a plasma cross-section.

Kaliski, S. <u>Generalized equations for laser heating of
a dual-temperature plasma with allowance for heat of
thermonuclear synthesis.</u> Biul. WAT J. Dabrowskiego,
v. 20, no. 12, 1971, 25-30 (RZhF, 5/72, no. 5G299)
(Translation)

Generalized equations are derived for laser heating of a plasma to
obtain fusion, for the case of different ion (T_i) and electron (T_e) tempera-
tures. The equations are based on the following simplifying assumptions:
bremsstrahlung depends only on T_e, heat yield only on T_i; radiation losses
are negligible; thermal conductivity of ions is small relative to that of elec-
trons; electron and ion densities are roughly equal; and the mechanical
parameters of the system are not distinguishable by ion and electron com-
ponent. Equations for laser heating of of the plasma are obtained for $T_i = T_e$.

Kazakov, A. Ye., I. K. Krasyuk, P. P. Pashinin, and
A. M. Prokhorov. <u>Experimental observation of laser
radiation amplification from the interaction of opposed
laser beams in a plasma.</u> ZhETF P, v. 14, 1971, 416-418.

Experimental data are briefly discussed on the effects of focusing
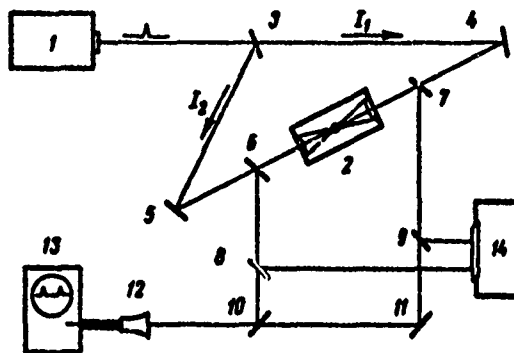opposed laser beams in an argon plasma. The test configuration (Fig. 1) used

Fig. 1. Colliding beam experiment.
1 - laser; 2 - Ar chamber; 3--11 - splitting
deflecting optics; 12 - coax; 13 - scope,
0.2 ns resolution; 14 - spectrograph.

a monopulse laser at $6943 \overset{o}{A}$ and 20-100 nsec duration, split and simultaneously
focused at f = 2 cm through opposite faces of the argon chamber. The optics
were assigned such that $I_2 < I_1$ by varying amounts, but both were above break-
down threshold. Records of exit intensities and spectra of the two pulses showed
two distinct effects: the weaker pulse was amplified by the stronger, and also
underwent a spectral broadening. These effects were more pronounced with
larger initial disparity between I_1 and I_2 intensities. An example given shows
I_2 increased by a factor of 1.32, where initially $I_2 = 0.2 I_1$. Stimulated Compton
scattering is suggested as the main mechanism for these results, and calculations
on this assumption show a good agreement with actual gain figures for the weaker
pulse. The spectral change in I_2 is not explained and must be clarified by
additional tests.

Kaytmazov, S. D., A. A. Medvedev, and A. M.
Prokhorov. <u>Effect of a 400 koe magnetic field
on the plasma of a laser spark.</u> ZhETF P, v. 14,
1971, 314-316.

An experiment is briefly described in which the controlling effect
is studied of an external magnetic field on the geometry of a laser spark
plasma. Two conditions must evidently be met for field control of spark

geometry, namely (1) field pressure must exceed gas kinetic pressure in the plasma, and (2) the skin layer should not exceed spark radius, r. This means that the external field must be sufficiently great that on lowering of plasma pressure to the magnetic pressure level, plasma temperature still remains high enough to preclude diffusion in the external field. The corresponding threshold for field control in the present case was calculated to be on the order of 300 koe. Tests to corroborate this were run at levels up to 500 koe, using a transformer-fed one-turn coil of 0.8 cm dia. instead of the usual capacitor bank. A 100 μsec field pulse was thus generated, which simplified the requirement of exact synchronization of laser spark and field pulse. Tests were run in ambient air, using a neodymium glass laser at 2--3 j in both giant pulse and spike regimes to produce breakdown. The comparative effect of the field is seen in Fig. 1, where the spark is confined to a cylindrical form with

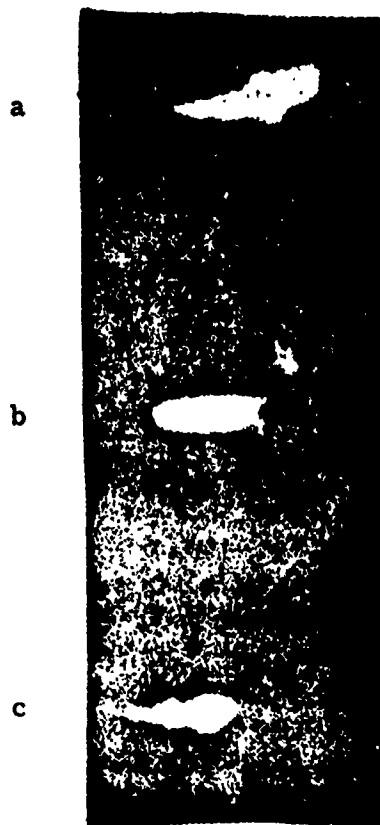Fig. 1. Field effect on laser spark. a, c - no applied field; b - field applied

a smooth boundary. In both laser regimes the field increased spark axial length by about 1.5 times; it follows that this formation should retard plasma cooling. Nominal spark parameters of r = 0.1 cm and time constant $\tau = 3 \times 10^{-7}$ sec led to the conclusion that the plasma temperature attained was at least 6×10^5 deg. K.

Knyazev, I. N., and V. S. Letokhov.
Stimulated radiation in the far vacuum u-v
from fast heating of an electron plasma
by ultrashort optical pulses. OiS, v. 33,
no. 1, 1972, 110-115.

Laser excitation in a rising electron avalanche is not advantageous in the short-wave range because: 1) as long as the neutral gas predominates in the plasma, the electron avalanche proceeds at a high speed but owing to photoabsorption there is no emission at short-wave transitions; and 2) when neutral gas burns out and the plasma becomes transparent for transitions in the far vacuum ultraviolet, ionization velocity drops drastically, hindering inversion. The authors propose using ultrashort pulses of an electric or optical field with $\omega > \omega_p$ for electron heating in a dense plasma where $n \cong 10^{18}$-10^{20} cm^{-3} and z~5. The heating should proceed until a temperature is reached sufficient to excite the upper operating level without substantially increasing the electron density. The use of short-wave electric pulses does not require the same high degree of initial plasma density typical of light pulses. The above method yields the maximum critical excitation velocity on the order of the collision frequency ν_{eff} between ions and electrons; energy absorbed by the plasma is used for electron heating. Optimal excitation of operating levels of the above type of short-wave laser occurs when electrons are heated to an energy that corresponds to the maximal cross-section, at a time $\Delta t \ll A_{12}^{-1}$, which is smaller than the reciprocal value of the operating transition probability; it is thus feasible to obtain amplification factors $\cong 10$-10^3 cm^{-1} in the vicinity of $\lambda \approx 500$Å. The authors calculate inversion excitation during propagation of ultrashort light pulses in plasma. Results suggest that by using a neodymium laser pulse of $\Delta t = 10^{-11}$ sec duration and 1 joule energy it is possible to heat plasma of $n_e \cong 2 \times 10^{19}$ cm^{-3} and z=5 to an energy of ~160 ev. This energy may be optimally used at an ~1.5 cm length and $\approx 10^{-3}$ cm^2 cross-section area.

Kochelap, V. A. <u>Negative absorption of light</u>
<u>in a dense ionized gas.</u> ZhTF, no. 2, 1972,
449-451.

The theoretical possibility is explored of achieving negative
absorption in a non-equilibrium dense ionized gas through electron radiative
capture by neutral atoms which exhibit affinity for the electrons (negative ion
continuum). The gain factor formula

$$\alpha\,(\omega) = c\omega \left[\frac{g_i}{2g_a} \left(\frac{2\pi\hbar^2}{m_e kT_e} \right)^{\!\!1/2} e^{-\frac{\hbar\omega - \epsilon_{a_i}}{kT_e}} n_a n_e - n_i \right].$$

(1)

(where ω is the cross-section of electron photodetachment from the negative
ion, g_a and g_i are multiplicities of degenerate atoms and ions; m_e is the electron
mass; ϵ_c is the atom affinity; and n_a, n_e, and n_i are concentrations of atoms,
electrons, and negative ions, respectively) was derived from consideration of
thermodynamics. This formula shows that a gain in the negative ion continuum
can be achieved, if n_i is maintained below its equilibrium value. An evaluation
of α was made for a nonequilibrium H plasma with T_e = 5,000° K using the
formula and the assumption that $n_i \longrightarrow 0$. It was shown that a significant gain
can be achieved under these conditions; e.g., at the frequency ω = 2.10^{15}
sec^{-1} and the degree of ionization x = 0.5, α attains a maximum value of
0.3 cm^{-1}. A predominance of photostimulated over spontaneous emission
from a nonequilibrium ionized gas interacting with a powerful light wave is show
to occur at a photon optical density $q > q_m$. The threshold q for H under
the cited conditions is q_m = 2 x 10^{13} cm^{-3}. A theoretical high quantum yield
can be obtained in the system studied. The low n_i values necessary for
realization of negative absorption in nonequilibrium plasma presumably may
be attained by cooling the electrons to T_a in a time τ_e significantly shorter
than the times of electron capture by neutral atoms and the electron
recombination with positive ions. A nonequilibrium plasma with the required
parameters can also be created by directing an $n_e \geq 10^{16}$ cm^{-3} electron beam
into a gas.

Liberman, M. A., and A. T. Rakhimov.
Penetration of e-m waves into a plasma with
allowance for nonlinearity. ZhETF, v. 61,
no. 3, 1971, 1047-1056.

· The authors examine the structure of an alternating electro-
magnetic field interacting with a weakly ionized plasma, for the case of
thermal nonequilibrium in the plasma. It is noted that nonlinear effects
begin to appear in such a case at relatively weak fields in comparison to
the characteristic plasma field. The discussion is limited also to the case
where the incident e-m field frequency is well above the electron-atom
collision frequency, but below plasma frequency. Using this model the
authors show that the effect of the e-m field on the local ion-recombination
balance in the plasma causes an appreciable change in the penetration
depth of the field into the plasma, according to the relation c/ω_p where ω_p
is electron frequency in the interaction region. Expressions are derived
illustrating the nonlinear decrement in e-m intensity with penetration, and
some sample calculations are given for the effect, using typical plasma
and beam parameters.

Omel'chenko, A. Ya., V. I. Panchenko, and
K. N. Stepanov. Absorption of an extra-
ordinary electromagnetic wave in a linear
layer of plasma in the hybrid resonance
region. IVUZ Radiofiz, no. 5, 1972,
660-664.

The article presents the results of numerical calculation
of the absorption coefficient and field distribution of an extraordinary
wave at normal incidence to an inhomogeneous magnetically active plasma.
The case is considered when the external field is homogeneous and is
normal to the direction of plasma density changes. It is assumed that
density changes linearly along the x-axis and that effective frequency of
electron collision with heavy particles ν is small in comparison to wave
frequency.

The equation defining the component of electric field E_y
in the plasma was solved by computer in two different ways, both
yielding identical results: using the Runge-Kutta method, and by
numerical summation of series for E_y by degrees $\xi = \omega_r^2/\omega^2 + \omega_H^2/\omega^2 - 1$.

Results of calculations are given for various values of the parameters $u = \omega_H^2/\omega^2$ and $\rho = \omega/c \; dx/d(\omega_r^2/\omega^2)$, as shown in Figs. 1 and 2.
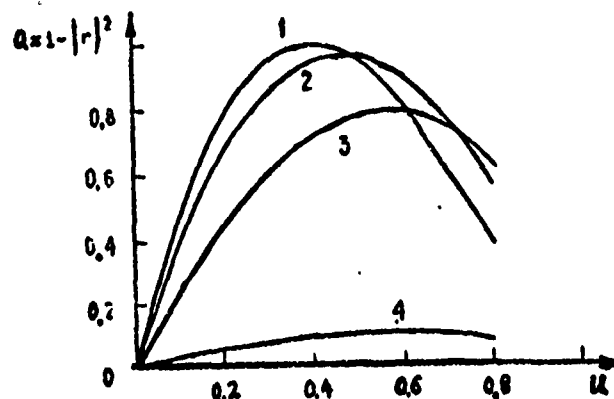

Fig. 1. Q(u) for a strongly inhomogeneous
plasma at $\rho = 1(1)$; 0.8 (2); 0.5 (3) and 0.1 (4).

Fig. 1 illustrates the dependence of the absorption coefficient Q on the value of the parameter u in a strongly inhomogeneous plasma, for $\rho = 0.1 - 1$. For a weakly inhomogeneous plasma $\rho = 10 - - 20$; and for a moderately inhomogeneous plasma the value of $\rho \approx 3-5$. The corresponding graphs for weak and moderately inhomogeneous plasma are given in the article.

Fig. 2 shows the distribution of electric field in a strongly inhomogeneous plasma for $\rho = 0.5$ and $u = 0.57$. The article contains some additional data on the distribution of the variable ξ in relation to various values of the parameters u and ρ. The results obtained are qualitatively evaluated. The absorption coefficient is appreciable only in those cases when the distance between the first point of reflection and the resonance point is comparable with the wavelength in plasma. In a

weakly inhomogeneous plasma $(\rho \gg 1)$ this can occur only in a weak magnetic field $(u \ll 1)$. In the case of strong inhomogeneity $(\rho \lesssim 1)$ strong absorption may take place even at $u \sim 1$.
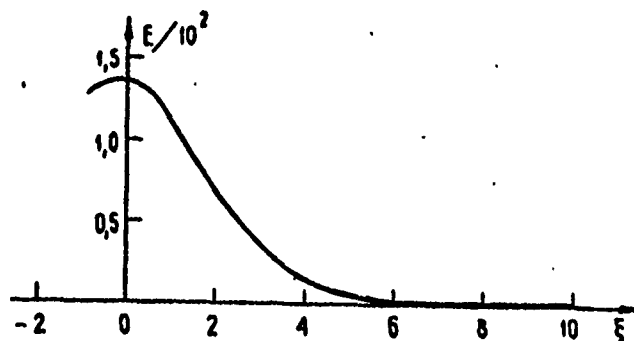
Fig. 2. Field distribution at $\rho = 0.5$, $u = 0.57$.

Popov, S. P. Stationary regime of the radially-symmetrical motion of laser heated vapors, taking temperature and ionization nonuniformity into account. ZhPMTF, no. 4, 1972, 3-7.

This is a theoretical study concerning the effect of temperature and ionization honequilibrium on the motion of vapor products generated by laser interaction with a solid surface. The case is considered for stationary motion of a radially symmetrical vapor cloud, generated by power densities $q = 5\text{-}20$ Mw/cm^2 and focused radius $r_o = 0.01\text{-}1$ cm. In an earlier paper on this problem, Nemchinov (PMM, v. 3, no. 2, 1967, 300-319) considered the coefficient of beam absorption to be constant or to vary according to a power law as a function of temperature and density. The conditions for a stationary regime were then established in terms of vaporized mass, surface pressure, maximum vapor temperature, and vapor cloud radius.

Popov extends this treatment to account for a more realistic behavior of absorption coefficient as a function of temperature and density, referring to a stationary regime at $T = 20,000°K$ and $q = 100$ Mw/cm^2, i.e. in the range where transition from the nonshielding to the shielding situation occurs. Nemchinov and Popov have previously analyzed the effect of temperature nonequilibrium on plasma heating in this model, showing that it acted to reduce the critical flux q_o at which shielding begins. (February 1972 Report, p. 5). Popov shows that an analogous situation applies to the stationary mode; in fact, for the assumed parameters of the cited beam-target model, q_o drops by a factor of 2-2.5 when thermal nonequilibrium is taken into account. Graphical solutions are given comparing transition region characteristics for the two cases.

Pustovalov, V. K. <u>Self-similar gas motion behind a shock wave front sustained by radiation.</u> DAN BSSR, no. 12, 1971, 1079-1081.

The author analyzes a simple model which relates to the optical plasmatron described by Rayzer and others (see for example the February 1972 Monthly Report, p. 11), i.e. a continuous local plasma sustained by a laser beam. The present model assumes a half-space $x > 0$, filled with a cold ideal gas of constant density ρ, where the surface $x = 0$ is the boundary between the gas and vacuum. At time $t = 0$ a strong shock wave begins to propagate from the boundary in to the gas, impelling the gas to expand into the vacuum. Energy from an optical flux q is absorbed by the gas and uniquely determines the propagation of the shock wave; gas expansion is assumed to be adiabatic. Using this model, the author develops self-similar equations in Euler coordinates defining gas pressure, density, velocity in terms of adiabatic index γ and the self-similar index ξ. It is shown that for the sustained shock condition γ must lie between 1 and 1.5. The case of $q < 0$, i.e. energy radiating from the shock wavefront, is also briefly considered.

Rezvov, A. V. Effective boundary
conditions in the theory of e-m wave
penetration into plasma. ZhTF, no. 6,
1972, 1120-1129.

    The spatial structure of an e-m field in a semi-bounded
plasma is calculated for incidence of a p-polarized plane wave at an angle
θ (vector E lies in the plane of incidence), or surface wave propagation
along the boundary. The specific case is analyzed of a frequency range
satisfying the inequalities $\omega^2 \gg \nu^2$; $\omega^2 \gg \nu_T^2/c^2 \cdot \omega_p^2$; $\omega - \omega_p > \omega_p \, \nu_T^2/c^2$
sin θ, which permits omission of the effects of particle collisions. A
Maxwellian distribution of particle velocities is assumed. The author procee
from expressions for Fourier components of the e-m field which were
obtained from a simultaneous solution of the Maxwell equation and the
Boltzmann kinetic equation.

    The spatial distribution of a plasma e-m field includes both
plane waves and a spatially anharmonic component, and comprises a
superposition of free oscillations. The latter are determined from the analytic
properties of permittivity dispersion functions and particle interactions with
the plasma surface. Solutions are given for the mirror reflection model
and for the conditions of particle diffuse scattering on the plasma boundary.
Based on the values obtained for longitudinal and transverse wave amplitudes
induced in plasma, the author concludes that the same results may also
be obtained by the standard phenomenological method if the boundary condition
of the e-m field components are supplemented or slightly modified. Such
effective boundary conditions are outlined by the authors in solving the
problem of plane e-m wave incidence on a plasma boundary at the angle θ.

Semenova, V. I. <u>Electromagnetic wave</u>
<u>reflection during oblique incidence on a</u>
<u>moving ionization front.</u> IVUZ Radiofiz, no.
5, 1972, 665-674.

An extensive theoretical analysis is given of the
interaction of a monochromatic wave with a plasma boundary. The
particular case considered is of inclined incidence of monochromatic
TE and TM waves upon a sharply defined boundary of a plasma half-
space, where the plasma is generated by ionizing radiation acting on
a neutral gas. For simplicity the incident pulse is assumed arbitrarity
narrow and the dielectric constant outside the plasma is taken to be
unity. It is shown that with the E-field normal to plane of incidence,
the solution for the inclined incidence case is essentially the same as for
normal incidence. With the TM wave, however, inclined incidence is
shown to generate two axial waves in addition to the transverse ones, at
any given frequency of the incident wave. Formulas for the reflection
and transmission of the latter are obtained and analyzed in terms of the
idealized plasma parameters.

Tyurin, Ye. L., and V. A. Shcheglov.
<u>Radiant heat wave in a moving plasma.</u>
ZhTF, no. 8, 1972, 1586-1590.

The article presents an analytical solution to a problem
of heated plasma flow with a preset density and random time dependence
of flow velocity $v(t)$. At the boundary $x = 0$, a laser energy flow occurs
with a random time form $I_o(t)$. This corresponds to the physical condition
when plasma is heated by powerful laser radiation in the energy range of
10--100 joules per pulse, and pulse duration r which agrees with the gas-
dynamical plasma dispersion r_{gd}, and equals 10^{-9} sec. Plasma heating

by two or more pulses is examined which improves the heating quality when the process is essentially unstable and absorption is determined by the number of discharge particles.

Radiation transfer and energy conservation equations are solved for a medium where n = const and $v \ll c$ at the preset boundary conditions. The solutions describe the process of heat wave propagation in a moving radiation absorbing medium. The solutions are applicable to any form of absorption coefficient K temperature dependence and cover a broad range of initial conditions. Heating of sufficient intensity generates a sharp front wave $x = x_o$, where $\partial t / \partial x$ is maximal and the temperature T_{fr} = const. As a function of current time t and setting time t_s when $dx_{fr}/dt = 0$, two heat wave propagation modes were noted: at $t < t_s$ the heat wave motion is unstable and it propagates into the plasma; at $t = t_s$ the front comes to a stop, and its motion and other wave parameter variations are subsequently dependent on changes in the plasma flow velocity $v(t)$ and radiation energy velocity $I_o(t)$. In other words, when $t \geq t_s$ the heating process becomes stabilized and at the boundary $x = 0$ this leads to equality between plasma radiation energy flow $I_o(t)$ and heat energy flow. Heat wave parameters were computed under two conditions: 1) v = const is the plasma flow average velocity under the pulse effect; and 2) $v \sim \sqrt{T_o}$ accounts for an increase in plasma velocity during the heating process. It was proven that variations in velocity in relation to heating had only a slight effect on the time t_s but doubled the heating time. Numerical estimates are given for t_s and the maximum depth of heat wave penetration into plasma x_{max}, under typical laser heating conditions. At $I_o = 10^{13}$ w/cm^2, $n = 10^{21}$ cm^{-3}, and $v = 2 \times 10^7$ cm/sec, the values $t_s = 5 \times 10^{-9}$ sec and $x_{max} = 5 \times 10^{-2}$ cm were obtained. At a relatively high pulse energy ϵ expressed in joules per square centimeter, the heat wave possibly approaches the non-transparent plasma layer where $n \geq n_{crit}$, which leads to the reflection of laser energy from the target.

The solutions obtained by the authors permit estimates of the optimal duration τ_{opt} of single or pulse packets from specific ϵ, n, v and plasma absorption layer thickness values with non-reflecting characteristics and under maximum temperature conditions. It was also demonstrated that only about one half of radiation energy was used for plasma heating, the remainder being dissipated in the plasma.

Volosevich, P. P., and Ye. I. Levanov.
On self-similar motions of a two-
temperature plasma. IN: Sbornik.
Teplo- i massoperenos, v. 8. Minsk,
1972, 29-35. (RZhMekh, 9/72, no.
9B119) (Translation)

A self-similar solution is analyzed to the problem of
dispersion of an ionized gas in vacuum, occurring from a laser-target
interaction. The case is considered for a powerful laser source inter-
acting with a plane solid surface. The plasma is treated as a two-
temperature hydrodynamic approximation, taking into account the
energy exchange between electrons and ions; electron thermal
conductivity; and ion drag. The self-similar solution has the form
of a temperature wave propagating through a given "noise" level at
a finite velocity. Between the temperature wave front and the vacuum-
target interface a shock wave occurs, at whose front the electron
temperature is continuous while the hydrodynamic parameters and ion
temperature undergo discontinuities. At the target face the ion
component of temperature goes to zero, while the electron component
has a non-zero value. Calculations show that there are two distinct
modes of heat propagation, namely subsonic and supersonic.

Yevtushenko, T. P., V. Kh. Mkrtchyan, and
G.,V. Ostrovskaya. Spectroscopic studies of a
laser spark. IV. Absorption spectrum of a spark
in hydrogen. ZhTF, no. 12, 1971, 2581-2589.

This is the fourth report in a series by the authors on laser
spark spectroscopy; the previous article was reported in Effects of High
Power Lasers, Dec. 1971, p. 7, on spark spectra in air, He and Ar. In
the present tests the absorption spectrum of hydrogen at 6 atm was measured
and compared to the continuous spectrum of an air breakdown. The
same method was used as in the earlier tests, as shown in Fig. 1, using
two Nd glass lasers to generate the sparks. The lasers were identical
and developed giant pulses of 0.5 j using a driven prism Q-switch
rotating at 27,000 rpm. A large amount of graphical data on spark
parameters, deduced from the spectral response, is presented and
analyzed including the time characteristics of absorption, N_e, and
plasma temperature. An example is given in Fig. 2, showing temperature,
pressure and density variation in the center of the spark. In conclusion
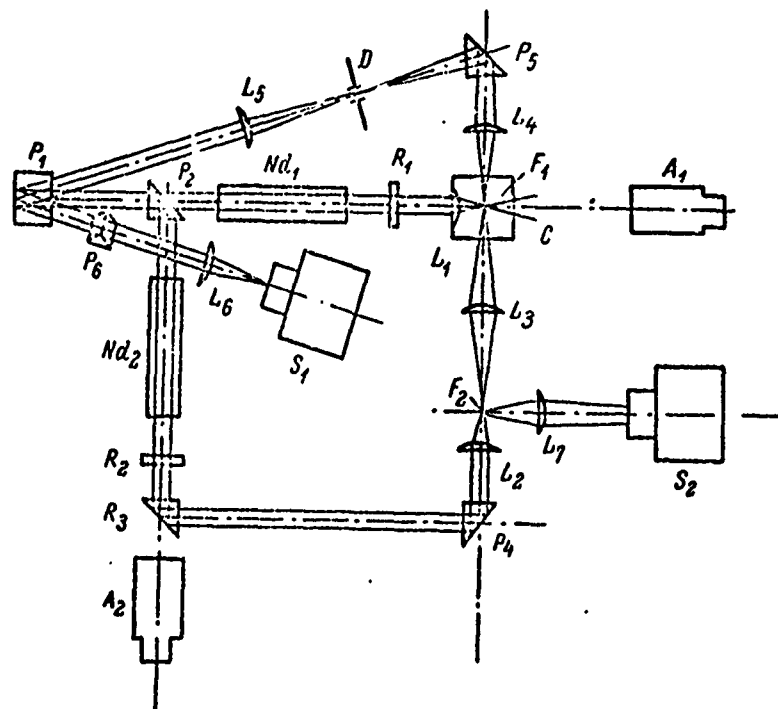
Fig. 1. Schematic for spectral study of a
laser spark in hydrogen. A_1, A_2 - monitor tubes;
C - hydrogen vessel at 6 atm; F_1, F_2 - sparks;
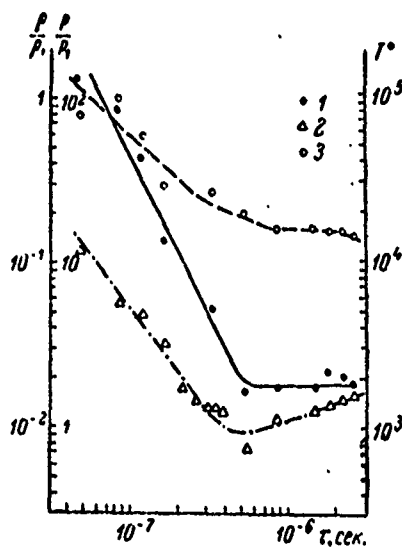S_1, S_2 - spectrographs.

Fig. 2. T, p, ρ(t) in the center of a laser
spark in hydrogen. 1 - pressure; 2 - density;
3 - temperature.

the authors discuss the accuracy of the spectral method for deducing
the cited spark parameters.

Zakharov, S. D., Ye. L. Tyurin, and V. A. Shcheglov.
On the propagation of monochromatic radiation through
a plasma. ZhETF, v. 61, no. 4, 1971, 1447-1451.

A rigorous analytical solution is obtained to the problem of propagation
of pulsed monochromatic radiation in an absorptive plasma. The laser pulse
is assumed to have an arbitrary waveform, and a radiation frequency well above
plasma frequency; the volumetric change in electron density is also assumed
to occur smoothly. With these assumptions reflected radiation may be neglected.
It is further assumed that electron collision frequency ν_e meets the condition
$\nu_e \ \tau \gg 1$, where τ is the characteristic time to alter the mean electron energy
in the plasma; this permits use of the concept of electron temperature. Expressi
are then derived for pulse intensity as a function of penetration into the plasma
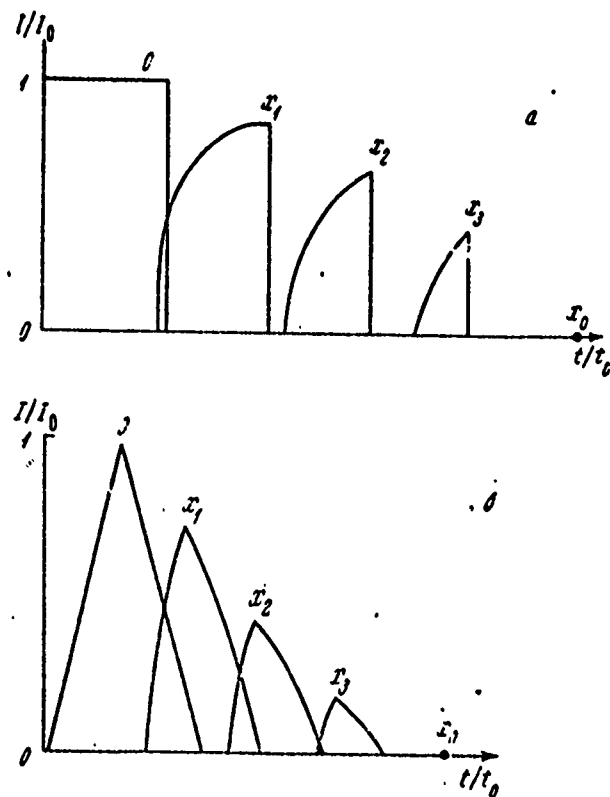and for absorption coefficient, assuming a bremsstrahlung mechanism.

Fig. 1. Variation in pulse waveform
vs. penetration into plasma.

Fig. 1 shows theoretical degradation of an initially rectangular and triangular
laser pulse vs. penetration depth. Other idealized solutions are presented,
based on typical parameters of an Nd glass laser and a hydrogen plasma.

Zaritskiy, A. R., S. D. Zakharov, P. G. Kryukov, Yu. A. Matveyets, and A. I. Fedosimov. Variation in the back-scatter radiation spectrum from laser heating of a plasma. ZhETF P, v. 15, no. 4, 1972, 184-188.

$(CH_2)_n$, $(CO_2)_n$, D_2O ice, and Al were used as targets in spectrum measurements of laser beams reflected from plasma. The emission source was a mode-locked neodymium glass laser comprising a generator and a six-stage amplifier. The spectral measurements and the plasma heating were carried out on a fundamental frequency $\lambda = 1.06\mu$ as well as the second harmonic $\lambda = 0.53\mu$. Harmonic conversion was effected at an efficiency of up to 50% by a KDP crystal. The initial oscillation spectrum was contracted to ~ 0.05 Å by inserting Fabry-Perot axial mode selectors into the resonator. The laser pulse was thereby lengthened to 1 nsec.

Spectrograms for four laser bursts on a LiD target (objective f = 4.5 cm, $\lambda = 0.53\mu$) show that a large number of equidistant lines can be seen in the light spectra reflected from the plasma. The lines generally are situated both in the Stokes and the anti-Stokes portions of the spectra. The number of lines is a function of the energy and, as a rule, the greater the burst energy the greater the number of lines. The width of each line is within the resolution limits of the equipment (0.05 A). At an output-energy level of about 5 j, spectra were recorded with variable focusing: objective f = 4.5 cm and lens f = 30 cm. In the first case line multiplication was continuous, while in the second case it was observed in about half of the bursts; this reflects the threshold character of the effect, since the focal spot diameter was one order greater for the lens.

Supplementary measurements show that the equidistant lines in the reflected-emission spectra are linked to the presence at the incident-emission line of weaker companion lines (at least one hundred times less intense). The distance between the companion lines is equal to the interval between the lines of reflected light. These lines were found to be due to the selection in the generator modes of exceptionally weak interferometer optical element parasitic reflections.

Zayko, Yu. N., L. I. Kats, N. N. Kireyev, and S. A. Smolyanskiy. Electromagnetic wave propagation in a rarefied plasma in a variable magnetic field. TVT, no. 2, 1972, 232-242.

The complex index of refraction is calculated for a single-component, spatially homogeneous infinite Lorentz plasma in a spatially uniform alternating magnetic field $\vec{H}(t) = \vec{h}_o H_o \cos \Omega t$. Stress vector orientations of stationary and alternating external fields, the magnetic fields and the electromagnetic wave are arbitrary. The alternating magnetic field $\vec{H}_1(t)$ and the induced electric field $\vec{E}_1(t)$ are regarded as strong, and $\vec{E}_2(t) << \vec{E}_1(t)$ is the weak electric field of the wave. The response of the system to the plasma electric field is analyzed for $E = \vec{E}_1(t) + \vec{E}_2(x, t)$. The average oscillation value for the alternating magnetic field is not derived. When computing the tensor of plasma electric conductivity, the authors based their calculations on the equation of electron motion in a nonrelativistic approximation.

A perturbation theory approximation method is used to solve the specific problem $\lambda = \dfrac{H_1}{H_o} << 1$. Results yielded: 1) a relationship that determines the plasma conductivity matrix by a value order (the

matrix may also be determined by approximations, disregarding perturbation theory); and 2) an explicit expression for the complex plasma refraction index; $n_m(\omega) = n'_m(\omega) + in_m''(\omega)$. The complex formulas are analyzed for five physically different cases when the vectors k, h_o and h_1 are paired perpendicularly or are parallel. Since the final formulas for the complex refraction index are too cumbersome, only those results are given that agree with $|n'_n(\omega) >> n_n''(\omega)|$.

The left-hand and right-hand wave polarizations are examined. Conditions are established under which resonances occur. The resonances are evidently a function of the alternating magnetic field amplitude, which results in additional resonance points. The signal cutoff pattern is recorded for the five cited physical cases and the two wave polarizations. Conditions are given for the occurrence of windows in some of the cases, i. e. when $n'_n(\omega) = 1$, $n''_n(\omega) = 0$. Exact formulas must be used to determine the complex refraction index. In all cases, plasma brightening becomes feasible due to the position of the magnetic field variable component.

3. Laser Interaction with Metals

Anisimov, S. I., B. I. Dmitrenko, L. V. Leskov, and V. V. Savichev. Effect of surface reflectance on evaporation of metal by intense optical flux. FiKhOM, no. 4, 1972, 10-14.

The question of conditions for optimum vaporization rate of a metal target by laser beam has been treated by several authors (cf. Komotskiy, Effects of High Power Lasers, Dec. 1971, 36; Plyatsko et al., ibid., 38). The problem is typically attacked from the point of view of finding the limit intensity parameters beyond which a transition from an evaporative to explosive regime occurs. In the present paper the authors analyze a somewhat idealized model of this problem, in which the vapor products are correlated primarily to heat reflecting properties of the metal surface. The case is limited to a one-dimensional vaporization front, and also considers only those laser pulse energies and durations for which optical absorption in the vapor products can be assumed negligible. For simplicity the optically absorptive surface layer of the metal is also neglected.

The problem thus reduces to solving a thermal conductivity equation with nonlinear boundary conditions at the moving vaporization front, given as follows for origin of coordinates moving with the vapor front:

$$\frac{\partial T}{\partial t} = a \frac{\partial^2 T}{\partial x^2} + V(t) \frac{\partial T}{\partial x}$$

$$-\varkappa \frac{\partial T}{\partial x}\bigg|_{x=0} = Aq_0 - \rho V \Delta w \tag{1}$$

$$T(x, 0) = T(\infty, t) = 0$$

where $a = \varkappa / c\rho$ is metal thermal conductivity; A = temperature absorptivity; V = velocity of the phase boundary; and Δw is enthalpy jump at vaporization; treating the vapor as an ideal gas, $\Delta w = \lambda - RT/2$ where λ = specific heat of vaporization at 0° K.

In view of the complexity of the boundary conditions, the authors resort to an approximation proposed earlier by Anisimov (TVT, no. 1, 1968, 116), which treats the problem in two stages. The initial stage is considered a transient one in which the vapor front accelerates from zero to some maximum value, carrying a layer of heated matter before it. This is followed by a stationary motion stage, in which virtually all absorbed energy is utilized in vaporization; this accounts for the bulk of the vaporization, so for the present argument the first stage is disregarded as "lost time". It is shown that this approximation is valid for temperatures well below λ/R.

Following an analysis of the "lost time" interval, the authors then derive expressions for optimum pulse flux density q_o^* and optimum pulse duration τ^* to achieve maximum vaporization in terms of the given physical parameters. The analysis also yields an expression for maximum travel of the vaporization front in terms of incident flux density; this is useful for cases in which vaporization should be kept below some tolerable maximum, e.g. in laser welding.

Arifov, U. A., M. R. Bedinov, and K. Khaydarov.
On the nature of ion generation from the effect of laser radiation on solid matter. DAN Uzb SSR, no. 7, 1971, 25-26.
(RZhF, 1/72, #1G151)

A study was made of ion generation from focused radiation of a free-running ruby laser on a solid target, and was correlated with laser energy and target type. Ion sources included targets of Ni, Mo, W, Zn and Si in a 10^{-6} torr vacuum; plasma components were registered with a cylindrical collector and a photomultiplier. For Mo, Ni and Si targets and an energy range of 0.2-1.3j, the ion current showed a spike shape similar to the laser pulse. Ion current pulses appeared at once, but were shorter than the laser pulses and appeared predominantly at pulse start. For W and Zn targets, ion generation was mainly c-w in nature. Electron current for all targets and laser energies maintained a spiked characteristic. The pulse shape of the ion current was dependent on optical and thermophysical propertie of the target, and also on the plasma generated in the beam focal region. A considerable change in power density in this region, following microcraterin of the target surface, led shortly to a drop in ion current near the end of the laser pulse.

Avotin, S. S., E. P. Krivchikova, I. I. Papirov,
P. I. Stoyev, and V. I. Tereshin. Change in
electrical resistance of beryllium from laser
radiation. ZhETF, v. 62, no. 1, 1972, 288-293.

Transient and long-term effects of laser irradiation on resistivity
of beryllium are described. Tests were run on 0.2 mm thick Be foil
strips, exposed to pulsed radiation from a GOR-100M laser (not identified)
generating 1 millisecond pulses at 40 j, focused to a 2.5 mm dia. spot
on the foil surface. Resistivity ρ was measured during and after exposure
with a constant 1 a current passed through the specimen. Variation of ρ
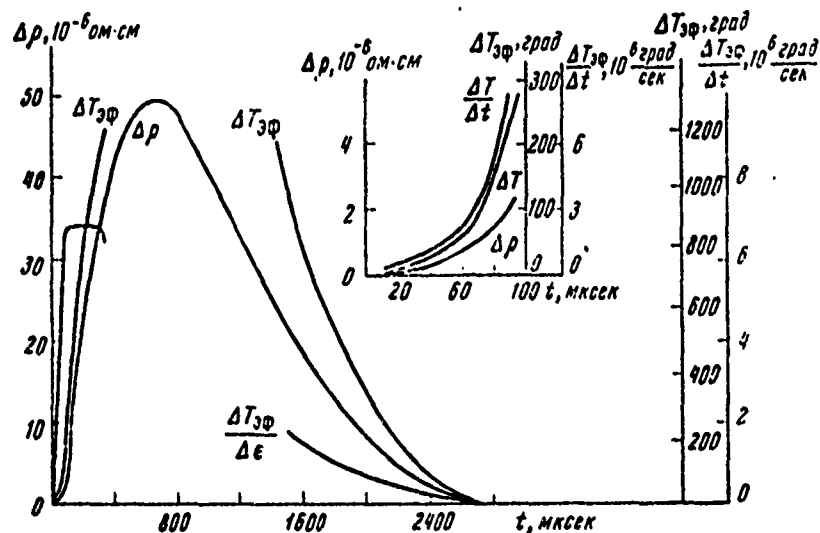during exposure is illustrated in Fig. 1, with calculated values of local

Fig. 1. Resistivity variation in laser-irradiated
beryllium.

temperature rise ΔT_{eff} also included. A detailed examination shows three
distinguishable stages in $\Delta \rho$ (t) up to the 700 μsec point, as indicated by
the curve form. In the initial stage (< 100 μs) a local heating rate of about
10^6 deg/sec was calculated to exist in the impact region. It is noteworthy
that a full anneal back to pre-exposure values of ρ occurs when the test is
done in a 300°K ambient, whereas at 77°K, ρ continues to increase for an
interval following irradiation, and after several hundred microseconds
levels off at a value some 9% above the original value. The latter effect is
ascribed to an increase in structural defect density during the high temperature
anneal.

Batanov, V. A., F. V. Bunkin, A. M. Prokhorov, and V. B. Fedorov.
Vaporization of metal targets from high-intensity optical radiation. ZhETF, v. 63, no. 2, 1972, 586-608.

In an extensive study of laser interaction with metals, theoretical and experimental data are given on metal liquid-vapor phase transition, the increased transparency wave in metals, ejection of matter and recoil impulses at the target, and laser irradiation of Bi and Pb targets. Calculations indicate that when the intensity of incident radiation exceeds some threshold value I_{thresh} the target surface temperature of a $\sim 10^{-3}$ cm thick layer will be higher than either the normal boiling temperature or melting temperature; the vaporization consequently proceeds from the liquid metal.

Evidence is shown that at a critical intensity I_{md} a "transparency wave" appears in the vapor products, at the front of which the metal vapor takes on dielectric properties. The authors then trace the behaviour of the complex dielectric permittivity of target matter when radiation intensity passes through the point I_{md}. At this moment, the coefficient of reflection R from the target drops to one fifth of its initial value, but with further increases $I > I_{md}$ the coefficient decreases more slowly (see Fig. 1).
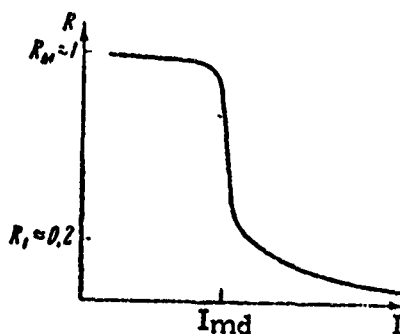

Fig. 1. Dependence of reflection coefficient R on intensity I of incident light. Decrease of R in the region $I \gg I_{md}$ follows the law $R \sim 1/I^2$.

An increase of radiation intensity above I_{md} does not increase the target surface temperature; rather the resulting energy is used in moving the front of the increased-transparency wave deeper into the target. The velocity of the increased-transparency wave D in relation to "cold" metals is computed from the laws of conservation of matter, pulse and energy. It is shown that at the initial stage of increased transparency, when the excess intensity I over the transparency threshold $I_{\mu d}$ (μ is the absorption coefficient) is low, D is linearly dependent on I.
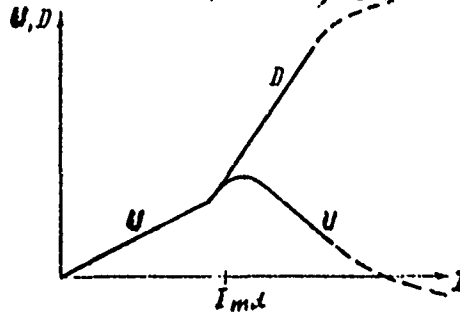

Fig. 2. Dependence of the rate
of front vaporization U and the velocity
of the increased-transparency wave D
on incident light intensity.

Dependence of the rate of vaporization of the front wave U on intensity I of incident radiation is also examined. A sharp deviation of linear dependence U(I) at the threshold point I_{md} is caused by an increase in absorptive capacity (1 - R) of the target surface. At $I = I_{md}$ the velocity of U reaches a maximum, but a further increase of I stops the vaporization front (U= 0), and immediately removes it from the "cold" metal (U<0), as seen in Fig. 2.

Ejection of matter and recoil impulses provide additional experimental data on processes at the target, as predetermined by conditions at the phase boundary. Formulas are given for specific values of the recoil pulse J and ejected mass Δm with respect to their relations to total energy E_o in the radiation pulse. Experiments were conducted with

lasers of up to 10 J at a pulse duration of $\tau = 0.8$ millisec, permitting operation on large radiation-exposed spots to achieve uniform vaporization. Tests were carried out at atmospheric pressure using Bi and Pb targets. Experimental data were obtained that verified the suggested mechanism of metal vaporization under the impact of a high-intensity laser beam. From experimental relations D/E_o, maxima were traced at the I_{md} values $\approx 3 \times 10^6$ w/cm^2 for bismuth, and $\approx 2.5 \times 10^7$ w/cm^2 for lead. The corresponding values for T_{md} were $\approx 2500^\circ$ K for Bi and $\approx 3350^\circ$ K for Pb.

Aluminum targets were also tested and it was determined that the crater shape had a strong effect on the recoil impulse. The authors present additional data on the vaporization of metal targets by high-intensity laser beams and conclude that the gas-dynamic structure of a plasma flare is time-independent; its shock wave is fixed with respect to the target, and the ambient pressure is < 1 atm. This is of particular importance for the evaluation of ejecta, since it bypasses the role of the liquid phase, in contrast to the usual method of weighing the target before and after the test.

Barmin, A. A., and A. G. Kulikovskiy.
Boundary conditions at the surface of a
discontinuity, occurring from the interaction
of powerful radiation with metal. IN: Sbornik.
Nauch. konf. In-t mekh, Mosk. universiteta,
Moskva, May 22-24, 1972. Abstracts of papers.
Moskva, 1972, 7. (RZhMekh, 9/72, no. 9B920)
(Translation).

The structure is studied of the narrow transition zone
which appears upon the interaction of powerful beamed radiation with
metal, for the case in which the incident radiation is entirely absorbed.
A complete system of boundary conditions is obtained for the surface
discontinuity which is used to model the transition zone.

Bedilov, M. R., K. Khaydarov, and Kh. Babadzhanova.
Nature of radiation defects formed on the surfaces of
solids by ruby laser radiation. IAN UzbSSR, Ser. fiz-
mat. nauk, no. 2, 1972, 66-68.

Results are described of an experimental investigation of damage
processes on the surface of solids from ruby laser radiation in a free-
running regime. Radiation energy was 1-3 joules and maximum power
density was $\sim 10^7$ watt/cm^2; the beam was focused using a f = 50 mm lens.
Targets were W, Mo, Ni, Zn, and Si, purified by laser radiation and
placed in a 10^{-6} torr vacuum. Radiation processes were studied using
microscopic and oscillographic methods, which provided data on integral
and time characteristics of target surface defects during the laser pulse
period. Integral defects formed by 800 μsec exposure were studied by
microscope. In the 0.6-2 joules energy range, growth of surface radia-
tion defects was strongly dependent on the nature of target and laser energy.
At 0.6-1.0 joules, the target structure was predominantly band-like; but
melting zones and craters did not appear. Individual 150-200 μ microcraters
were formed however on the surface due to the intensive laser pulse peaks.
With an increase of energy to 2 joules, the band structure disappeared and
macrocrater and melting zones were observed on the target. The macro-

craters were almost identical, nearly circular and their size was a function of target type, varying between 800 and 1050 μ. For W, Mo, Ni, and Zn targets, macrocraters attained 800, 1050, 950, and 1200μ respectively, at a laser energy of 2 joules. Ion current variations were recorded by an oscillograph in synchronism with the laser pulse to determine the defect formation rate, energy absorption and changes in crater structure with time. Typical oscillograms of ruby laser pulsed radiation at 0.6 and 2 joules and simultaneously obtained pulsed ion current with a tungsten target are shown in Fig. 1.
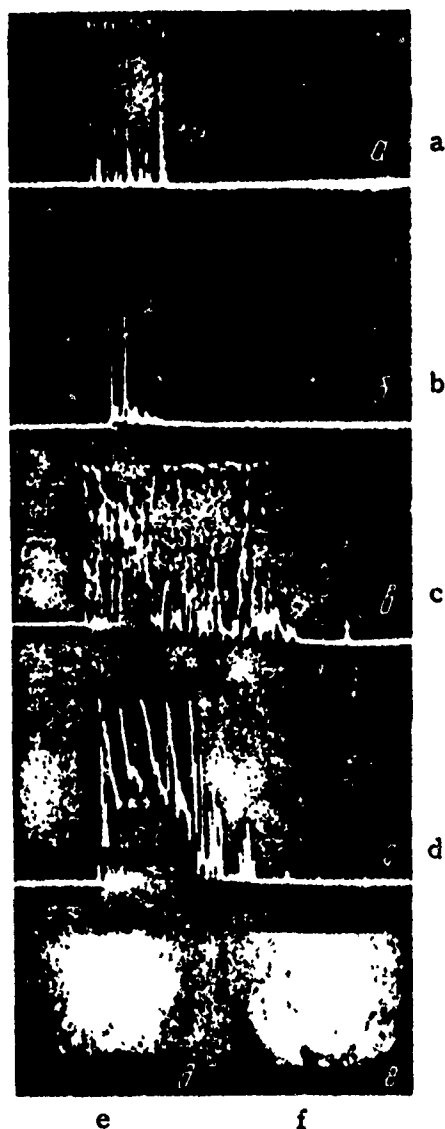

Fig. 1. Oscillograms of laser radiation at 0.6 joule (a), and 2 joules (c); ion currents of W target at 0.6 joule (b) and 2 joules (d); and defects formed on the surface of W target at 0.6 joule (e) and at 2 joules (f).

From the oscillographic results, the authors conclude that at low laser energies, ion currents assume a peaking character, are short in duration, occur after the start of the laser pulse, and are possibly connected with the formation of band structures and microcraters; at higher

energies, ion currents have a quasi-continuous character, and increase in duration and amplitude, which is related to formation of craters and melting zones.

Boyko, Yu. I., Ya. Ye. Geguzin, and A. K. Yemets. Character of deformation in the region of pulsed laser beam action on a CsI single crystal. FTT, no. 10, 1971, 3096-3097.

A brief description is given on alteration and damage effects in CsI single crystals exposed to a neodymium laser. The beam was focused within plane-parallel specimens 3 mm thick to a spot size of 200 microns; energy was 2--3j at a 500μsec pulse width, which is above the damage threshold. Depending on plane orientation to the beam, surface disfigurations of generally square or rhombic form were observed in all cases, at some distance from the destruction center. Two photos of the described figures are included. The autho suggest the effect is due to the crowdion mechanism proposed by Indenbom (ZhETF P, v. 12, 1970, 526), or at least the results would permit the crowdion mechanism, whether or not that would be a sufficient explanation. Analogous disfigurations are noted to have been recently reported in CsI under fast-acting pc loading, as described for example by Rozhanskiy et al (FTT, 1971, 411).

Kapel'yan, S. N., and A. M. Yudovin. Duration of vaporization after termination of a powerful thermal flux. DAN BSSR, no. 3, 1972, 214-216.

Theoretical expressions are developed which define post-pulse vaporization duration, as well as depth of the vaporization layer, for the case of laser irradiated metals. The work is based on heating concepts reported by Anisimov (Effects of High Power Lasers, Dec. 1971, p. 24) and uses his thermophysical model. This asserts that the thermal field at the conclusion of a rectangular pulse can be given by

$$T(x) = T_0^* \exp(-\beta x) \tag{1}$$

where $1/\beta = a/v_0$ is a characteristic dimension of the heated region, and T_0^* is the temperature at the vaporization front. Following the laser pulse the vaporization front will continue to expand until T^* drops to vaporization threshold. This interval can be found from a transcendental equation expressing vapor kinematics and target thermal parameters; the authors obtained solutions by simple iteration using a Minsk-22 computer. Results for several metals are seen in Fig. 1, showing that at a given laser flux
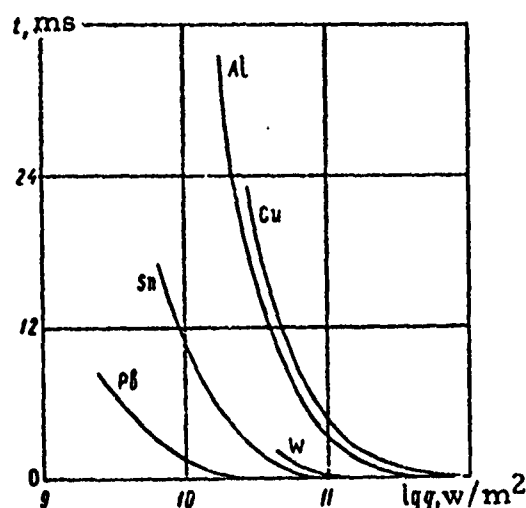

Fig. 1. Post-pulse vaporization duration
vs. laser intensity

the longest post-vaporization will occur in Cu and Al, and the shortest in Pb. The sharp decrease in post-pulse vaporization with rise in pulse intensity is shown to be consistent with the thermal storage mechanisms in the impact region.

Mirkin, L. I. Dynamic deformation of low-carbon steel from the effect of a laser beam. IN: Sbornik. Vysokoskorostnaya deformatsiya. Moskva, Izd-vo Nauka, 1971, 109-112. (RZhMekh, 3/72, #3V1469)

Structural effects are studied in low-carbon steel exposed in vacuums to focused laser pulses in the 1 millisecond range, at energies up to 35 j. The amount and distribution of resultant twinning was measured. A physical model of the beam action is postulated to explain the simultaneous presence of a thermal and mechanical interaction zone.

Orekhov, M. V., and B. S. Slavin. On the nature
of material ejection from the action of laser radiation
on materials with varying thermophysical properties.
ZhPS, v. 16, no. 1, 1972, 153-155.

A comparative beam-target study on ejecta behavior is reported for two target materials of widely differing thermal conductivities. A ruby laser was used developing 10j pulses of 1 millisec duration, and focused at f = 75 mm on steel and ferrite targets at a density of approximately 10^7 w/cm^2. A portion of the beam was split off to drive a high-speed scope, so that an extended view of laser pulses and the corresponding target flares could be seen. This display showed a cyclic nature in flare amplitude for the steel target, not evident in the ferrite target. The difference in behavior is linked by the authors to the substantially greater thermal conductivity of steel, as a result of which a portion of the crater walls melts during repeated pulse action and provides a periodic shielding effect to the incoming pulse. For ferrite, with several orders lower conductivity, the beam effect remains relatively localized and no periodic variation occurs. This is shown in the cross-sections of laser craters in the two specimens in Fig. 1, where evidence

Fig. 1. Crater generation from free-running
ruby laser impact on ferrite (a) and steel (b),
X60.

of melt and run-down is seen for the steel target, while the ferrite crater is comparatively clean.

Osadin, B. A., and G. I. Shapovalov. <u>Pulsed</u>
<u>vaporization in a vacuum.</u> TVT, no. 2, 1972,
361-367.

Works on the effects of laser radiation on substances in a conden
state by Anisimov, et al. (Nauka, 1970) and Afanas'yev and Krokhin (IN:
Trudy FIAN, v. 52, 1970, 118), which considered evaporation under the
influence of high-intensity heat fluxes, have as a rule examined the quasi-steady
stage of the process, characterized by a constant velocity of the evaporation
w ave moving into the substance. The present paper deals with the non-steady
stage of the process at moderate heat fluxes ($Q = 10^5 - 10^8$ w/cm^2) which,
besides lasers, can also be created by electron beams in an electric discharge.

A computer-aided solution of the equation of thermal
conductivity was obtained for aluminum, copper, and titanium. Consideration
was given to evaporation from the surface into a vacuum at heat fluxes of
$10^5 - 10^8$ w/cm^2 to the surface. The time relationships of the process of pulsed
evaporation in a vacuum are discussed, as well as the application of the
obtained solution.

Plyatsko, G. V., M. I. Moysa, and L. P. Karasev.
<u>Using a laser to eliminate residual weld stresses.</u>
F-KhMM, no. 6, 1971, 87-89.

Laser heating of a butt weld to relieve residual stress is briefly
described. The test specimens were type VT-14 steel cylinders of 300 mm
ID and 3 mm wall thickness, welded by argon arc at a rate of 12 m/hr.
Following the weld operation a 10 mm long section of the weld external surface
was subjected to laser irradiation sufficiently intense to cause a slight surface
melting, but no metal ejection (no other data on laser parameters are given).
After laser exposure, strain gage data showed the impact area to have returned
to a nearly unstressed state, from post-weld stress levels as high as 18 kg/mm
The effect is attributed to two factors: generation of thermoelastic waves
which permit dynamic relaxation of stress, and the creation of a surface layer
whose physical properties differ from those of the base material. Further
study of the technique is planned to clarify the relief mechanism.

Petukhova, T. M., V. V. Bukhalenkov, and V. I. Grokhovskiy. Metal surface condition after laser irradiation. EOM, no. 4, 1972, 28-31.

An analysis is given of physical and chemical changes in the surface of several iron and steel targets following laser irradiation. The laser used was a type K-3M free-running ruby with 3 millisec., 1.5 j pulses, and focused on the target surface at f = 10 mm. A wide range of crater geometries was obtained by profilometer, as listed in Table I.

Table I. Crater Characteristics

Structure type	Material and heat treatment	Crater dia., mm	Crater depth, mm	Max. ejecta ridge hgt., mm	Ejecta range, mm
Perlite	U 12 steel, heated to 850°C, oven-cooled	0.40	0.030	0.060	0.65
	Iron with globular graphite, heated to 890°C, air-cooled	0.30	0.030	0.035	0.75
	Ductile iron, heated to 870°C, air cooled	0.30	0.035	0.040	0.75
Austenite	1X18N8 steel, heated to 1100°C, water quenched	0.30	0.010	0.010	0.40
Martensite	U 12 steel, heated to 850°C, water quenched	0.40	0.030	0.080	0.70
	Iron with globular graphite, heated to 890°C, oil quenched	0.45	0.030	0.040	0.80

Similarities and differences in the crater profiles are
discussed; Fig. 1 compares ejecta profiles for austenite and martensite
types. Laser hardening effects were also recorded; it was noted that
ejecta peaks give   anomalously high hardness readings, whereas the
base material in some cases suffers a loss in hardness after irradiation.
Strain hardening patterns are illustrated, together with data on
exoelectron emission variations which can be used to detect phase change
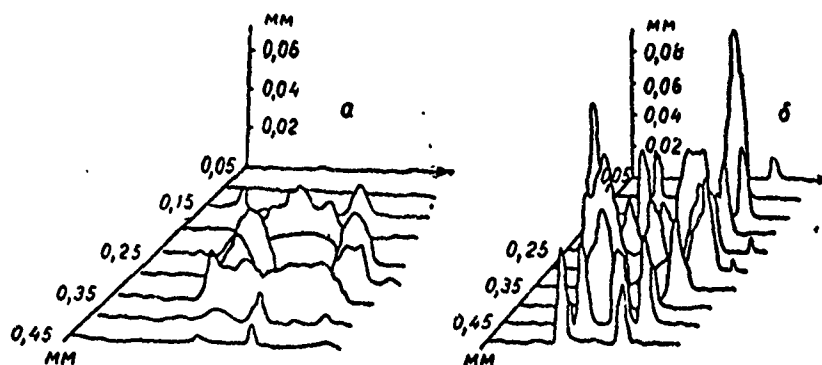in the target material.

Fig. 1. Relief profiles in the crater
region for austenite (a) and martensite
(b) targets. Vertical - x 1000, horizontal-
x 200.

This is a continuation of an earlier study by the authors on characteristic
of condensed ejecta from laser impact with metals (Effects of Strong Explosions,
no. 2, 1971, 38). The same laser parameters were used, i.e. a free-running typ
GSI-1 generating 1 μ sec, 7 j pulses, and using a focal distance of 200 mm. In
the present tests a transparent rotating disk was interposed between the beam
source and target face, so that a time pattern of condensate products was obtained
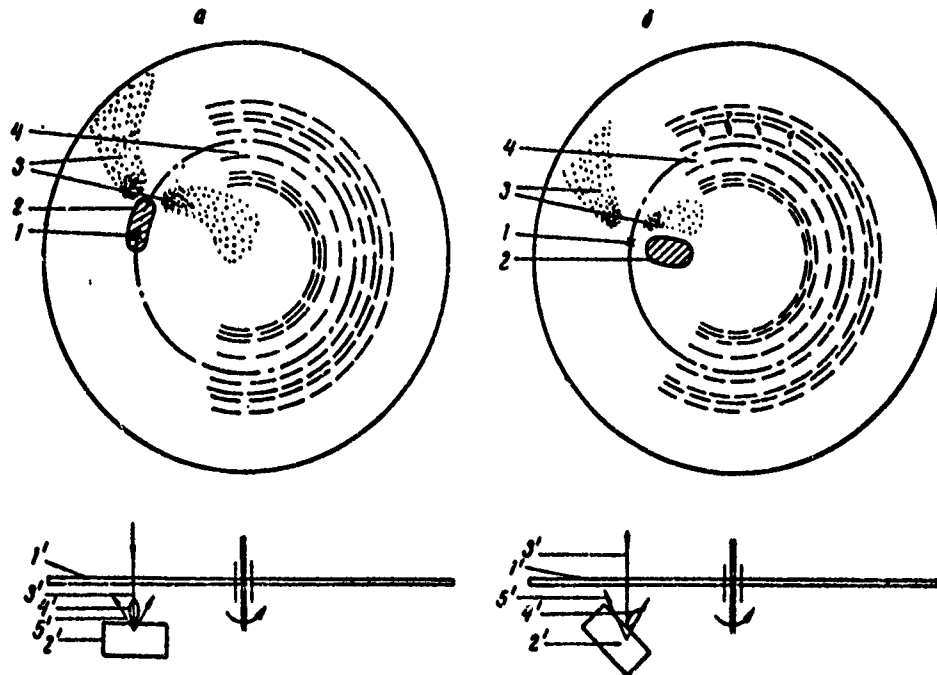

Fig. 1. Condensate distribution, lead target
a - normal, b - 45° beam angle. 1 - beam impact
point; 2 - condensed vapor; 3 - particle rays;
4 - large particle bands. Disk speed = 3,000 rpm;
distance between target and disk = 12 mm.

Fig. 1 shows two examples of condensate distribution for normal and inclined bear
angle, using a lead target. Three discrete types of condensed forms can be
distinguished with preferential positioning, depending on beam angle. Flare photo
are also given for an iron target (Fig. 2), which show that the flare axis will
deflect during flare development to line up with incident beam direction, for the
case of an inclined beam. Data show that the limit velocity of ejecta was about
100 m/sec. The technique is useful in identifying type and pattern of ejected
material during the course of a laser pulse. The results indicate that pulse width
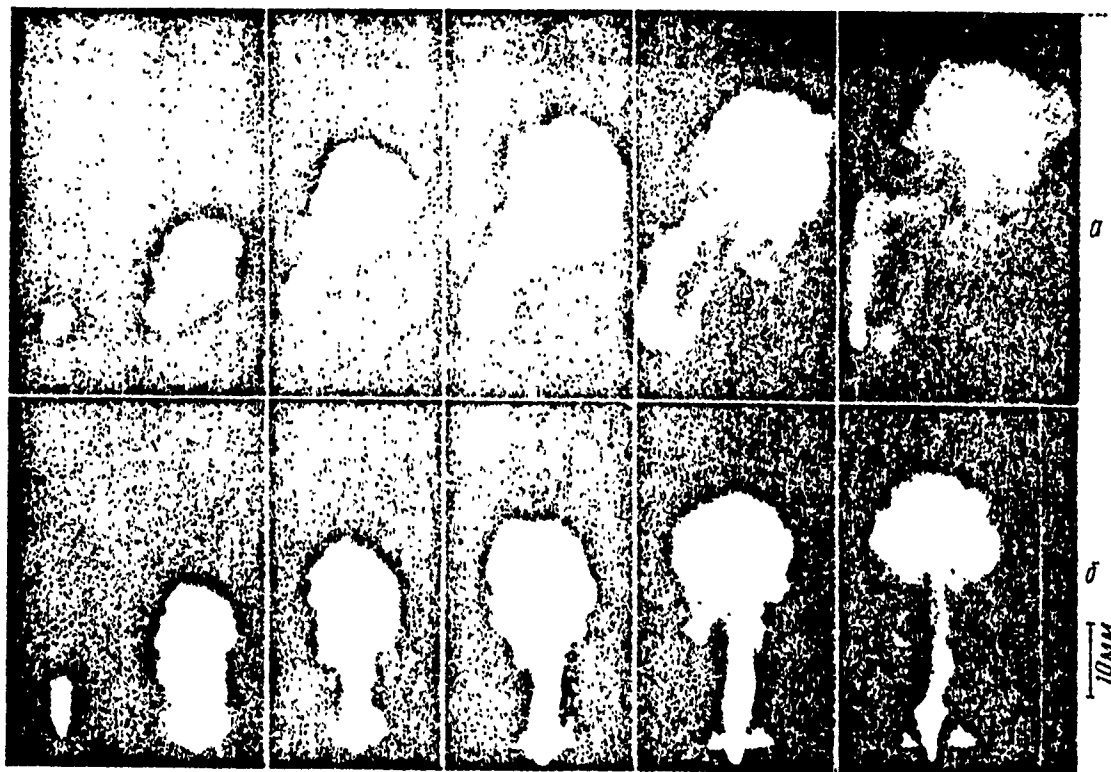need not exceed 200 μ sec, since most of the vaporization occurs well before this
time.

Fig. 2. Flare development, iron target.
a - 45° beam angle; b - normal. 64μsec
between frames.

Siller, G., E. Buchelt, and H. B. Schilling. <u>Properties
of an electron source with laser-induced electron emission.</u>
IPP-Berlin, 1971, 25 p. (RZhF, 1/72, #1A386)

A pulsed electron source with currents on the order of several hundred
amperes and a 10^{-8} sec duration is described for a ring accelerator. A
principle requirement was to obtain a beam with minimal emittance. To achiev
this, a focused laser beam on a metallic cathode is used as an emitter, with
a working area of 10^{-4} -- 10^{-2} cm^2. Data are given on measurements of
emittance and energy distribution of electrons in the emitted pulse.

Uglov, A. A., A. A. Zhukov, A. N. Kokora, M. A. Krishtal, and M. Kh. Shorshorov. "Shift" of critical points under laser heating of carbon-iron alloys. FiKhOM, no. 2, 1972, 3-8.

The "shift" of critical points in steel heated by a laser beam is analyzed. Allowance is made for nonuniform distribution of specific heat flux on the metal surface, and hence different volumetric heating rates. Under conditions of rapid heating and cooling rates, as in metal treatment by a laser beam, "shift" of critical points becomes important in micrographic determination of temperature within the metal after cutoff of the laser pulse. Using a theoretical formula, numerical data were obtained for heating rates $dt/d\tau$ in ShKh15 perlitic steel at various depths z and distances r from the center of a beam spot on the metal surface. Concentration coefficient $k = 80$ cm^{-2} was used in calculations of power density distribution on the surface. The calculated $dt/d\tau$ versus r plots (Fig. 1) show that, at $q_o = 0.92 \times 10^5$ w/cm^2, $dt/d\tau =$
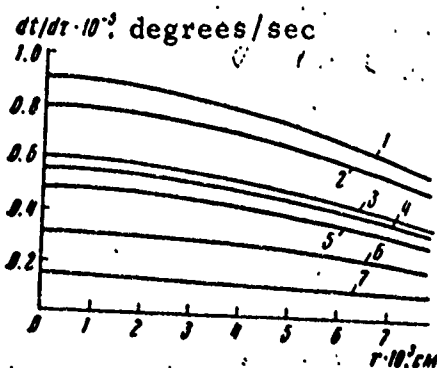

Fig. 1. Heating rate of ShKh15 steel by laser pulses of 0.5 millisec width versus r at z(cm) = 3.10^{-3} (1), 2.10^{-3} (2), 1.10^{-3} (3), 5.10^{-3} (4), 0 (5), 6.10^{-3} (6), and 7.10^{-3} (7).

10^5 degrees/sec, and that dt/dτ can vary by a factor of five in the region where temperature may exceed the perlite-to-austenite transformation point (A_1). At the cited dt/dτ , the shift t_x of point A_1 for ShKh15 steel was calculated to be ~ 200° C from

$$t_x = \left(\frac{k_1^2 x^2}{4D}\right)^{1/2} \cdot v^{1/2}$$

where k_1 = 110 degrees is the angular coefficient determined from the Fe-Fe$_3$C phase diagram; $\nu = 0.5 \times 10^5$ deg/sec is the heating rate in the critical temperature range, and $\bar{D}$ is the coefficient of carbon diffusion in austenite. The maximum Tx variation due to difference in v within the metal was 1.7. It was concluded that steel of a complex composition is not suitable for a study of temperature fields under conditions of a very rapid heating. In view of this conclusion, a micrographic study was made of type 45 and U8 hypoeutectoid carbon steels in a surface area casehardened by laser radiation. The micrographs show that the temperature range of A_1 transformation is enlarged up to the liquidus, and the A_3 transition point practically disappears with the ferrite lattice coexisting with melted austenite. A sample result of U8 steel exposure is shown in Fig. 2.
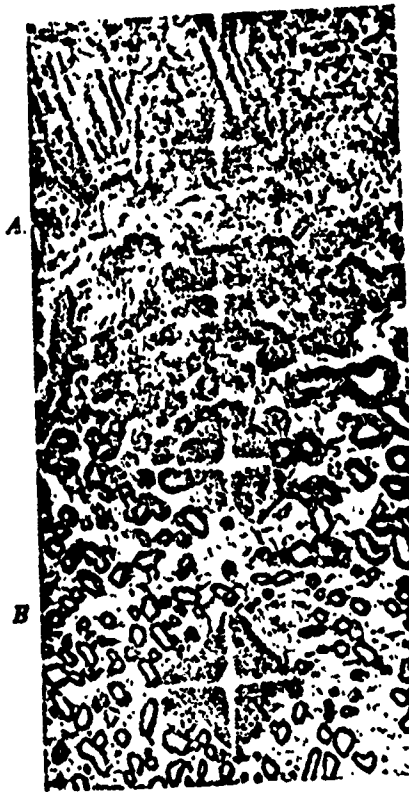
Fig. 2. Microstructure of type V8 steel with a perlite
structure in the laser heating zone. A- fusion
boundary; B- limit of thermally affected zone.
(X 1300)

4. Laser Interaction with Dielectrics

Anan'in, O. B., Yu. A. Bykovskiy, M. Ya. Minakov, and A. N. Petrovskiy. Self-focusing of ultrashort pulses in transparent media. FTT, no. 11, 1971, 3465-3467.

A comparison of self-focus damage in several dielectrics is briefly given. Filamentary damage tracks were observed in specimens of R-8 glass, quartz, $LiNbO_3$ and KDP, from self-focus effects of picosecond pulses from an Nd glass laser. The laser operated in a mode-locked regime, generating trains of 8-10 picosecond spikes with 10 ns spacing, and pulse power of 1.5×10^9 w. The beam was focused within the target specimens at f = 8cm. Significant differences in damage mechanism are pointed out, e.g. in quartz, $LiNbO_3$ and K-8 glass, filaments appeared directly at threshold, whereas in KDP damage at threshold was initially in discrete point form, becoming filamentary only at intensities well above threshold. The results suggest the usefulness of repeating the tests with a single spike, rather than a series, for better identification of the filament formation process.

Anoshin, A. N., G. M. Zverev, Ye. A. Levchuk, and V. A. Pashkov. Study of the surface resistance of nonlinear crystals to laser radiation. Sixth All-Union Conference on Nonlinear Optics, Minsk, July 1972 (Preprint).

This is apparently a rework of the paper already reported by Zverev et al on anomalous damage effects to lithium niobate and lithium tantalate (October 1972 report, p. 1), and includes octahedral specimens of $Ba_2Nb_5O_2$ as a target specimen. The findings are essentially those of the cited earlier paper.

A set of experiments is described on interaction of powerful
laser radiation with type K-8 glass, with the object of determining the
criteria for shock wave generation at the focal point. A Q-switched ruby
was used generating 50 Mw pulses, focused to a 0.2 mm spot both internally
and on the glass surface. A holographic plus high-speed framing method
was used to determine wave propagation velocity. Results confirmed that
the transition from a longitudinal sonic wave to a shock wave generally
occurred near the damage threshold. Wave velocity was observed to be a
function of pulse intensity, as well as of delay time in pulse.application,
as seen in Fig. 1. In theory the sonic wave converts to a shock wave when
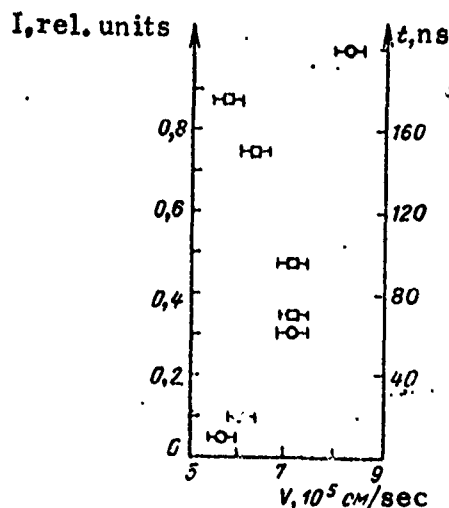
Fig. 1. Wave velocity vs. delay (squares)
and laser pulse intensity (circles).

pressure p in the focal region attains a value of $\rho_o C_o^2$, where ρ_o is glass
density and C_o is the sonic velocity in the glass. A sample calculation based
on actual parameters was made on this assumption, showing that shock
wave velocity should be 1.3 times sonic; this agreed closely with measured
results. With the beam focused on the surface a dual spherical wave was
typically generated, as shown in Fig. 2. Their characteristics were essentially
the same as for the internally focused pulse.

Fig. 2. Dual wave generation from
surface irradiation.

Basov, N. G., O. N. Krokhin, N. V. Morachevskiy,
and G. V. Sklizkov. Internal and surface effect of laser
radiation on optical glass. ZhPMTF, no. 6, 1971, 44-49.

The authors describe an experiment with laser irradiation of glass at
energy levels both below and above damage threshold. It is noted that transparer
dielectrics generally are an interesting subject for laser effects since they displa
a wide range of damage characteristics depending on material quality and inciden
energy parameters. The test was done by a high-speed interferometry method,
using a free-running neodymium laser as the active beam and a ruby laser in the
giant pulse mode for illumination of the impact region; the method was similar
to one reported earlier by Basov et al (Effects of High Power Lasers, Dec. 1971
80). At an Nd laser level of 100 j and 1 millisecond pulses, a series of interfero
grams were made of the glass, showing growth of inhomogeneities in the target
region at intervals up to 800 μ sec following pulse termination. The results show
no time correlation of inhomogeneity development with laser pulse parameters,
hence the alteration is concluded to be an integral effect. The most probable
mechanism for this is concluded to be the accumulation of thermoelastic stresses
from continuous absorption of the laser energy. Basov includes theoretical and
experimental data to support this hypothesis. Tests were also made with beam
energy increased by 10 to 15%, which exceeded the damage threshold of the glass
interferograms of the resulting flare are presented.

Belobrovik, V. I., G. I. Borovkov, L. V.
Volod'ko, V. S. Sokov, B. I. Taurotinskiy,
A. P. Khapalyuk, and A. V. Chaley. Thermal
self-focusing of laser radiation in plexiglas and
polystyrene. The Sixth All-Union Conference
on Nonlinear Optics. Minsk, July 1972 (Preprint).

The phenomenon of self-focusing of powerful neodymium laser
radiation in plexiglass and polystyrene was studied under a free-running regim
Laser pulse energy was 200 joules, duration of a single pulse was 2 μsec;
burst duration was 600 μsec, with a nominal interval between pulses of
5 μsec. The length of damage filaments, the threshold of their onset,
their relation to radiation energy, and the size of the focal region, were all
analyzed, together with the form of the pulse transmitted through the
specimen. A ruby laser pulse of 1 joule and 5 microsecond was used to
determine the dependence of the damage type on laser radiation polarization.
It was observed that damage was localized in the plane normal to the E-field
plane laser radiation. A thermal mechanism is believed to be responsible
for the cited phenomena.

Belozerov, S. A., G. M. Zverev, V. S.
Naumov, and V. A. Pashkov. Self-focusing
of ultrashort laser pulses in solid dielectrics.
The Sixth All-Union Conference on Nonlinear
Optics. Minsk, July 1972 (Preprint).

Characteristics of filamentary damage from laser-irradiated
glass, fused quartz, crystalline quartz and leucosapphire are reported.
Damage was induced by self-focusing of a single ultrashort pulse as well
as a series of ultrashort laser pulses at λ = 1.06 μ and 0.53 μ. Under

the impact of ultrashort pulse sequences, filaments were formed in all tested materials, in which local recurrent damages were detected. When irradiated with a single ultrashort pulse, no local damage was observed. It was proven experimentally that the presence of local damage in self-focusing filaments is caused by independent effects of single ultrashort pulses in a burst. Threshold power densities for the formation of self-focusing filaments are given for glass, quartz and leucosapphire; estimates of critical values of self-focusing and n_2 values are also given.

Belozerov, S. A., G. M. Zverev, V. S. Naumov, and V. S. Pashkov. <u>Destruction of transparent dielectrics by radiation from a mode-locked laser.</u> ZhETF, v. 62, no. 1, 1972, 294-299.

A comparative test was made on damage thresholds in various dielectrics from pulsed laser radiation. The main purpose was to illustrate the difference in effect of single pulse (10 ns) and a train of short pulses (30 x 4 ns) from a mode-locked Nd laser on dielectric breakdown. The test materials included type K-8 glass, fused and crystal quartz, leucosapphii and ruby with and without color centers. The test conditions and findings generally duplicate those of Orlov et al (<u>Effects of High Power Lasers</u>, Dec. 1971, p. 49), who also advised on the present experiment. A typical filamentary breakdown in the short-pulse regime indicated self-focusing, evidently not thermal, which was not apparent in the monopulse regime. The tests verify that while energy densities for threshold are of the same order of magnitude for all dielectrics tested, the power density threshold for the short-pulse mode is typically several orders higher than for the 10 ns monopulse, and was found to go as high as 10^{14} w/cm^2. This suggests a thermal relief mechanism operating between pulses in the pulse train case. Photos are also included comparing filament appearance of the ruby with color centers to that in the remaining specimens.

Butenin, A. V., and B. Ya. Kogan. The mechanism of
optical breakdown in transparent dielectrics. IN: Sb. Kvantovaya
elektronika. Moskva, Izd-vo Sovetskoye radio, no. 5,
1971, 143-144.

A test is described which demonstrated the strong effect of air
particle content on the optical breakdown level of transparent dielectrics.
It is shown that in particles in the 0.1-0.3 micron range, which attain $10^5/cm^3$
concentrations in urban areas, can sharply lower threshold even at pulse
energies on the order of 1j. Tests were run on thresholds of heptane, ethanol
and methylmethacrylate, using a Q-switched ruby at maximum energies of
0.8j, focused at 4 cm. An elaborate dual-chamber system with heating and
filtering was used to obtain progressively purer liquid samples, while breakdown
level was continuously recorded. Fig. 1 shows relative rise in threshold for
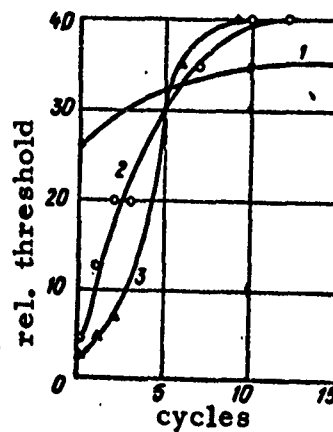

Fig. 1. Breakdown threshold vs.
cleaning cycles. 1 - heptane; 2 - ethanol;
3 - methylmethacrylate

the three specimens as a function of the number of cleaning cycles. In addition
the clean ethanol sample was re-exposed to ambient air, after which it reverted
to its original low threshold. The evidence points to the limiting effect of
particle inclusions in active laser elements.

Danileyko, Yu. K., A. A. Manenkov, V. S. Nechitaylo, A. M. Prokhorov, and V. Ya. Khaimov-Mal'kov. Role of absorbing inclusions in the destruction of transparent dielectrics by laser radiation. ZhETF, v. 63, no. 3, 1972, 1031-1035.

A theory is presented on the process of thermal destruction of transparent dielectrics, accounting for nonlinearities of the absorbing inclusions as well as the surrounding matrix. The theory attempts to prove that the destruction is clearly of a threshold nature and is always accompanied by high-temperature radiation spark similar to laser break-down in gases.

An equation of thermal conductivity is used to describe the laser heating of an absorbing spherical particle of radius a and its surrounding medium. For temperature nonlinearities of the value $Q(I, T)$, representing the thermal source power, various laws and approximations may be used based on the radiation absorption mechanism or the temperature interval. The authors selected an experimental temperature dependence for the $Q(I, T)$ value, and an inversely proportional dependence for the thermal conductivity $K(T)$ value. Two solutions for the thermal conductivity equation were analyzed as a function of the laser pulse duration. For long pulses when $t \gtrsim \tau_x = T_o C_1 \rho_1 a^2 / \alpha_1$, (where T_o is the initial specimen temperature; and C_1, ρ_1, α_1 are the specific heat, density and the constant of the particle matter, respectively), the solution of the thermal conductivity equation is given in the form of an implicit integral relationship between t_{thresh} and Q_{thresh}. The t threshold value denotes the time preceding the moment when the temperature in the center of an inclusion begins to rise rapidly, similar to an avalanching and equivalent to the onset of destruction. The other threshold value, Q, is the threshold capacity of destruction. The analysis indicates that the destruction process is of a thermal explosion nature. The maximum

attainable temperature in the absorbing inclusion is not pertinent in determinations of destruction thresholds. The latter temperature value governs the magnitude of maximum stresses in the surrounding matrix; and consequently, also the nature, scope and the dynamics of destructions in the matrix. For short laser pulses when $\tau \ll \tau_x$, it is concluded that it is not necessary to determine the critical temperature in order to estimate the Q_{thresh} for medium-size nonlinearity parameters.

The theory developed in the article proves that the threshold of destruction strongly depends on the size of inclusions, the thermal and optical constants, and the temperature nonlinearity. Numerical estimates are given for the threshold destruction of glass with $2a = 10^{-5}$ cm platinum inclusions from a laser pulse of $\tau = 3 \times 10^{-8}$ sec, yielding an I_{thresh} of $\cong$ 8×10^7 watt/cm^2. For ruby crystals with $2a = 3 \times 10^{-6}$ cm nickel particle inclusions and pulse duration $\tau = 3 \times 10^{-8}$ sec, with $\tau \gg \tau_x$, $Q_{thresh} \cong 2 \times 10^{14}$ watt/cm^2 and $I_{thresh} \cong 7 \times 10^9$ watt/cm^2 values are obtained.

Frolov, V. V. Temperature fields in multi-layer translucent coatings under conditions of pulsed radiation heating. I-FZh, v. 22, no. 4, 1972, 755-756. (Annotation of deposited paper.)

A summary is given of an analysis of heat transfer in a multi-layer coating system under beamed irradiation. The problem is treated as nonstationary and one-dimensional, with distribution of absorption taken into account. Reflection and concentrated absorption at layer interfaces are treated; the absorption process is considered to be linear.

As an example the temperature distribution is calculated in a two-layer heat shield in which the heat load is assumed to be applied in triangular pulses of a given energy, at durations ranging from 10 to 60 seconds. Owing to changing boundary conditions, it is shown that the system must be solved as a class of piecewise-discontinuous functions. On this basis graphical solutions are obtained showing the time characteristic of heat absorption as a function of absorption coefficient and pulse duration. Instantaneous temperature distributions are also presented for the cases of absolutely opaque as well as semitransparent coating systems.

The analysis shows that failure to account properly for internal heat absorption can lead to significant errors in theoretical temperature fields and level of total absorption; furthermore, the error increases with reduction in pulse width.

Garber, R. I., Ye. I. Stepina, and A. A. Stepanov. Features of the destruction of calcite crystals by laser radiation. FTT, no. 1, 1972, 243-245.

An experiment is briefly summarized which was designed to examine laser damage characteristics of a transparent dielectric, for the case where the dielectric has a relatively low absorption coefficient at the irradiation wavelength. This was done with calcite specimens, which have a coefficient on the order of 10^{-4} -- 10^{-5}, using both ruby and neodymium lasers. A variety of energy and power densities were used with the beam focused at the target surface as well as internally; a high dependence of threshold and damage type on orientation of the crystal axis was found. Crack patterns and cratering geometries are discussed also as functions of impact beam polarity. Damage effects were evident only at the higher power density ruby exposure up to 10^{10} w/cm^2; the Nd laser, although at a higher pulse energy, did not attain threshold, which emphasizes power density as the main destructive facto It is also noted that the damaging power levels were several orders less than the predictable levels for nonlinear effects that typically cause damage; hence in the present case a thermal explosion mechanism is indicated. Crater and defect photos are included.

Geguzin, Ya. Ye., A. K. Yemets, and Yu. I. Boyko.
Lowered optical strength of transparent solids with macro-
scopic defects. FTT, no. 5, 1972, 1565-1566.

An experiment is briefly described which attempted to correlate
the degree of porosity in glass with its optical strength σ in laser
applications. The case considered assumes that the characteristic
linear dimension of the pore is greater than laser wavelength λ ;
in such cases for glass or ionic crystals, as much as 70% of light
incident on the pore may be reflected, resulting in interference with
the transmitted beam and generation of thermal damage centers.
Tests to show this effect were done with a silicate glass containing a
dispersed powder, sintered to form a porous medium with pore
size $\approx$ 5 microns and a mean pore spacing of 30 microns.
The porous glass was exposed to a He - Ne laser beam at $1.06\,\mu$
and a 50 msec pulse width, together with a non-porous glass.
Results show that for the latter, σ was 6×10^{14} erg/cm$^2 \cdot$ sec,
dropping to 2.5×10^{14} erg/cm$^2 \cdot$ sec for the porous specimen.
The relation of the pore structure to color centers is noted as having
a definitive effect on the optical strength characteristics. In another
step of the test the porous medium was modelled on a larger scale
by using spherical quartz glass beads, suspended in a medium with a
higher refractive index than the beads. No other data are given for
this portion; however, Fig. 1 shows the medium, and an interference
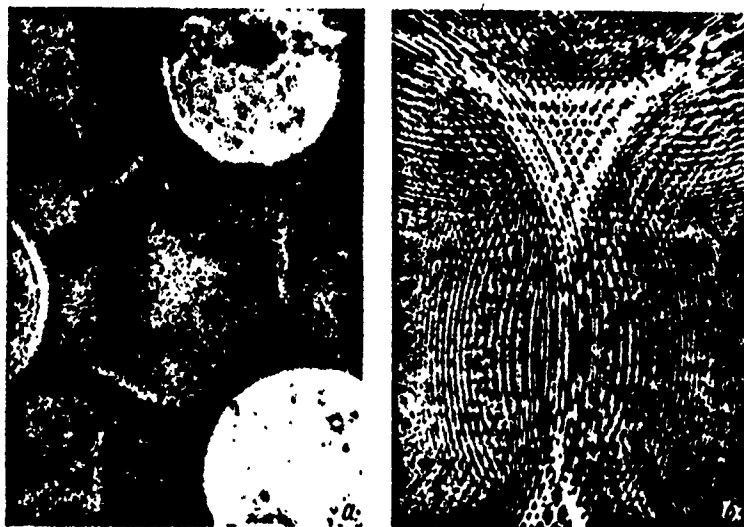pattern obtained also at $\lambda = 0.63\mu$. The results with the

Fig. 1. "Pore" model, and interference
pattern parallel to equatorial plane. X240.

model were effectively identical to those with the original sintered
glass.

Khazov, L. D. Effect of a powerful optical field on
transparent dielectrics. IN: Trudy Gosudarstvennogo
opticheskogo instituta, v. 41, no. 172, 1971, 22-29.
(RZhF, 6/72, no. 6D1230)

A review is given of basic experimental results and qualitative
concepts on the interaction of powerful single-pulsed optical radiation
with transparent dielectrics. Particular emphasis is given to surface
destruction. The experimental results are explained on the basis of
an intense internal photoeffect, generated at the dielectric surface by the
high density of local surface electron states. It is proposed that the sur-
face strength of transparent dielectrics could be increased by reducing the
density of surface defects.

-74-

Kuznetsov, A. Ye., A. A. Orlov, and
P. I. Ulyakov. Pulsed regime for
vaporizing optical materials by CO_2
laser radiation. IN: Sbornik.
Kvantovaya elektronika, Moskva.
no. 7, 1972, 57-60.

An analysis is given of experimental results on the
interaction of CO_2 laser radiation (λ = 10.6μ; constant power density =
(0.5-2) 10^4w/cm^2) with a series of optical materials, as reported by
Bubyakin et al (FIAN, 1969, 34p), where a shielding effect in the evaporation
process of the substance and cavity formation were noted. Time characteris-
tics of cavity depth ℓ_k and the length of the luminous part of the flare ℓ_f
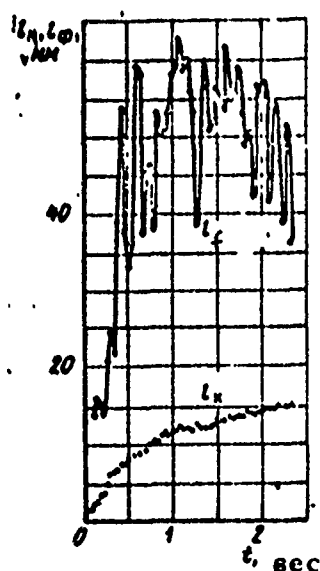for KV quartz glass are plotted in Fig. 1. The evaporation displays a clearly

Fig. 1. Relationship of cavity
depth ℓ_k and flare length ℓ_f to
irradiation time for quartz glass
(q = 1.9x10^{14}/cm^2)

pulsating character with an irregular oscillating frequency of 5-10 Hz.
Average deepening rates in the pulsating period and in steady-state
evaporation are tabulated for various materials. This qualitative
characteristic was observed in all experiments, with quartz as well
as with other optical materials. The only variation was in the
pulsation amplitude and the steady-state regime discharge time. Two

main processes, namely gaseous phase dispersion and emission shielding lead to the pulsating nature of cavity formation. The pulsation damping of LK-5, K-8 and other glass types occurred more rapidly than with quartz glass. A steady self-adjusting evaporation regime was observed through to the complete piercing of a 60 mm thick quartz specimen, and with splitting of other materials. The pulsating nature of the process up to the self-adjusting regime is apparently common to all substances. The damage products of these substances also exhibit absorptivity at the active irradiation frequency. The authors conclude by giving a system of approximate equations for the dynamic low-temperature evaporation of dielectrics, taking vapor absorption into account.

Kuznetsov, A. Ya., I. S. Varnasheva,
A. A. Poplavskiy, and G. P. Tikhomirov.
Destruction of reflective dielectric coatings
by laser radiation. OMP, no. 3, 1972, 39-42.

The resistance of reflective coatings to laser radiation was studied using zinc sulfide and magnesium fluoride coatings. The coatings were applied by thermal evaporation in a vacuum, and the reflection factor was $R = 90\%$ at $\lambda = 0.7\,\mu$. The flux falling upon the specimen was controlled by glass filters at a constant radiation energy of a single-pulse multimode ruby laser, with a ≈ 40 nsec pulse duration. The purpose was to find the number of bursts the coating would endure at various energy-density values below the limit value, i.e., to find the threshold of destruction for multiple radiation effects. The reference threshold of destruction was the number of bursts n at which the mirror transmissibility increased by 30%. The energy density limit (threshold of destruction) at which the coating was destroyed with one burst was also measured. The reference density criterion in this case was the appearance of plasma, recorded photoelectrically or visually.
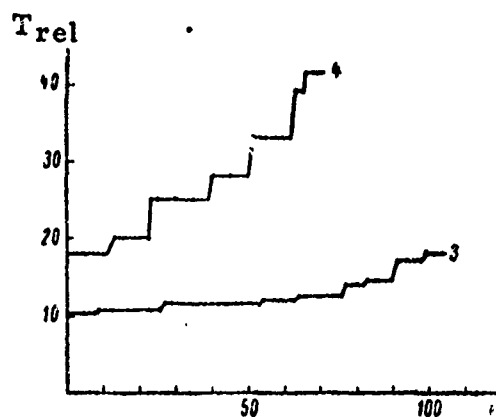
Fig. 1. Transmissibility variation
in relative units for multiple radiation
effects on two coatings.

Experimental relationships for the threshold enerɡy density W, at
which destruction begins at the n-th burst as a function of the number
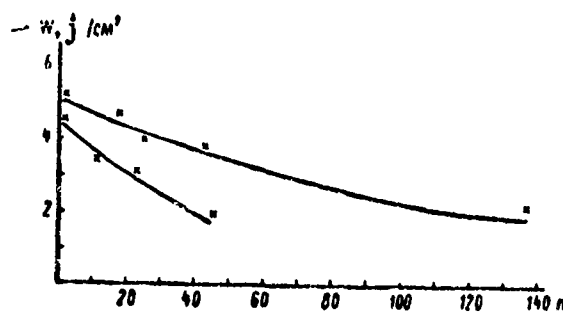of exposures n, are presented in Fig. 2.

Fig. 2. Threshold characteristic, x- experimental
values up to n = 140

The values in Fig. 2 are approximated by a function of the type

$$W_n = W_1 \times e^{-\beta (n-1)},$$

where W_1 is the threshold of destruction for one burst, W_n is the threshold
of destruction for n bursts, and n is the number of bursts. The coefficient
β for coatings produced ₋y the same technique is 0.0030-0.0160. This
ratio is an approximate one since it was determined for n = 140; however,
it can be seen from (1) that the relationship of the destruction threshold
to the number of bursts is cumulative. Although the coating properties
for β were not determined, this value is always higher for coatings with

-77-

a one-burst lower destruction threshold. Coating transmissibility increases substantially with a burst increase prior to the appearance of plasma (Fig. 1), although coating destruction is not observed visually. Electron-microscope observations show that, prior to the plasma appearance, the transmissibility increase is accompanied by microdestruction of the coating surface, which increases with the number of bursts. This form of destruction begins even before the change of coating transmissibility.

Assuming the destruction process is a thermal one at the absorption centers (microimperfections), a formula is presented for determining the index of absorption of the microimperfections, together with an example of its application.

Laboratory of laser beam mechanics. Nauka i zhizn', no. 2, 1972, 54-56.

Tests on mechanical effects of laser beams on optically transparent polymers are discussed. The destruction of plexiglass when exposed to a laser beam is explained by the presence of structural inhomogeneities. This was proven by experiments using a measured quantity of fine dust particles added to a polymer test specimen. After laser exposure, the maximum number of damage centers was found to correlate with the number of injected microadmixtures. The polymer destruction process takes place in three stages: 1) generation of opaque centers; 2) heating and decomposition of material in the center region, and ») destruction of the material surrounding the center. The cause of the thermal centers in polymers exposed to laser beams is not known, but it is assumed that thermal stress produces cracks in polymers, which strongly absorb radiation energy. Three photographs are given illustrating the destruction of a clear plastic by laser beam.
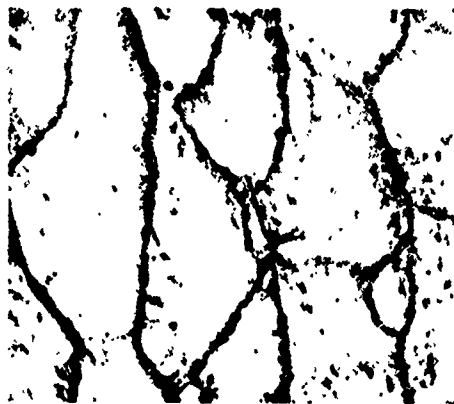
Fig. 1. Microstructure of
plexiglass. Distinct
boundaries divide the sub-
stance into separate aggre-
gates of a size on the order
of a   micron.

Findings of investigations of the relationship between the
strength and structural properties of polymers are briefly
reviewed.   Laser beam radiation caused destruction of polymers,
usually along the boundaries of structural formations.   The
structural bond of a plexiglass was about 10 times weaker than
the molecular strength; accordingly, destruction was noted along
the bonds well before molecular destruction.   Molecular
destruction can be caused by both heat and light.   The wavelength
of laser radiation is such that at low intensities unstressed polymer
molecules do not absorb the waves; but internal destruction does
take place and cracks are observed.   The aggregate structure of
the substance plays an important role; e. g. the less the
aggregate size, the greater the amount of cracks in polymers.   The
investigations show that organic glass and other amorphous polymers
contain hyper-molecular structures.   Figure 1 shows the micro-
structure of a plexiglass.

Lisitsa, M. P., and I. V. Fekeshgazi. Study of the
dynamics of flare development, formed by laser radiation
on the surface of transparent dielectrics. IN: Kvantovaya
elektronika. Kiyev, Izd-vo naukova dumka, no. 5, 1971,
251-256.

In a companion article to one by Fekeshgazi (p. 92), the authors
describe the methods used to record flare development in the interaction of a lase
beam with type I⁻ 5 glass and NaCl. The main effort was in registering flare
brightness and in relating flare development time and pulse shape to the incoming
laser pulse; this was done with a photomultiplier and a fast sweep scope giving
a flare front velocity resolution of 2.5 nsec. A dual optical grid system was usec
in the flare development region for velocity measurements; at a grid separation
of 3 mm, this permitted velocity measurements up to 10^8 cm/sec. Data on
velocity characteristic and density of evaporated material in the flare are given,
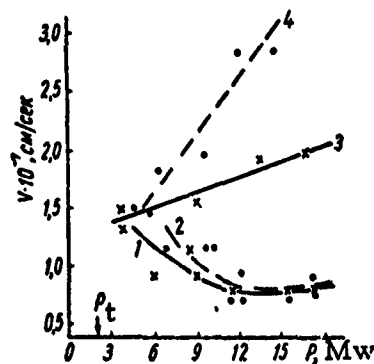primarily for glass specimens, for flare generation at both entrance and exit face

Fig. 1. Flare velocity in beam direction (3, 4)
and density of flare atoms (1, 2) vs. laser power.
1, 3 - NaCl; 2, 4 - glass, P_t = damage threshold.

Fig. 1 is an example of flare dynamics at the target face, using a Q-switched
ruby with 30 nsec, 18 Mw pulses. Analogous data for flares at the exit face
show a secondary peak in luminosity, indicating development of a shock wave
during flare lifetime.

Lukhov, Yu. N., V. S. Mospanov, and

Yu. D. Fiveyskiy. Optical surface strength

of a transparent dielectric and formation

of a thermal lens. Sixth All-Union Conference

on Nonlinear Optics, Minsk, July 1972 (Preprint).

Stress dynamics and thermal lens formation were studied
in the vicinity of the surface of an optically transparent solid isotropic

dielectric when a giant laser pulse was passed through its surface.
The laser pulse had a Gaussian form and a rectangular dependence
(sic) on time. The study was concentrated on the near-axis region
(parabolic approximation) and accounted for both surface and internal
absorption of radiation; surface fusion was not considered. The
thickness of the surface absorption layer was 10^{-6} cm; in this layer the
fraction of absorbed energy of the incident radiation was $\sim 10^{-4}$; the
dielectric surface was assumed to be mechanically free. Calculations
showed that at pulse termination the compressive stresses σ_{rr} and σ_{xx}
were maximal within the temperature-affected surface layer of $a_o \sqrt{\tau_i}$
$\cong 10^{-5}$ cm, where a_o^2 is the thermal conductivity coefficient of the
dielectric, and $\tau_i \cong 10^{-8}$ sec is the pulse duration.

The critical value of the pulse power density W_{cr} causing
surface destruction is derived from a formula for maximum values of
stress half-sums, $1/2 (\sigma_{rr} + \sigma_{xx})$ and of the stress $[\sigma_r]$, which leads to
compressive destruction of the dielectric. Tensile stresses σ_{rr} reach
their maxima when the distance from the surface is $v\tau_i \cong 10^{-3}$ cm, where
v is the speed of sound in the dielectric, at pulse power density W_c; at this
density the tensile stress is not sufficient to destroy the surface layer
by tension. It should be noted that the results obtained refer to the exit
face of the target specimen.

The probable damage mechanism is given as follows:
compressive stresses generated by surface heating break down
crystalline bonds; tensile stresses cause a dielectric layer to split off.
Absorption of laser radiation in the dielectric surface layer leads to tensor
change of the dielectric constant of the matter owing to thermoelastic
stresses under continuously changing temperatures. In the case of
radiation focused deep into the dielectric by external optics, the position
of focal point varies with time. It should be noted that for short pulses

($\sim 10^{-8}$ sec), distortion of the flat dielectric face is negligible; however on the laser optical axis at a power density of W_c, surface displacement is 10^{-7} cm. Within the laser pulse duration the focal point shifts at a constant velocity whose direction is determined by $(\partial n / \partial T) u_{ik}$, where n is coefficient of refraction, T = absolute temperature, and u_{ik} is the deformation tensor. At W_c the net shift in focal distance ΔF at pulse termination amounts to 5% of the focal distance value of the external optics.

Novikov, N. P., and A. A. Kholodilov. Destruction of thermoplastics by the combined action of gas and powerful thermal flux. I-FZh, v. 22, no. 4, 1972, 618-626.

This paper is a repeated treatment of an experiment reported by the authors previously (Effects of High Power Lasers, Dec. 1971, 48), in which the destruction characteristics of several polymers are compared under combined laser and hot gas impact. In the present case only PMMA and polystyrene specimens were used; surface heating was provided by a CO_2 laser plus a coaxial high-speed flow of heated nitrogen over the specimen. The gas jet diameter was more than double the specimen diameter so that the process could be treated as one-dimensional and stationary. The resulting liquefaction, cavity formation and ejection rate of material are discussed as functions of beam power density and jet velocity; the conclusions are as stated in the cited earlier work. The main emphasis is on the differences in destruction characteristics which depend on the chemical structure of the target material. Thus polystyrene shows a monotonic rise in destruction rate with beam intensity and gas velocity, whereas PMMA may show a definite peak in destruction rate for the same heating, as seen in Fig. 1. This is evidently caused by a temporary shielding effect by ejecta in PMMA for two of the four curves in Fig. 1(a), which dissipates at higher gas velocities; no similar effect was found for polystyrene. Rough calculations were also made of the amount of ablated material for the polystyrene target, as a function of beam intensity and flow rate. An extensive theoretical analysis of the observed destruction mechanisms is included.
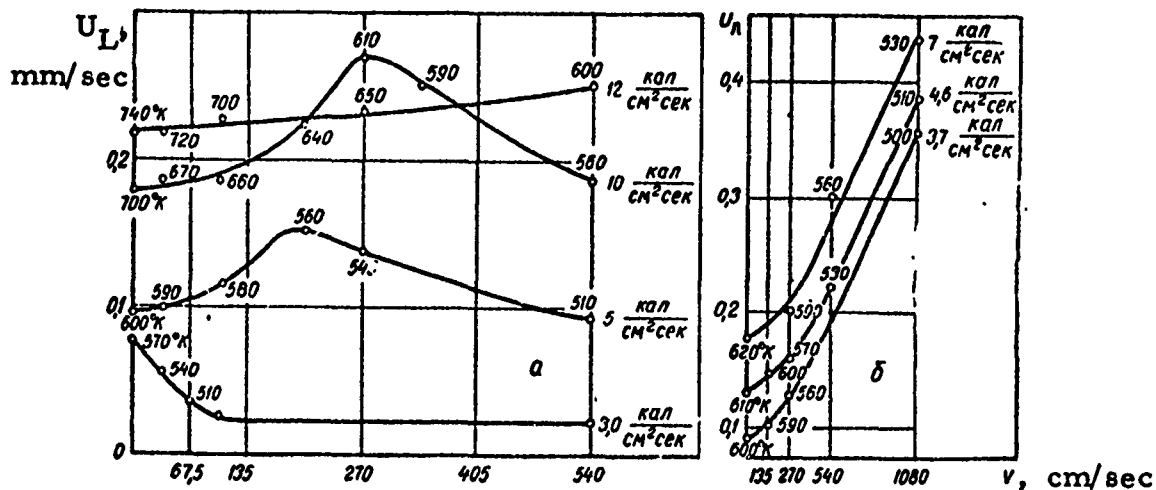
(Fig. 1 on page following)

Fig. 1. Linear destruction rate U_L as a function of
laser intensity and gas velocity.
a- PMMA
b- polystyrene
Surface temperatures are shown on each curve.

Novikov, N. P., V. P. Perminov, and
A. A. Kholodilov. Stationary one-
dimensional destruction of thermoplastics
by intense fluxes of beamed energy. I-FZh,
v. 23, no. 2, 1972, 257-266.

In a previous work Novikov et al (June Report, p. 8)
described damage effects to polymers from a combination of hot gas and
laser irradiation. The present report is a variant of the technique in
which polystyrene (PS) and PMMA elements were irradiated by a CO_2
laser whose beam width was substantially greater than target diameter.
At 10.6μ these materials are effectively opaque, so all incident laser
energy was considered to be absorbed. Cylindrical specimens 4 mm in
diameter were exposed in vacuo to a 6 mm diameter beam of unspecified powe
polished wafers of NaCl were interposed opposite the impact face to
intercept disintegration products from the heated area. In addition, a
series of thermocouples was initially imbedded in the specimens at
prescribed distances from the original impact surface.

With this configuration the destruction dynamics of PS and
PMMA were recorded and are described in detail. Results showed that

the impact surface temperature rose with increased laser power but attained a maximum of 500° C which could not be exceeded. The effect can be described by a time-temperature function in terms of depth into the specimen, as seen in Fig. 1. Four damage zones
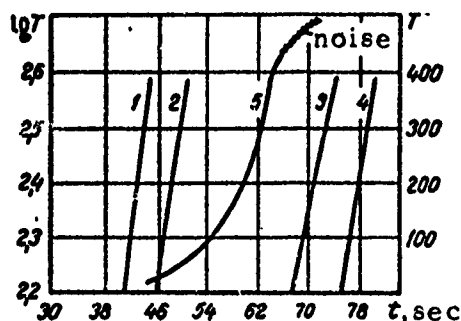

Fig. 1. Temperature vs exposure time, PS and PMMA. Original thermocouple depths = 7 mm (1); 8 mm (2); 12 mm (3); 13mm (4); and 10 mm (5). Curve (5) is T(t), others are lgT(t).
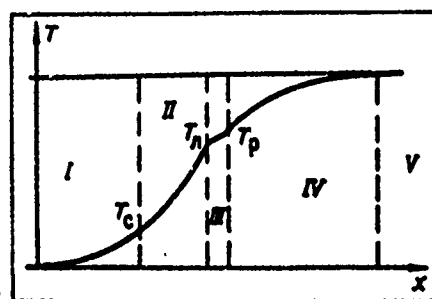
Fig. 2. Zone temperature characteristic of thermoplastics.

are claimed to be discernible, as shown in Fig. 2. Zone I, the farthest from the impact face, is solid polymer which obeys a Michelson exponential temperature response up to the softening point, T_c, where an abrupt shift in thermal capacity occurs. Zone II is a highly elastic state; Zone III is a quasi-liquid with inception of pyrolysis, and Zones IV and V are in the form of fine droplets of fused polymer. Photos of the debris deposited on the NaCl wafers show both droplet and solid particle ejecta occurring; a distribution analysis of particle formation is given. The results show in general that the damage process is uniform throughout the laser exposure and can be considered as one-dimensional and stationary.

Poplavskiy, A. A., G. P. Tikhomirov, and T. S.
Turovskaya. <u>Electron microscope examination
of radiation damage in dielectrics</u>. ZhTF, no. 7,
1972, 1462-1463.

A brief description is given of laser radiation damage to glass
and a combination of ZnS plus MgF_2 on a glass substrate. In all cases the
beam intensity was below visual damage threshold, ranging from low levels
up to 85% of critical. Fig. 1 gives a magnified view of laser effect on polished
type K-8 optical glass, showing the increasing fusion effect as threshold is
approached. The overall damaged region was noted to be considerably
greater than laser beam area.

a   b

Fig. 1. Subthreshold damage to glass.
Fused region in (b) is 6μ in diameter.

In contrast, the layered dielectric coating showed damage
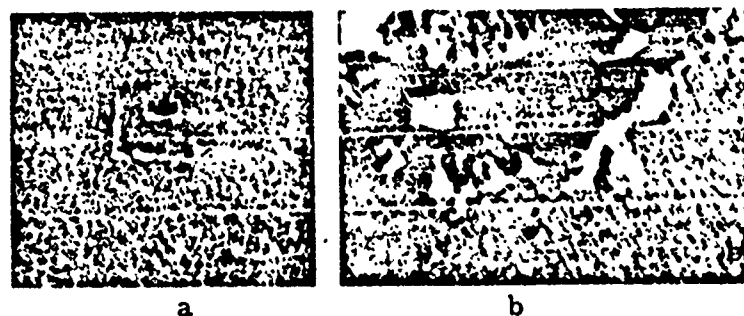beginning at a much lower energy density. Fig. 2 shows cavities on the

a   b

Fig. 2. Subthreshold damage to $ZnS+MgF_2$ on
glass a- at $0.4 Q_{thr}$; b- at $0.85 Q_{thr}$

order of 2μ appearing at $0.4Q_{thr}$. The tests thus verified that the damage effect in the two cases was different at low laser energies but becomes qualitatively the same as threshold is approached. The damage patterns suggest that energy is absorbed in a subsurface layer, in accordance with the results of Bonch-Bruyevich et al on optical glass (cf. Effects of High Power Lasers, Dec. 1971, 52)

Rysakov, V. M., and V. A. Marushchak.
Processes of self-focusing and destruction
in glass. Sixth All-Union Conference on
Nonlinear Optics. Minsk, July 1972 (Preprint).

A study is described on the form of damage tracks, speed of penetration of damage filaments, and their direction of growth, in a number of laser-irradiated optical glasses. These parameters are analyzed in relation to the laser pulse power (ruby or neodymium), to lens focal length, to divergence, and to the spectral width. The results obtained have shown that damage processes and self-focusing can be definitely ascribed to the development of a collapsing elastic cylindrical wave formed by electrostriction, according to the nonstationary theory of self-focusing advanced by Kerr. The studies were also concerned with incident light propagation and its scattering; to the light generated by the damage regions; and the dynamics of these spectra with time. It was discovered that by using pulses of $\sim$50 nsec no other changes in pulse spectra are observed but those produced by Raman scattering. This corroborates the hypothesis that in this case self-focusing is determined by electrostriction and not by low-inertia processes; the latter, if they take place in solids, evidently develop only by picosecond laser pulses.

Sultanov, M. A. Study of the destruction of polymer
films by a laser beam, as a function of type and structure
of the material. Mekhanika polimerov, no. 6, 1971,
1092-1093.

A photographic analysis is given of a variety of laser damage types to
polymer films, using both focused or nonfocused beams. Test materials cited
were oriented and nonoriented thin films of polyethylene, dacron, polypropylene,
an α-methyl styrene-plus-styrene copolymer, teflon, and kapron. Film thickness
varied from 85 to 350μ; irradiation was by an Nd laser at 3-5j, 1-5 millisecond
pulses developing a power density of 3×10^9 w/cm^2. For focused beam damage
tests f = 35 mm. Results are presented as microphotos of surface (270X) and
internal (600X) damage; one example given compares effects on Soviet and
Hungarian brands of polyethylene. Characteristic crater formation and ejecta
patterns for each polymer type are discussed. In the case of teflon the usual
pattern was absent; instead a surface fusion was observed at depths of 3--5 micro
with beam effects detectible down to 20 microns. It is noteworthy that up to 60%
of incident laser energy was reflected or scattered by the teflon surface, whereas
reflection from all other materials was negligible. The test results prove that
the nature of damage in polymers is strongly governed by the physicochemical
properties of the material. However, a generalization can be made on damage
mechanism according to irradiation type, i.e. for a nonfocused beam, photolysis
is called the major destructive factor, whereas a focused beam generates a
hydrodynamic explosion with plasma and shock wave formation.

Sultanov, M. A. Razrusheniye nekotorykh

prozrachnykh dielektrikov pod deystviyem

neodimovogo i rubinovogo lazerov v rezhime

svobodnoy generatsii. (Damage in various

transparent dielectrics from free-running

ruby and neodymium lasers). Fiz-tekhn.

institut AN TadzhSSR. Dushanbe, 1970, 19p.

(RZhF, 5/72, no. 5D1093)

It is shown that a powerful laser beam interacting with various
polymer materials will generate a hydrodynamic explosion process, which is
accompanied by a shock wave and plasma formation in the material. The
destruction mechanism in transparent dielectrics is postulated in the beam
focal region as well as behind it.

Sultanov, M. A. Destruction of transparent
dielectrics under the action of free-running
neodymium and ruby lasers. Mekhanika
polimerov, no. 2, 1972, 359-360.

The author notes that a variety of theories exist on the basic
destruction mechanism of laser interaction with transparent solids; among
these are thermal explosion, acoustic phonons from stimulated Brillouin
scattering, and photolysis of the target material. Experiments are described
which were designed to clarify the predominant mechanism of laser damage
in several dielectrics, including polymethyl-methacrylate, polystyrene and
several types of glass. Both ruby and neodymium crystal lasers were used,
in free-running regimes at energies of 3 to 15 j. Characteristic platelets of
cracks at angles up to 90° from the beam axis were observed for both laser
types; however in the Nd target specimens the damage area was more
extended along the beam axis, whereas the ruby damage was localized near
the beam focus. (Repeated reference is made to damage photos, which are
unfortunately omitted from the text.)

The test results lead Sultanov to the following concept of the
damage process. On focusing a sufficiently powerful beam in the transparent
dielectric, a local region is heated to a liquid state in which further energy
is absorbed by inhomogeneities, and crack propagation begins. A plasma is
generated which expands at high velocity; thus the effect is that of a powerful,
instantaneous point explosion. The process is a hydrodynamic one, including
shock wave generation which causes further destruction both before and
behind the beam focal point. Examples of remote damage regimes in PMMA
specimens are cited in added support of the theoretical model.

Zverev, G. M., Ye. A. Levchuk, V. A. Pashkov,
and Yu. D. Poryadin. Optical destruction of the
surface of lithium niobate. ZhETF, v. 62, no. 1,
1972, 307-312.

Anomalous breakdown thresholds of laser-irradiated $LiNbO_3$
are examined and the types of destruction mechanisms taking place are
suggested. In contrast to most dielectrics, $LiNbO_3$ has both a markedly
lower breakdown threshold at room temperature, as well as a distinctly
irregular change in breakdown level with increase in ambient temperature.
This was observed in radiation tests with a focused Q-switched Nd glass
laser at 1.06μ on polished $LiNbO_3$ specimens, in which 20 ns, 0.1 j pulses
were applied at f = 15 cm. Threshold at room temperature (120 Mw/cm^2)
increases with ambient temperature as seen in Fig. 1, exhibiting step jumps
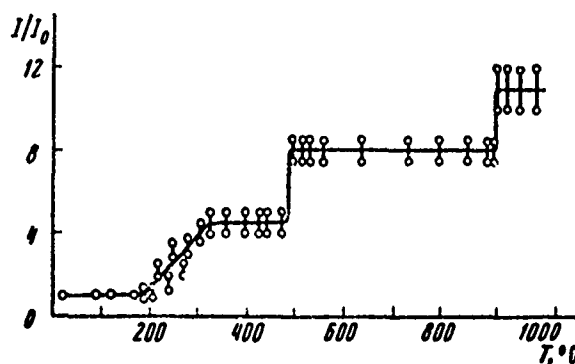at the Curie points. In contrast, the threshold characteristic of $LiTaO_3$

Fig. 1. Relative threshold intensity vs. temperature, LiNbO$_3$.

and BaTiO$_3$ were found to have no temperature dependence until the Curie point was reached, while for ruby and glass, no temperature dependence of threshold could be found between 20--700°C. At lower temperatures a cumulative effect of laser pulses on threshold is also noted in LiNbO$_3$ which is shown in Fig. 2. An analysis of these findings
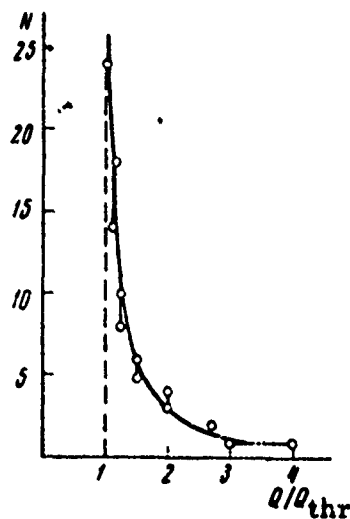

Fig. 2. Relative threshold vs. total laser pulses, N.

indicates that for temperatures below 330°C, surface damage is a function of light absorption in small trapping centers, whereas at higher temperatures the predominant mechanism is absorption by free carriers in the surface layer.

Zverev, G. M., Ye. A. Levchuk, V. A. Pashkov, and Yu. D. Poryadin. Surface damage in lithium niobate and tantalate from laser radiation. Kvantovaya elektronika, no. 8, 1972, 94-96.

This is a more detailed analysis of experiments recently described by the authors (April Monthly Report, p. 2) on laser damage thresholds of $LiNbO_3$ and $LiTaO_3$. An Nd glass laser was used in both free-running and single pulse modes to establish the threshold characteristic of wafer speci...ens with initially polished surfaces. In the single pulse regime the second harmonic (0.53μ) was also used, but this showed no significant change in damage threshold over the fundamental. As reported earlier, the point of emphasis is the anomalous cumulative effect of pulses on lowering the threshold, which distinguishes these materials from other transparent dielectrics such as ruby or glass. The comparative effect is seen in Fig. 1 for the two test materials.
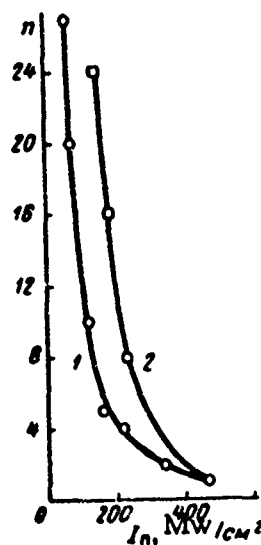

Fig. 1. Damage threshold in $LiNbO_3$ (1) and $LiTaO_3$ (2) vs. number of laser pulses

The authors cite numerous observed effects to indicate that nonlinear absorption does not play a part in the damage process here; for example, threshold was virtually independent of the level of surface polish in the target specimens. It was also noted that, beyond a certain focused spot size, threshold became independent of spot size, as seen in Fig. 2. The following mechanism is therefore proposed: for $LiNbO_3$,
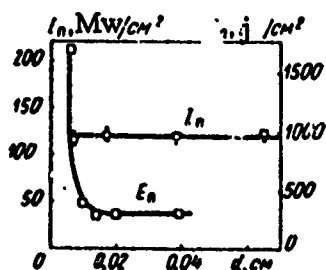

Fig. 2. Damage threshold in $LiNbO_3$ vs. beam diameter

existing concentrations of Nb^{5+} ions on the surface cause a preferential surface heating under the laser pulse leading to Nb^{4+} formation and a further surface absorption; this process is cumulative under repeated pulsing until threshold is reached by local heating. The same would hold for the $Ta^{5+} \rightarrow Ta^{4}$ reaction, although this requires a higher temperature (600-700° C), which would explain the higher threshold characteristic of $LiTaO_3$ in Fig. 1. The authors also note that the natural piezoelectric properties of $LiNbO_3$ may be a factor in its damage threshold, owing to a surface charge layer, and propose further tests along this line. Sample damage photos are given in Fig. 3.

Fig. 3. Surface damage to laser-irradiated $LiNbO_3$. a- single-pulse regime, after 6--8 pulses at threshold (x 300); b- after 20--30 pulses (x300); c- after free-running exposure (x 150)

5. Laser Interaction with Semiconductors

Brekovskikh, V. F., Z. I. Mezokh, A. V. Ovodova,
A. A. Uglov, A. K. Fannibo, and V. A. Yanushkevich.
Dislocation structure of germanium subjected to a
laser beam. FiKhOM, no. 6, 1971, 6-10.

Crystallographic alterations in laser-irradiated Ge are discussed. Single crystals of Ge both with and without initial dislocations were subjected to pulsed radiation from a ruby laser which was run in either a spike or spike-free regime. Pulse width was 1 millisec, energy was 0.5 j and density was 2×10^4 w/cm^2. Specimens were cut in the (111) plane with the impact surface being polished before testing. Exposure was done in air at temperature from room up to 550°C, while dislocation characteristics were observed for both specimen types and laser regimes. Resultant dislocation density in all cases was clearly greater for the spike mode. The results also verify that polygonization in semiconductors with a high dislocation level will proceed at considerably lower ambient temperatures than previously stated in the literatur Microphotos of generated dislocations are included.

Epshteyn, E. M. Thermal instability of a
semiconductor in a laser beam. IVUZ Radiofiz,
no. 1, 1972, 33-37.

A theoretical study is presented on a possible mechanism of laser-induced destruction of a semiconductor. The case is limited to photon energies less than the width of the forbidden zone, so that the main exchange mechanism is absorption by free carriers. In the general case a cumulative heating and increase in free carriers will occur, resulting in a stationary temperature field. However, above some laser threshold level the stationary field breaks down and a rapid thermal reaction sets in which is analogous to breakdown in a d-c field, or the thermal explosion from an exothermic chemical reaction. To examine the governing phenomena the author assumes the simplest case of a cylindrical semiconductor target, axially excited by a uniform-intensity laser beam such that $\lambda \ll \rho \ll R$, where λ is laser wavelength, and ρ and R are beam and cylinder radii. Expressions are derived for the limit conditions of the stationary field solution, and the corresponding threshold power of the laser is determined. Finally, it is shown that the elapsed time required to reach threshold under practical conditions will lie in the 1 millisec - 1 sec range - i.e. demanding in effect a c-w laser regime. Therefore the described mechanism cannot account for breakdown observed, for example, in transparent dielectrics under nanosecond pulse exposure.

Test results are described of damage to GaAs single crystals exposed to 500 μs pulses from a neodymium glass laser. Specimens were 1--2 mm thick and were polished on both entrance and exit faces prior to exposure. At the 1.06 μ wavelength the specimens then had absorption coefficients in the 1 to 3/cm range. Damage at the exit surface was the particular object of study; at incident power levels of about 5×10^5 w/cm^2 damage began to appear in the form of pits with a mean depth of 80 μ, as seen in Fig. 1 (a). Evidence is cited to show that the damage occurs from post-pulse heating of the surface layer; this is supported by measurement of GaAs dissociation, twinning, and a sharp increase in dislocation density, all of which are high temperature effects. Further tests were made to measure local photoluminescence response in the damage regions using a focus beam area of 500 μ^2 from a He-Ne laser, which was appreciably smaller than the damaged area. Fig. 2 compares the change in photo response for two types of n-GaAs, one doped with Te and the other with trace Cu. The reasons for the observed response are discussed in terms of crystal lattice structure.

Fig. 1. Exit face of GaAs crystal in beam
region (x270)
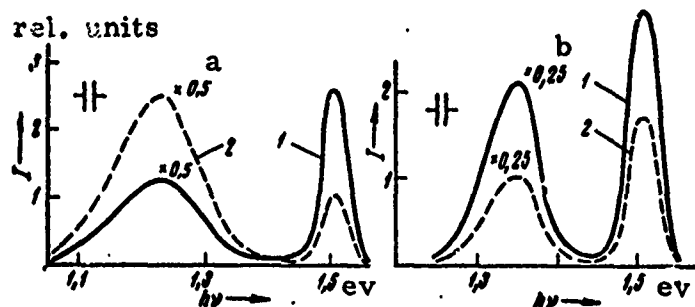
a- before etching; b- after etching.

Fig. 2. Photoluminescence spectra of n-GaAs
doped with Te (a) and Cu (b),   T = 77°K.
1- damaged area; 2- undamaged area.

Lisovets, Yu. P., I. A. Poluektov, Yu. M. Popov, and
V. S. Roytberg. Passage of a coherent ultrashort optical
pulse through a semiconductor. IN: Sbornik. Kvantovaya
elektronika. Moskva, Izd-vo Sovetskoye radio, no. 5,
1971, 28-36.

Analytical solutions are obtained describing the passage of an ultrashort
laser pulse through a semiconductor. A resonance interaction with the semi-
conductor is assumed, where the laser pulsewidth is less than the polarity
relaxation time of the medium. Conditions are specifically examined for self-
transparency, under which the pulse can ideally propagate with no energy loss
to the medium. It is shown that the resultant stationary pulse may propagate
at a velocity an order of magnitude below the speed of light in the given medium

Nikiforov, Yu. N., V. A. Yanushkevich, and A. V. Sandulova. Change in electrical properties of p-Si crystal whiskers from the action of giant laser pulses. FiKhOM, no. 3, 1972, 132-134.

Laser-induced change in the resistivity ρ of p-Si whiskers is described. The whiskers were grown along the [111] axis, had a hexagonal cross section, and ranged in length from 3 to 7 mm. Specimens were exposed to 50 nsec giant pulses from a ruby laser, with the laser beam normal to the crystal axis. Impact densities were varied over several tens of joules/cm^2, up to the damage threshold which was in the range of 35 - 45 j/cm^2. The data are presented as resistivity variation $\Delta R/R_o$ in exposed specimens as functions of whisker geometry, ambient temperature and initial ρ. Typical results at an exposure of 22 j/cm^2 show a sharp rise in R by about 12-15%, followed by an exponential decay back to about the initial value, at a time constant $\cong 20$ milliseconds. Of the possible mechanisms considered for the alteration effect (photoeffect, crystal heating, piezoeffect, defect formation) it is shown that point defect formation is the most probable factor. Defect levels, estimated to reach 10^{17}/cm^3, were effectively annealed out in all cases in 30 milliseconds or less.

6. Laser Interaction with Liquids

Askar'yan, G. A., E. Ya. Gol'ts, and T. G. Rakhmanina. Alteration of the propagation and reflection of ultrasound under the effect of an intense light on the surface of a body in liquid. ZhETF, v. 62, no. 3, 1972, 1072-1074.

A new effect was investigated experimentally in which the propagation of sound is changed due to intense light acting on the medium. A flash of an unfocused and unmodulated neodymium laser beam sharply reduced the reflection and transmission of ultrasound through the surface of a steel plate immersed in water. Strong change is found when the surface temperature T is high enough to form vapor or gas. An expression was derived for determining this temperature. In the experimental arrangement (Fig. 1), a laser beam
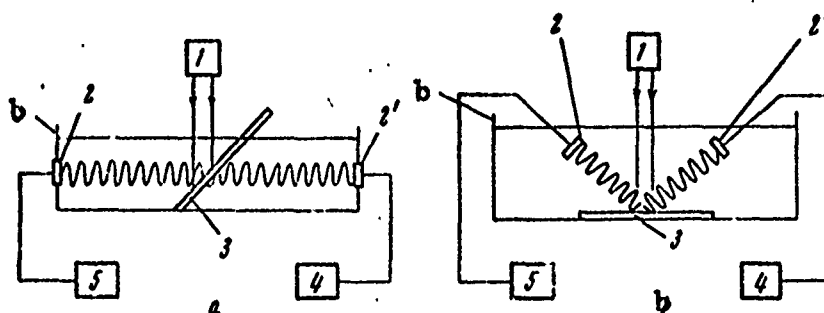

Fig. 1. Experimental sketch for investigating alterations of (a) propagation and (b) reflection of sound due to an unfocused laser beam on the surface.

from 1 falls on the surface of a steel plate 3, immersed in water in vessel 6. An ultrasonic transmitter 2, a piezoelectric element of 1 cm radius, transmits a directional ultrasonic wave at a frequency of 2 MHz from generator 5, in such a way that the sound wave passes through the surface region, illuminated by the laser pulse. The piezoelectric receiver 2' records the ultrasound radiation, passing through (Fig. 1a) or reflected by the plate (Fig. 1b). Two series of experiments were conducted: a) using a free-running laser with a maximum energy ~10 joules, pulse duration ≈0.5 msec, and beam radius 1 cm; and b) using an unfocused, Q-switched laser with a pulse width of 30-40 nsec. Seven oscillographs obtained during the experiments are given to show the effects of light on the reflection of sound. The build-up time of the interaction effect, connected with the formation of vapor-gas bubbles or of a non-uniform film, was commensurate with the energy release time.

Duration of interaction increases with an increase of flux density and at a light flux density of ~10kw/cm^2 lasts for ~200 msec, which significantly exceeds the laser pulse duration (~1 msec). At high laser powers with Q- switching a rapid film formation was observed, which eliminated propagation and changed the sound reflection. Possible applications include: the interruption and elimination of reflection and propagation of sound, and ultrarapid modulation of sound, when short laser pulses are used.

Bozhkov, A. I., and F. V. Bunkin. Optical
excitation of surface waves in transparent
condensed media. ZhETF, v. 61, no. 6,
1971, 2279-2286.

The excitation of surface waves in condensed media by two mutually interfering plane monochromatic waves is discussed. Optical excitation of surface waves in such a case proceeds by a striction mechanism which involves a ponderomotive force jump from the normal to the surface component. The mechanism is not related to radiation absorption and hence is primarily applicable to transparent media. The proposed method of surface wave excitation is examined for two coherent monochromatic waves incident on a liquid surface. Mathematical treatment of an equation of motion of the liquid-atmosphere interface, with allowance for ponderomotive forces, produced general formulas of the velocity component V_z and the function ζ (x, y, t) describing surface deviation from the z = 0 plane. These formulas led to the conclusion that two plane electromagnetic waves stimulate vibrations of the liquid surface with amplitude $|\zeta_o|$, a wave vector q = k_{t1} - k_{t2}, and a beat frequency $\Omega = \omega_1$ - ω_2. In these expressions, k_{t1} and k_{t2} are the wave vector projections on the liquid surface, and ω_1, ω_2 are the frequencies of the two optical beams. A formula was derived for $|\zeta_o|^2$ as a function of q, Ω, which is applicable also to a total Fresnel reflection, when the liquid occupies a space z > ζ (x, y, t). Analysis of frequency characteristic $|\Delta|^{-2}$ variations as a function of Ω in the regions of low and high Ω revealed that $|\Delta|^{-2}$ for viscous liquids decreases continuously with increases in Ω, and the $|\Delta|^{-2}$ characteristic for low viscosity liquids is a resonance frequency in the region of high Ω. For Ω = 0, the $|\zeta_o|$ of the static surface wave is independent of viscosity γ and in the cases of $\Omega = \Omega_o$ (q) and $\geq \Omega_o^2 / v_q^2$ the surface wave travels with $|\zeta_o|$ dependent on v, surface tension and α, dielectric constant of the liquid, and independent of v and α, respectively. Conditions are given for the application of the $|\zeta_o|$ formulas to a laser excitation source. Examples of numerical evaluations of the optical beam intensities required to stimulate surface waves in a high or a low viscosity liquid show that striction can stimulate these waves with an amplitude much higher than thermal excitation, and in certain cases may determine the radiation resistance of transparent laser materials.

Chastov, A. A. Transmission of a
powerful beam in semicolloidal dye
solutions. ZhPS, v. 16, no. 4, 1972,
649-653.

Ruby laser beams in semicolloidal dye solutions were
investigated under the condition that the size of micelles and the
inhomogeneities formed around them was smaller than the beam wave-
length. Aluminum chlorophthalocyanine in o-dichlorbenzene, vanadyl
phthalocyanine in chloroform, and 1.2-aluminum phthalocyanine in o-
dichlorbenzene and quinoline solutions were used. Experiments have shown
that with increased radiation intensity the transmissibility of colloidal
solutions first rises and then drops; intensities of the order of several Mw/cm
produce nonlinear scattering.

The author computed the attenuation of a parallel light
beam in a semicolloidal dye solution and concluded that the scattering
coefficient has a square-law dependence on radiation intensity. An initial
stage of increased transmissibility was traced to the brightening of dye
monomers. The dye linear absorption decreased under weak and moderate
fluxes and the number of aggregated molecules increased. At strong fluxes
the transmission characteristic of the solution dropped and the number of
bonded molecules rose from the increased nonlinear scattering. The
difference in the transmissibility of semicolloidal solution layers of various
thickness is reduced with an increase of radiation intensity. The
phenomena discussed are cited as having application in the study of inter-
actions of powerful radiation with absorbing solutions. The author suggests
using the factor of a decrease of transmission in semicolloidal solutions
exposed to high radiation intensities for detecting tiny concentrations of
aggregates, when spectral methods are insensitive.

Results are described for the droplet dispersion patterns obtained from
laser explosion of a water drop. As reported earlier, the critical point at which
explosion occurs depends on the product ϵK_p, where ϵ is incident energy density
and K_p is a dimensionless factor indicating absorptive effectiveness; the present
tests were done above the critical point. The test configuration (Fig. 1) used a
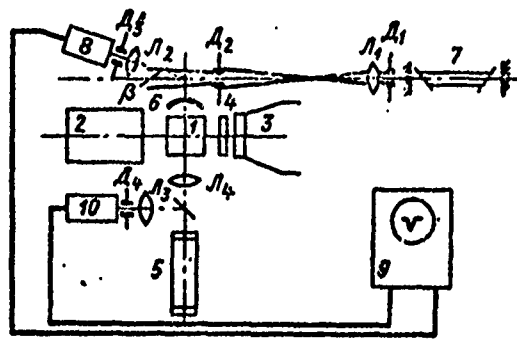
Fig. 1. Water drop explosion experiment.
1 - water drop on movable plate; 2 - camera;
3, 4 - illumination; 5 - ruby laser; 6 - coated
screen; 7 - LG-55 laser; 8, 10 - photomultiplier;
9 - scope.

free-running ruby laser to evaporate water drops on a glass plate; the ejected
droplets were collected on a coated screen and their distribution patterns were
recorded. In addition, droplet velocity was recorded by a second transverse lase
beam in the ejecta path, where intersection of droplets was registered as noise
in the beam detector system; synchronization with the activating beam gave
droplet time of flight. Data presented include directional patterns and velocity
characteristics; droplet sizes varied in the range of 5 to 80 microns, depending
on the size of the initial target drop. The tests verify the non-central explosion
point in the drop, and resultant anisotropic patterns of energy propagation and
ejecta motion.

7. Laser Interaction with Miscellaneous Materials

Adam, A., D. Horvath, P. Hrasko, Zs. Kajcsos, and M. Labadi. Positron annihilation in a laser radiation field. Kozp. fiz. kut. intez. no. 72, 1971. (RZhF, 5/72, no. 50196) (Translation)

Positron annihilation in NaCL crystal was observed in the presence of a laser field. It was established from time spectral analysis that the decay constant of long-lived components was approximately 20% greater under laser radiation than without it.

Aseyev, G. I., and M. L. Kats. Destruction mechanisms of alkali halide crystals and multi-photon ionization of impurity centers. FTT, no. 5, 1972, 1303-1307.

The destruction of a series of natural and impure alkali halide crystals (NaCl, KCl, KBr, NaBr, KCl-Eu, KCl-Ag, KCl-Tl, and KCl-In) under the effect of ruby and neodymium lasers was investigated in a free-running regime (energy = 1.5 joule, duration = 500μsec). Beam focusing on the specimens was done by $f = 50$ and 150 mm lenses. The destruction mechanism in crystals is explained in terms of Brillouin forced dispersion and local heating. The temperature at the damage site was approximately $5000^\circ C$ at a near critical power density. Forced dispersion components were not observed. Results show little likelihood of destruction due to hypersonic phonons and high-frequency breakdown; the primary destruction mechanism is rather the local heating associated with absorption of a portion of the laser energy by crystal structure defects. The dynamics of the destruction process and causes of optical fatigue in alkali halide crystals are outlined. It is shown that a decrease of at least one unit of the suggested photon level of the multi-quantum excitation process in photoconductivity of activated alkali halide crystals is associated with the thermal ionization of excited states of impurity centers. Graphical and photographic data of experimental results are included.

Aseyev, G. I., and M. L. Kats. __Multiphoton excitation and ionization of Tl$^+$ in alkali halide crystals.__ Sixth All-Union Conference on Nonlinear Optics, Minsk, July 1972 (Preprint).

Multiphoton excitation of photoconductivity and luminescence was studied in NaCl, KCl and KBr crystals activated by thallium ions, and exposed to ruby and neodymium laser radiation in spike and spikeless generation regimes. A study of the concentration dependence of photocurrent power i and of the dependence of i on laser photocurrent values F has shown that phosphor photoconductivity is the result of three-to four-photon-excited thallium centers when the specimens are irradiated by ruby or neodymium lasers. By comparing photoelectric signals corresponding to spike and spikeless generation pulses it was established that the photocurrent amplitude in the spike regime is some two orders higher than for spikeless pulses. Spikes can also generate a larger photocurrent than can monopulses; this is accomplished at the expense of reduction in parameters such as duration and area of localization of spikes.

Luminescence studies related to laser excitation have shown that in different specimens either of these two phenomena can take place: a simultaneous excitation of thallium centers of two types, or excitation of the second type only. This is due to the magnitude of resonance detuning between the effective quantum $k\hbar\omega$ and the maximum absorption band. Depending on the value of F, two types of luminescence Tl$^+$ centers were observed: intracentral and recombination types, the latter being accompanied by crystal photoconductivity. In making measurements it was noted that from burst to burst the intensity of short-wave luminescence of the specimen decreased, whereas, in proportion to this decrease, the long-wave luminescence increased. This is the result of redistribution of impurity concentrations in favor of the second-type thallium centers, owing to formation of additional crystal defects by the laser beam. The data permitted computation of quantum yield as well as probability, cross-section and the multiphoton absorption coefficient for the KCl - Tl phosphor.

Aseyev, G. I., and M. L. Kats. Damage
mechanisms in alkali halide crystals and
multiphoton ionization of impurity centers.
Sixth All-Union Conference on Nonlinear
Optics, Minsk, July 1972 (Preprint)

An experimental study was made to analyze damage formation
in a series of nominally pure and impure alkali halide crystals from
radiation of free-running ruby and neodymium lasers, and to determine the
damage thresholds. The value of critical power density P_{cr} was found not
to depend on parameters such as impurity concentration, optical wavelength,
radiation polarization, or orientation of wave electric vector with respect
to crystallographic axes. The governing criterion is the level of nonselective
crystal absorption of the laser generation frequencies. It was shown that
the effect of laser optical fatigue is caused by a decrease in background
transparency of specimens following repeated pulsing. In the case of
indium and silver phosphors, the fatigue is evidenced by the formation of color
centers.

To explain the mechanism of damage to alkali halide crystals,
attempts were made to detect the presence of stimulated Brillouin scattering
and of local heating in the specimens. No scattering components were
detected up to values of $P \cong P_{cr}$. Temperatures in the focal region were
100-500° C at a density ~1/5 P_{cr}, rising to ~5000° C at $P \cong P_{cr}$.
Measurements show that hypersonic phonons and high frequency breakdown
cannot cause damage in alkali halides if the laser operates in a free-running
regime. The basic mechanism is the local heating of specimens, related
to the absorption of some portion of laser energy by nonselective crystal
defects.

A relation was established between the damage mechanisms /
and the multiphoton ionization of activation centers. It is demonstrated
that a unit decrease in the assumed degree of photon generation, in
relation to the process of photoconductivity excitation of activated alkali·
halide crystals, as observed by the authors,is due to thermal ionization
of excited impurity centers.

Assovskiy, I. G., and A. G. Istratov. Combustion of
powders under optical radiation. ZhPMTF, no. 5, 1971,
70-77.

It is noted that the bulk of the literature on optical ignition of powder
does not consider the further effect of optical flux on combustion characteristics
following ignition. An analysis is accordingly made to correlate combustion
rate of a powder with intensity of optical excitation, using both a stationary
combustion regime and one in which optical flux varies in some harmonic manner
It is assumed that incident flux is absorbed in the condensed phase according to
the exponential Bouguer-Lambert law, at a constant transparency index. In
stationary combustion of the powder the optical radiation is shown to be equivalen
to raising the initial powder temperature, which permits analysis without conside
ation of radiation parameters. In the nonstationary case with periodically varyin
optical flux the model of Novozhilov (PMTF, no. 4, 1965) is used to define
combustion behavior. A correction factor to average burn rate, proportional to
the square of the optical flux amplitude, is introduced; in the case of an exponen-
tial ratio of combustion rate to initial temperature, this correction is a negative
one. The authors also discuss the effect of radiation on the stability of combustio
in the stationary mode.

Bayramov, B. Kh., B. P. Zakharchenya, and
E. M. Khashkhozhev. Self-focusing of argon laser
radiation and light scattering by phonons in bismuth
germanate crystals. FTT, no. 11, 1971, 3412-3414.

Self-focusing effects are discussed on the basis of results with a c-w argon laser (4880Å) propagating through bismuth germanate ($Bi_{12}GeO_{20}$). Laser power was well below damage threshold at 0.3w, and was adjusted to a 3 mm diameter beam at f = 270 mm. Visual effects showed generation of irreversible color centers acting as self-saturating absorption regions in the beam path. The saturation effect ceased after 20 to 30 sec following exposure, depending on beam intensity. A typical annular beam cross-section pattern in the crystal region was also observed. One factor causing a change in refractive index was evidently local heating and resultant non-uniform stress patterns, since $Bi_{12}GeO_{20}$ is strongly piezoelectric. Spectral data are included which show regions of substantial variance in optical phonon scattering between first-order and nonlinear scattering; however no shift, split or broadening of phonon lines was observed. A brief mention is also made of the effect of argon laser self-focusing on phonon scatter of He - Ne laser light (6328Å).

Boyko, Yu. I., and A. K. Yemets. Study
of laser self-focusing in alkali-halide single
crystals, according to data on shift of the
damage center. DAN, v. 206, no. 2, 1972,
319-322.

Experimental results are described of laser damage phenomena in KCL and KBr crystals, with the object of determining the extent and effect of self-focusing in the crystal. A free-running ndt glass laser was used developing 100 μsec pulses to a maximum of 16 j. Target specimens were parallelepipeds 30x30x100 mm; the laser beam entered normal to an end face as shown in Fig. 1, using a lens with f = 55 mm.
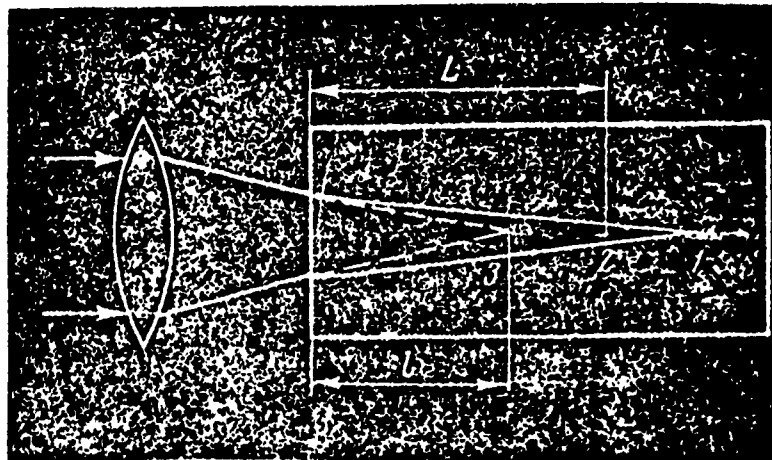
Fig. 1. Configuration for self-focusing experiment.

Results were analyzed in terms of the actual distance L of beam focus
from the entrance face, and lens focal distance ℓ (Fig. 1). In the absence
of nonlinear effects the approximate linear relation $L \cong n_o \ell$ should apply,
where n_o = nominal refractive index; this proved to be the case for KCL,
whereas for KBr the damage center was found to shift toward the laser
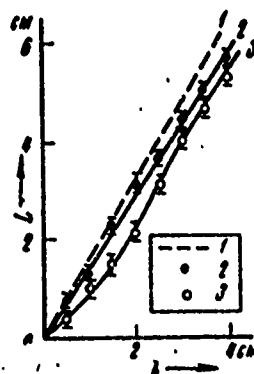source such that $L \sim \ell^2$. The effects are compared in Fig. 2, showing the

Fig. 2. Shift of damage center vs. lens focal distance
1 - calculated for KBr; 2- KCl; 3- KBr, actual

nonlinear self-focusing response of KBr. The latter effect suggests a
thermal mechanism, which was confirmed by further tests on KBr
specimens in a heat chamber in which $n_o(T)$ as well as $dn_o/dT(T)$ were
measured. This showed that at $0.6 \, T_{fusion}$ and above, dn_o/dT takes on
positive values which would account for the observed self-focusing in KBr.

Fekeshgazi, I. V. Structure of the flare formed at the
input surface of alkali-halide crystals by a laser beam.
IN: Kvantovaya elektronika. Kiyev, Izd-vo naukova dumka.
No. 5, 1971, 256-259.

A beam-target study is described using a Q-switched ruby on specimens
of NaCl, KCl, KBr, and LiF. The laser was run in a spike mode with spikes
controlled from one to six or more. Spikes were of approximately equal ampli-
tude, 30--40 nsec wide and separated by 100-150 μ sec; power was from 2 to 8 M
The main effect of interest was the appearance of luminous centers in the specim
each of which corresponded to a single spike in the laser pulse. Sample photos
are given showing the effect of a six-spike pulse, which generates a train of six
centers starting at the surface. The mechanism appears to be that of a vapor
cloud generated by the first spike, which diffuses into the crystal and is illuminat
by succeeding spikes; luminosity decays monotonically with rise in number of
spikes. Cloud diffusion rate appeared to be essentially constant within a
3--6 x 10^3 cm/sec range. A spectrographic study confirmed that the luminosity
was from the metal line of the particular specimen.

Kasatochkin, V. I., M. Ye. Kazakov, V. V. Savranskiy,
A. I. Nabotnikov, and N. P. Radimov. Synthesis of a
new allotropic form of carbon from graphite. DAN SSSR,
v. 201, no. 5, 1971, 1104-1105.

Applying a free-running neodymium laser beam to a pyrographite target,
the authors obtained vaporized deposits which proved to be a new allotropic form
of carbon. In one test a pyrographite substrate opposite the target face was used,
with a center aperture for the laser beam (Fig. 1); one millisecond pulses were
used, at energies of 250 and 500 j. In another variant the target specimen was
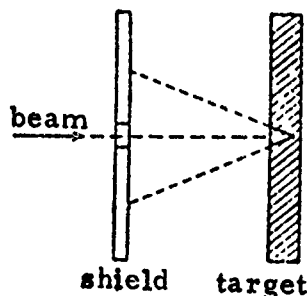

Fig. 1. Irradiation of graphite.

placed in an evacuated glass ampoule, with the vapor products depositing on the inner surface. The deposits typically were silver-white, surrounded by a black border. X-ray studies of the silvery deposit showed a polycrystalline structure having a mean crystallite dimension of 10^{-5} cm; images of the black deposits were characteristic of a highly dispersed substance with diffused diffract bands. A complete identity was established between electron diffraction patterns from single crystals of both silvery and black deposits, indicating the structural identity of the two products. The black form is identified as carbyne, which has previously been obtained by oxidative dehydropolycondensation of acetylene. The difference in color was attributed to the high degree of dispersion in carbyne as well as the presence of amorphous carbon impurities. It is noted that this allotropic form has been discovered earlier in natural graphite and in meteoric material, and later was produced by electric discharge in pyrographite under vacuum and high temperature (Whittaker et al, Science, v. 165, 1969, 589). The authors intend further publication on the atomic structure and properties of the new allotropic form.

Korotin, A. V., and L. P. Semenov. Vaporization of crystals under the effect of external excitation. IN: Institut eksperimental'noy meteorologii. Trudy, vyp. 30. Fizika aerodispersnykh sistem. Moskovskoye otdeleniye gidrometeoizdata, Moskva, 1972, 65-71.

The authors present a straightforward thermodynamic analysis of the interaction of a concentrated heat flux with a crystal surface, for the case in which an appreciable melt zone appears prior to evaporation. The analysis assumes a constant-intensity beam normal to a semiinfinite crystal face, and arrives at expressions for melt zone boundaries, growth rate and limit conditions, and time to melt, in terms of target and beam parameters. It is shown that in the general case the maximum temperature will occur at the outer melt surface, and also that an optimum beam intensity exists for which the melt area will be maximum, decreasing at higher or lower intensities. It is interesting to note that the numerical examples given assume an ice target; results on the ice-water parameters are given for beam densities ranging from 25 to 200 w/cm^2. In ice, for example, the depth of the melt zone is only weakly dependent on beam intensity.

-108-

An experimental study was made of the radiative energy transfer in optically thin loose fibrous layers bound by diffusely radiant and reflecting surfaces. Allowance was made for the effects of induced radiation and scattering from the medium in approximation of local thermodynamic equilibrium. The fibrous layers were made of a superthin (1-2μ) fiberglass or ~30μ thick caprone fibers bound by oxidized aluminum and copper or polished aluminum surfaces. The effective thermal conductivity λ_T of the plane-parallel optically thin layers was measured in an electric calorimeter with a special heat-insulating shield in high vacuum. The maximum λ_T error was 5%. The experimental λ_T data are plotted in Fig. 1 in comparison with the theoretical $\lambda_T(\tau)$ dependence calculated from

$$\lambda_T = \frac{1}{\dfrac{1}{\lambda} + \dfrac{1}{4\epsilon_r \sigma T^3 L}} \tag{1}$$

where λ is the radiative thermal conductivity of an optically dense layer, σ is the Stefan-Boltzmann constant, T is the arithmetic mean of the layer temperature, L is the geometric thickness of the layer, and ϵ_r is the reduced emissivity of the boundary surfaces, which was experimentally measured in the absence of the loose fibrous layer. Allowance was made, when calculating λ_T, for the coefficient $\bar{\mu} = 3/2$ of angular distribution of radiation flux intensity incident on the boundaries. The experimental and theoretical λ_T/λ versus τ plots for two different ϵ_r values were similar. The data indicates that λ_T dependence on L and τ of the layers with diffusely reflecting surfaces is described with a good approximation by (1) and similar formulas. In contrast, the experiments with a polished aluminum boundary (cold) surface
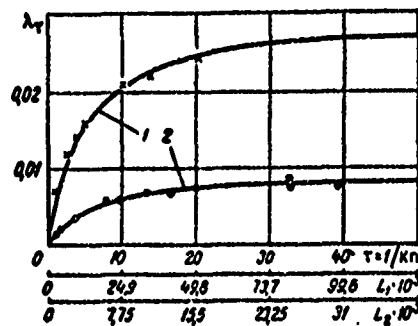

Fig. 1. λ_T in W/m/degree vs. optical thickness τ and L(m m) of a loose fibrous layer of 30 kg/m³ volume density, ϵ_r = 0.27. Solid lines are calculated by (1) .
1- caprone fiber, 2- super-thin glass fiber

revealed a significant discrepancy with the theoretical data calculated by (1). It was concluded that the $\bar{\mu}$ = 3/2 value is acceptable only for gray, diffusing boundary surfaces of thin layers of any τ, i.e. the boundary boundary has the effect of increasing τ by a constant value.

Zakharov, V. P., V. N. Chugayev, V. I. Zaliva, and
Yu. G. Poltavtsev. Study of the graphitization process
of thin carbon films from the effect of powerful light
pulses. UFZh, no. 2, 1972, 279-283.

An experiment in optical graphitization of a carbon film is
described, which complements the work of Zakharov reported previously
(March 1972 monthly report, p. 9 and April report, p. 130). Instead of a
laser a type IFP flashlamp was chosen in the present case, having a spectral
peak at 0.4 micron, and used to irradiate a 10^{-5} cm pure carbon film at
various distances and flash intensities. The bulk of the experiment was devoted
to recording change in optical transmission of the film, giving an index of the
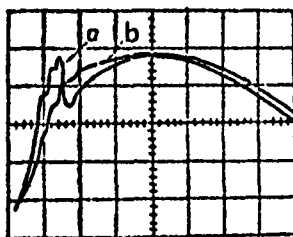induced graphitization process. A typical result is shown in Fig. 1.

Fig. 1. Change in transmitted flux of irradiated
carbon film.
        a- after first pulse;
        b- after second pulse
        major division = 10^{-4}sec.

For this case a film area of 1 cm^2 was determined to be raised to the order
of 1000°C per pulse. Curve (a) in the figure shows the inflection interval
where graphitization occurs; the reduced response of curve (b) then held true
for subsequent pulses. In this case graphitization occurred in about 10^{-5}
sec.; correspondingly increased times were required for reduced film
treating rates. The authors suggest a two-step process occurring, beginning
with a rapid formation of crystallites, and followed by a more extended period
of crystallite reorientation and grouping into the graphite structure. Additional
tests on r-f transmissibility of the exposed film confirmed the assumed
process.

Zakharov, V. P., and Yu. M. Pol'skiy. Velocity of
the temperature front in carbon films during their
interaction with laser radiation. FiKhOM, no. 6, 1971,
3-5.

A simple technique is described for determining the mean radial
velocity of a temperature front, generated by focused laser radiation on a
carbon thin film. The carbon film is overlaid with a thin Ge film and two
photomultiplier arrays are aimed in the vicinity of the impact point, offset
by a known distance (200 microns in the example given). At a sufficient laser
exposure the Ge film melts, causing a discrete change in optical density; the
time for the melt region to reach the remote monitored point then yields
mean temperature front velocity. In the cited tests a free-running ruby laser
was used, giving a mean front velocity of 1.5 - 2 m/sec, although the rate
nearest the impact region was evidently higher. The results also indicate a
slower and more complex fusion mechanism in the Ge with increased distance
from the focal point, suggesting an interim reordering of its crystal structure
prior to melting. The resolution of the technique is limited by the dimensions
of the sensing photocathodes; for the tests described, error was put at not
over 25%.

8. Theory of Laser Interaction with Material

Alekseyev, E. I. **A description of the interaction of noncoherent radiation with matter.** ZhPS, v. 15, no. 6, 1971, 1090-1093.

A general probability expression is presented from which the interaction of radiation with matter can be approximately described. The model assumes most types of noncoherent radiation sources of macroscopic nature, and includes certain types of laser radiation as well; random noise sources are however excluded. A general expression defining radiation interaction with a density matrix of material elements is given, which can be treated as a system of ordinary stochastic differential equations with stipulated or random initial conditions. A rigorous solution for the assumed model could be obtained by a form of the Fokker-Planck-Kolmogorov equation; however for practical considerations a satisfactory solution may be had by using only the mean value of density matrix elements. The author illustrates the approach by examples of approximate equations describing differences of population levels in a two-level system, under the effect of radiation taken to be a normal stationary process with zero mean. The method is tedious, requiring computer solution, and is limited to systems with a few levels only, but in theory applies to radiative interaction of arbitrary intensity and spectral characteristic with matter, as long as the radiation may be considered as a normal stationary process.

Askar'yan, G. A., and T. G. Rakhmanina. **Scattering,refraction and reflection of sound under the action of intense light on a medium.** ZhETF, v. 61, no. 3, 1971,1199-1202.

An analytical discussion is given describing the effect of powerful optical absorption in a medium on acoustic parameters of that medium. Coherent or noncoherent radiation of sufficient intensity can cause substantial local changes in acoustical scattering, refraction and reflection owing to gas evolution, bubble formation, etc. The case of a liquid medium is treated here, with bubbles assumed to be formed by beam absorption, as this produces drastic changes in the cited acoustical parameters. An expression for mean bubble size is derived as a function of breakdown threshold and other parameters of the liquid medium. A comparison of theoretical scatter in bubbles with scatter in locally heated regions, at the same per unit energy absorption, shows that the bubble scattering

cross-section will exceed that of the heated regions by as much as 10^{13}, which indicates the predominant scattering effect of bubble formations. A brief treatment on sound refraction and reflection from optically disturbed regions is also given. The discussion in general is concerned with acoustic velocities ranging from supersonic to hypersonic.

Askar'yan, G. A., and S. D. Manukyan.
Acceleration of particles by a moving laser
focus, focusing front, or ultrashort laser
pulse front. ZhETF, v. 62, no. 6, 1972,
2156-2160.

An analysis is given of several ways in which the high field gradient in a laser pulse can be used to accelerate electrons or ions in a controlled fashion. If the mean force exerted on a particle in an e-m field of amplitude E_0 (r) and frequency ω is expressed as

$$f = -\frac{e^2}{2m\omega^2} \nabla (E^2)_{mean}$$

then it can be shown that, for example, a neodymium laser generating nanosecond pulses in the 30 Gw range will produce an effective field E_{eff} of approximately 1 Mv/cm, while a picosecond pulse of 3×10^3 Gw will yield 100 Mv/cm. Gradients of this magnitude when given a controlled lateral displacement (swept beam) or axial displacement (change in focal point or beam divergence) can in theory be used for selective particle acceleration. One method for doing this would be programmed refocusing of annular portions of the laser wavefront, using corresponding portions of a focusing lens; another would be a programmed refocusing of the beam along a selected path. In the latter case it is shown that a channel with reduced nonlinear absorption can be generated for charged particle motion. In the case of low coulomb attraction between electrons and ions, electrons would essentially be accelerated as if free; at sufficiently high coulomb forces an ion acceleration component would appear. In conclusion the authors suggest that the moving-focus technique could be extended to provide macroscopic particle acceleration (cf. Askar'yan et al. Light-reaction acceleration of macroparticles of matter. ZhETF P, v. 5, no. 8, 1967, 258-260)

Gurevich, V. I. <u>Pulse forms of a periodic point
source of heat on the surface of a large body.</u>
FiKhOM, no. 2, 1972, 19-22.

A study on the effect of pulse shape on laser interaction with
metals was mentioned by Baranov, Gurevich, and Heinrichs in a previous
report (April Monthly Report, p. 4). In the present paper Gurevich gives
a more extended analysis of pulse shape effect. The model assumes a
periodic pulse from either a stationary or moving source, and is used to
calculate a limiting temperature field in the impact region at the conclusion
of the laser pulse; for convenience a dimensionless temperature θ_i is intro-
duced. Analytical expressions for θ_i' (fixed) and θ_i'' (moving source) are
then obtained in terms of beam parameters and the Fourier (Fo) and Peclet
(Pe) criteria. A comparison of pulse shape effect on θ_i' is seen in Fig. 1
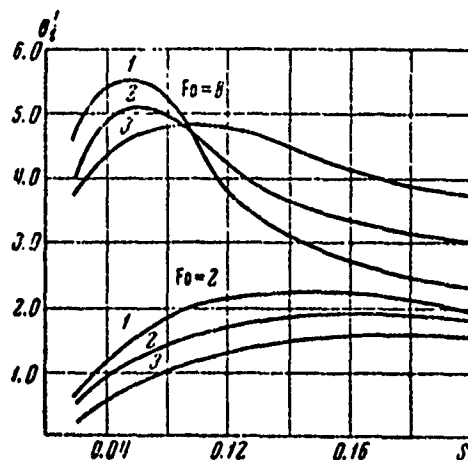for the fixed source case, showing the maximum effect of a sawtooth pulse

Fig. 1. Temperature θ_i' vs. duty factor S
1- sawtooth pulse, vertical leading edge;
2- rectangular pulse;
3- sawtooth, vertical trailing edge

with vertical leading edge, at the higher Fo levels. It follows that this
form would be preferable for fast local heating of a limited surface area,
despite the fact that a $\sin^2$ pulse generally gives most efficient energy
transfer in a given pulse width. Tabulated results are also included com-
paring the limit temperatures for a moving beam in terms of the cited pulse
shapes, again showing the superiority of the vertical-rise sawtooth.

Gurevich, V. I. Pulse forms of a periodic point
source of heat on the surface of a large body.
FiKhOM, no. 2, 1972, 19-22.

A study on the effect of pulse shape on laser interaction with
metals was mentioned by Baranov, Gurevich, and Heinrichs in a previous
report (April Monthly Report, p. 4). In the present paper Gurevich gives
a more extended analysis of pulse shape effect. The model assumes a
periodic pulse from either a stationary or moving source, and is used to
calculate a limiting temperature field in the impact region at the conclusion
of the laser pulse; for convenience a dimensionless temperature θ_i is intro-
duced. Analytical expressions for θ_i' (fixed) and θ_i'' (moving source) are
then obtained in terms of beam parameters and the Fourier (Fo) and Peclet
(Pe) criteria. A comparison of pulse shape effect on θ_i' is seen in Fig. 1
for the fixed source case, showing the maximum effect of a sawtooth pulse
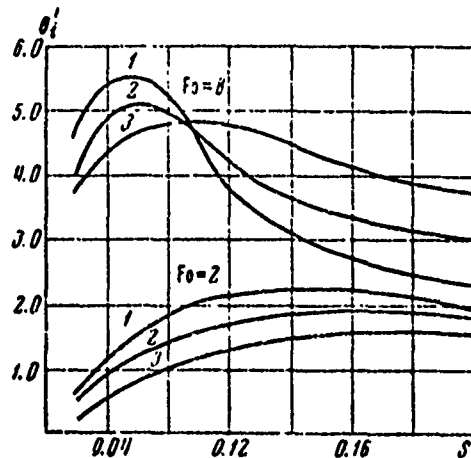

Fig. 1. Temperature θ_i' vs. duty factor S
1- sawtooth pulse, vertical leading edge;
2- rectangular pulse;
3- sawtooth, vertical trailing edge

with vertical leading edge, at the higher Fo levels. It follows that this
form would be preferable for fast local heating of a limited surface area,
despite the fact that a $\sin^2$ pulse generally gives most efficient energy
transfer in a given pulse width. Tabulated results are also included com-
paring the limit temperatures for a moving beam in terms of the cited pulse
shapes, again showing the superiority of the vertical-rise sawtooth.

Gurevich, V. I. **Pulse forms of a periodic point**
source of heat on the surface of a large body.
FiKhOM, no. 2, 1972, 19-22.

A study on the effect of pulse shape on laser interaction with
metals was mentioned by Baranov, Gurevich, and Heinrichs in a previous
report (April Monthly Report, p. 4). In the present paper Gurevich gives
a more extended analysis of pulse shape effect. The model assumes a
periodic pulse from either a stationary or moving source, and is used to
calculate a limiting temperature field in the impact region at the conclusion
of the laser pulse; for convenience a dimensionless temperature θ_i is intro-
duced. Analytical expressions for θ_i' (fixed) and θ_i'' (moving source) are
then obtained in terms of beam parameters and the Fourier (Fo) and Peclet
(Pe) criteria. A comparison of pulse shape effect on θ_i' is seen in Fig. 1
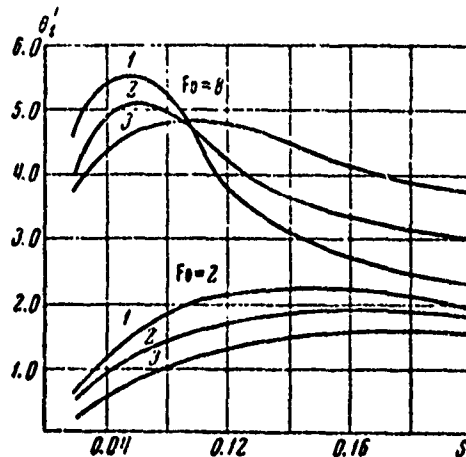for the fixed source case, showing the maximum effect of a sawtooth pulse

Fig. 1. Temperature θ_i' vs. duty factor S
1- sawtooth pulse, vertical leading edge;
2- rectangular pulse;
3- sawtooth, vertical trailing edge

with vertical leading edge, at the higher Fo levels. It follows that this
form would be preferable for fast local heating of a limited surface area,
despite the fact that a $\sin^2$ pulse generally gives most efficient energy
transfer in a given pulse width. Tabulated results are also included com-
paring the limit temperatures for a moving beam in terms of the cited pulse
shapes, again showing the superiority of the vertical-rise sawtooth.

Gusev, N. V., and A. A. Pyarnpuu. Quantitative study
of the ejection of matter from a solid surface by the action
of powerful radiation. ZhPMTF, no. 4, 1971, 127-133.
(RZhF, 1/72, #1G254)

A set of gas dynamic equations is derived and solved for the ejection
processes of a solid target under laser irradiation. Radiation energy
absorption is accounted for by postulating a discontinuity, at the boundaries
of which the gas dynamic parameters follow laws of conservation and, at the
initial moment, the Jouguet rule. At small energy densities surface vaporizat
does not occur, although electrons and ions are emitted. At increased q, the
vapor-flare condition appears; at still greater q, the flare region is sufficient
ionized to shield the target surface from the beam. For the small q case,
ejecta behavior is determined by vapor temperature and density distribution,
and degree of condensation; solutions of this type are presented graphically.
It is further shown that at higher q two flow modes can exist; in one of these
a shock wave propagates ahead of the "vaporization wave" (thermal mode).
In the other case the shock wave coincides with the discontinuity, giving the
"detonation" mode. It is noted that the appearance of shock waves, the
nonequilibrium of the processes, and other phenomena associated with absorpt
of powerful radiation, greatly complicate the examination of the problem.
It is suggested that a solution for the extended ejecta case may be obtained
by the approximation of a stepwise-variable absorption coefficient; this
enables comparison of results with a self-similar numerical solution.

Kolokolov, A. A., and G. V. Skrotskiy. Kinetics
of the self-focusing process for short optical pulses.
OiS, v. 31, no. 4, 1971, 650-652.

Factors determining the self-focus characteristics of short optical
pulses are analyzed. Pulse duration is assumed comparable to the time requ
for generation of nonlinear polarization in the medium, hence transient proce
in the medium must be taken into account. Using this model the authors
evaluate the degree of light absorption as a function of nonlinear polarization
relaxation, for the case of Kerr effect orientation and for striction. The
development rate of the lightguide filament is also determined for the strictio
nonlinearity case; it is shown from calculations that striction has a negligibl
effect on formation of narrow filaments.

Lokhov, Yu. N., G. V. Rozhnov, and I. I.
Shvyrkova. Kinetics of forming a liquid
phase from the action of a point heat source,
taking heat of phase transition into account.
FiKhOM, no. 3, 1972, 9-17.

The article presents a quantitative description of the melting
process of semiinfinite heat-conducting solids under the impact of a surface
point heat source of constant intensity with allowance for the phase transition
temperature. Analytical assumptions are: 1) the source surface power
density does not exceed $10^6 w/cm^2$, thus avoiding the problem of material
vaporization and the related gas-dynamic effects; 2) the material is an ideal
black body; 3) the liquid and solid phase thermophysical parameters are not a
function of temperature; 4) the material density remains constant during the
melting process and 5) the stabilization time of the maximum melting radius
for most metals does not exceed hundredths of a millisecond allowing the
heat exchange between the liquid and solid phases and the environment to be
ignored and reducing the problem to a spherically-symmetrical one.

The spherically-symmetrical problem is given as a set
of heat conductivity equations for liquid and solid phase temperature
distributions with corresponding initial and boundary conditions. For the
solution, the velocity of phase transition boundary motion is determined from
energy balance. For small time intervals the velocity is much higher than
that of diffusion in a liquid medium. Experimental data have shown that
turbulence in this medium controls the hydrodynamic nature of heat transfer
in a melted material. The turbulent temperature conductivity is of the order
of $0.1 cm^2/sec$, which results in a rapid mixing and levelling of temperature
up to the melting temperature T_m.

At specific material heat source parameters and thermo-
physical properties, the solution obtained enables the size of the melted zone to

be determined as well as the τ_m value, for the time of heat source exposure needed to form the melted zone. Both the zone size and the τ_m are dependent the melting temperature. The solutions obtained confirm the assumption that for most metals the liquid phase temperature is constant over the total time interval (steel is the only exception due to its low heat conductivity).

The authors demonstrate the qualitative agreement of estimates derived from the formulas with experimental data obtained using a focused laser pulse as a point heat source (energy - 0.1 joule, duration - $\tau = 1$ ms, under the conditions $\tau \geq \tau_m$). Temperature distribution data along the solid phase are also presented in computer-aided numerical solution form. It is shown that the stationary state stabilization and the heating depth of the solid phase are largely a function of the phase transition temperature.

Mirkin, L. I. Analogies between mechanisms of
destruction of transparent and opaque materials by a
laser beam. DAN SSSR, v. 201, no. 6, 1971, 1335-1337.

The author notes that laser damage to opaque materials is typically
evidenced as fusion and evaporation at the target surface, whereas for
transparent materials, damage appears as cracks typical of brittle failure.
In spite of the gross difference in destruction appearance, however, it is
suggested that in many cases a common damage mechanism applies to either
target type. Experiments with NaCl crystals irradiated by a neodymium
laser are cited to support this; the beam was defocused so that the effects of
cross-section intensity variation in the beam could be observed. Tests were
run both below and above threshold levels, and a precise examination of local
heating effects and crater profiles was obtained, using a scanning electron
microscope. The similarity argument is based on the fact that in transparent
media, local areas of less transparency will absorb heat preferentially and
with increased opacity become damage centers; following this stage the
destructive effects are analogous to those in metal or other opaque materials.
Therefore the evident differences in laser damage to transparent and opaque
targets arise only from their varying reaction to local thermal stress generated
by laser action.

Némchinov, I. V., and S. P. Popov. Shielding of a surface
evaporating under the action of a laser, for the case of
temperature and ionization nonequilibrium. ZhPMTF, no. 5,
1971, 35-45.

This paper is an extended treatment of a theoretical analysis published
earlier by the authors on the dynamics of shielding by vapor products of a target
surface under laser irradiation (Effects of High Power Lasers, Dec. 1971, 34).
From an extensive theoretical analysis and numerous citations from other curren
work on this subject, the authors establish that the critical flux density q_* at
which shielding is defined as beginning occurs at a substantially lower value than
that predicted by equilibrium ion and electron temperatures ($T_e = T_i$). It is
therefore postulated that $T_e \neq T_i$ at shielding onset and appearance of the flare
phenomenon. A description of thephysical processes is developed on this theory,
under certain simplifications concerning heat transfer, for flare propagation botl
in a vacuum and in a gas medium. Some calculations are given based on typical
experimental parameters, assuming a ruby laser source and an aluminum target
graphical solutions for these are included. The authors note in addition the
analogous finding of Popov on the shielding developed in front of a shock wave in
gas (ZhETF P, v. 9, no. 3, 1969, 176-179), which also commences earlier than
predictable by the equilibrium temperature theory. Another related work by Pop
et al has been reported previously (Effects of Strong Explosions, no. 2, 1971,
105), on this subject.

Nevskiy, A. P. Electron temperature at the surface of
metals subjected to powerful thermal fluxes. TVT,
no. 4, 1970, 898-899.

A theoretical treatment is given to conditions for generation of hot elect:
in a metal subsurface layer by external thermal flux, to achieve conditions
analogous to exploding wires. A formula was derived for temperature Θ of the
electronic subsurface layer in metals, as follows:

$$\theta = T + (l_\epsilon Q / \lambda) \qquad (1)$$

where $T \sim 10^3$ deg K is the temperature of the crystal lattice, Q is thermal flux
density on the metal surface, and l_ϵ and λ are thermophysical characteristics of
the metal. Formula (1) gives the Q necessary to establish a given (e.g. an order
of magnitude)differential between Θ and T, which occurs because of a significant
difference in time τ_e of establishment of a Fermi distribution in electron gas and
relaxation time τ_ϵ of electrons interacting with the crystal lattice ($\tau_\epsilon \geq \tau_e$). An
example shows that $Q \approx 10^5 - 10^7$ w/cm^2 are required to achieve an order of
magnitude differential between Θ and T in metals. These densities are presently
obtainable in interactions of concentrated laser and electron beams with the surfa
of solids, of powerful heat fluxes in arc discharges at the cathode, etc. In the
case of an arc discharge, this effect of "hot" surface electrons must be accounted
for in the analysis of electron emission.

Vodovatov, F. F., and M. S. Chupina. Interaction
of laser radiation with solid substances for the
purpose of mass-spectral analysis. IN: Moskovskiy
institut elektronnogo mashinostroyeniya. Trudy. No. 9,
1970, 89-98. (RZhMetrolog, 1/72, #1.32.1226)

The possibility is discussed of using a laser probe to vaporize and
ionize solids for subsequent mass spectrometry. Results are presented on
determination of degree of material ionization, and the possible dispersal
of kinetic energy in the generated ions.

9. Conferences

Cherkun, Yu. P., and I. N. Konopel'ko.
Current status of experimental and theoretical
studies in the field of combined heat exchange.
I-FZh, v. 22, no. 4, 1972, 757-758.

A brief summary is given of several papers on the subject
of radiation - induced heat exchange, presented at a session of a general
conference on mass and heat transfer held on Sept. 15-17, 1971 at the
Thermophysics Institute, Siberian Branch AN SSSR. The general theme of
the session was phenomena related to combination heat transfer mechanisms,
namely radiative - conductive and radiative - convective.

S. S. Kutateladze and D. I. Avaliani reported on experimental
findings of laser beam attenuation in liquid media with pulsating turbulence;
this work was judged important from a heat transfer viewpoint as well as in
regard to beam propagation in a turbulent medium. A related paper by
V. M. Kostylev and V. Ya. Belostotskaya dealt with the relation between
conductive and radiative heat transfer in optically thin layers of finely-dispersed
media; they show that in this case it is incorrect to use the hypothesis of
additive fluxes.

A report by N. A. Rubtsova and A. E. Berte covered the
thermal state of pure metal surfaces exposed to a constant thermal flux.
Results showed anomalies in surface temperature distribution (the Jacques
effect) on metals including Al, Fe, Sn and others; several possible models
for this phenomenon are advanced.

V. M. Yeroshenko discussed variants of ablation techniques
in which blowoff of dispersed media is used as a protection against radiative
flux; this refers to processes at levels of 100 atm and temperatures in the
20,000°C range. Several papers by other authors dealt with heat exchange
studies in various types of combustion reactions.

Special mention is given to a paper by A. I. Leont'yev and
A. M. Pavlyuchenko which is cited as giving the most complete picture
to date on temperature distribution in a turbulent boundary layer and laminar
sublayer in a thermal radiation field. As with Kostylev et al, these authors
also demonstrate the fallacy of the additive-flux hypothesis under their test
conditions.

In closing, S. Kutateladze stressed the need for further experi-
mental data on radiative heat exchange resulting from interaction of e-m
waves with materials.

Uglov, A. A. <u>Work presented in the seminar</u>
<u>on the physics and chemistry of materials</u>
<u>processing by concentrated energy beams.</u>
FiKhOM, no. 5, 1971, 158-159.

Highlights are given of selected papers in the 27th Seminar
on the title subject, held in Moscow during February, 1971. The seminar
was chaired by Academician N. N. Rykalin, and attended by over 80
leading researchers in the field from Soviet institutes. The bulk of the
articles deal with high-power laser interaction with metal and dielectric
targets, CO_2 lasers being most often mentioned. To a lesser degree,
particle-beam interactions are also discussed.

A paper by V. P. Veyko et al discussed the growth kinetics of thin
oxide films on metals from pulsed heating, and methods for optimizing
film control. Experiments with a c-w CO_2 laser have yielded a 40-50 $\overset{o}{A}$
oxide film on chrome at 1 millisec exposure, which is consistent with
calculated values. A number of test results by the same authors on poly-
mer targets was also discussed.

A. E. Kuznetsov et al presented their findings on vaporization
of dielectrics by 10.6 micron laser radiation, using quartz and other
optical glass under c-w CO_2 exposure. From their results the authors
have developed an approximate mathematical model based on the law of
mass conservation. Commenting on this, Yu. N. Lokhov noted the similarity
in characteristics between CO_2 destruction of dielectrics and the self-con-
sistent damage mode of metals under giant pulse exposure.

A paper by I. G. Stolyanova et al discussed aspects of laser
milling techniques in microelectronics; the authors have developed a
technique for producing laser-cut thin film resistors.

An interesting report by M. S. Baranov et al described computer
and experimental studies on the effect of laser pulse envelope in beam-target
tests. Results with rectangular, triangular and approximately sinusoidal
waveforms showed maximum metal vaporization for the triangular waveform
and minimum for the half-wave sinusoid. A criticism offered here by
A. A. Uglov, which applied generally to the laser beam-target tests, was
that attention tends to focus only on the strictly thermal effects occurring,

whereas chemico-thermal mechanisms also play a part and warrant more detailed examination.

Techniques for electron beam processing of materials are mentioned by A. N. Kabanov, D. B. Zvorykin et al, and Yu. D. Belotovskiy et al. These concerned nonthermal beam processing, electron lithography, and beam deposition techniques for metal films.

In summary, Dr. Rykalin observed that advances in laser tunability are needed to expand laser processing techniques, and that more detailed study of chemico-thermal processes is needed for both laser and particle beam techniques.

10. <u>SOURCE ABBREVIATIONS</u>

AiT	-	Avtomatika i telemekhanika
APP	-	Acta physica polonica
DAN ArmSSR	-	Akademiya nauk Armyanskoy SSR. Doklady
DAN AzSSR	-	Akademiya nauk Azerbaydzhanskoy SSR. Doklady
DAN BSSR	-	Akademiya nauk Belorusskoy SSR. Doklady
DAN SSSR	-	Akademiya nauk SSSR. Doklady
DAN TadSSR	-	Akademiya nauk Tadzhikskoy SSR. Doklady
DAN UkrSSR	-	Akademiya nauk Ukrainskoy SSR. Dopovidi
DAN UzbSSR	-	Akademiya nauk Uzbekskoy SSR. Doklady
DBAN	-	Bulgarska akademiya na naukite. Doklady
EOM	-	Elektronnaya obrabotka materialov
FAiO	-	Akademiya nauk SSSR. Izvestiya. Fizika atmosfery i okeana
FGiV	-	Fizika goreniya i vzryva
FiKhOM	-	Fizika i khimiya obrabotka materialov
F-KhMM	-	Fiziko-khimicheskaya mekhanika materialov
FMiM	-	Fizika metallov i metallovedeniye
FTP	-	Fizika i tekhnika poluprovodnikov
FTT	-	Fizika tverdogo tela
FZh	-	Fiziologicheskiy zhurnal
GiA	-	Geomagnetizm i aeronomiya
GiK	-	Geodeziya i kartografiya
IAN Arm	-	Akademiya nauk Armyanskoy SSR. Izvestiya. Fizika
IAN Az	-	Akademiya nauk Azerbaydzhanskoy SSR. Izvestiya. Seriya fiziko-tekhnicheskikh i matematicheskikh nauk

IAN B	-	Akademiya nauk Belorusskoy SSR. Izvestiya. Seriya fiziko-matematicheskikh nauk
IAN Biol	-	Akademiya nauk SSSR. Izvestiya. Seriya biologicheskaya
IAN Energ	-	Akademiya nauk SSSR. Izvestiya. Energetika i transport
IAN Est	-	Akademiya nauk Estonskoy SSR. Izvestiya. Fizika matematika
IAN Fiz	-	Akademiya nauk SSSR. Izvestiya. Seriya fizicheskaya
IAN Fizika zemli	-	Akademiya nauk SSSR. Izvestiya. Fizika zemli
IAN Kh	-	Akademiya nauk SSSR. Izvestiya. Seriya khimicheskaya
IAN Lat	-	Akademiya nauk Latviyskoy SSR. Izvestiya
IAN Met	-	Akademiya nauk SSSR. Izvestiya. Metally
IAN Mold	-	Akademiya nauk Moldavskoy SSR. Izvestiya. Seriya fiziko-tekhnicheskikh i matematicheskikh nauk
IAN SO SSSR	-	Akademiya nauk SSSR. Sibirskoye otdeleniye. Izvestiya
IAN Tadzh	-	Akademiya nauk Tadzhiksoy SSR. Izvestiya. Otdeleniye fiziko-matematicheskikh i geologo-khimicheskikh nauk
IAN TK	-	Akademiya nauk SSSR. Izvestiya. Tekhnicheskaya kibernetika
IAN Turk	-	Akademiya nauk Turkmenskoy SSR. Izvestiya. Seriya fiziko-tekhnicheskikh, khimicheskikh, i geologicheskikh nauk
IAN Uzb	-	Akademiya nauk Uzbekskoy SSR. Izvestiya. Seriya fiziko-matematicheskikh nauk
IBAN	-	Bulgarska akademiya na naukite. Fizicheski institut. Izvestiya na fizicheskaya institut s ANEB
I-FZh	-	Inzhenerno-fizicheskiy zhurnal

IiR	-	Izobretatel' i ratsionalizator
ILEI	-	Leningradskiy elektrotekhnicheskiy institut. Izvestiya
IT	-	Izmeritel'naya tekhnika
IVUZ Avia	-	Izvestiya vysshikh uchebnykh zavedeniy. Aviatsionnaya tekhnika
IVUZ Cher	-	Izvestiya vysshikh uchebnykh zavedeniy. Chernaya metallurgiya
IVUZ Energ	-	Izvestiya vysshikh uchebnykh zavedeniy. Energetika
IVUZ Fiz	-	Izvestiya vysshikh uchebnykh zavedeniy. Fizika
IVUZ Geod	-	Izvestiya vysshikh uchebnykh zavedeniy. Geodeziya i aerofotos"yemka
IVUZ Geol	-	Izvestiya vysshikh uchebnykh zavedeniy. Geologiya i razvedka
IVUZ Gorn	-	Izvestiya vysshikh uchebnykh zavedeniy. Gornyy zhurnal
IVUZ Mash	-	Izvestiya vysshikh uchebnykh zavedeniy. Mashinostroyeniye
IVUZ Priboro	-	Izvestiya vysshikh uchebnykh zavedeniy. Priborostroyeniye
IVUZ Radioelektr	-	Izvestiya vysshikh uchebnykh zavedeniy. Radioelektronika
IVUZ Radiofiz	-	Izvestiya vysshikh uchebnykh zavedeniy. Radiofizika
IVUZ Stroi	-	Izvestiya vysshikh uchebnykh zavedeniy. Stroitel'stvo i arkhitektura
KhVE	-	Khimiya vysokikh energiy
KiK	-	Kinetika i kataliz
KL	-	Knizhnaya letopis'
Kristall	-	Kristallografiya
KSpF	-	Kratkiye soobshcheniya po fizike

LZhS	–	Letopis' zhurnal'nykh statey
MiTOM	–	Metallovedeniye i termicheskaya obrabotka materialov
MP	–	Mekhanika polimerov
MTT	–	Akademiya nauk SSSR. Izvestiya. Mekhanika tverdogo tela
MZhiG	–	Akademiya nauk SSSR. Izvestiya. Mekhanika zhidkosti i gaza
NK	–	Novyye knigi
NM	–	Akademiya nauk SSSR. Izvestiya. Neorganicheskiye materialy
NTO SSSR	–	Nauchno-tekhnicheskiye obshchestva SSSR
OiS	–	Optika i spektroskopiya
OMP	–	Optiko-mekhanicheskaya promyshlennost'
Otkr izobr	–	Otkrytiya, izobreteniya, promyshlennyye obraztsy, tovarnyye znaki
PF	–	Postepy fizyki
Phys abs	–	Physics abstracts
PM	–	Prikladnaya mekhanika
PMM	–	Prikladnaya matematika i mekhanika
PSS	–	Physica status solidi
PSU	–	Pribory i sistemy upravleniya
PTE	–	Pribory i tekhnika eksperimenta
Radiotekh	–	Radiotekhnika
RiE	–	Radiotekhnika i elektronika
RZhAvtom	–	Referativnyy zhurnal. Avtomatika, tele-mekhanika i vychislitel'naya tekhnika
RZhElektr	–	Referativnyy zhurnal. Elektronika i yeye primeneniye

RZhF	–	Referativnyy zhurnal. Fizika
RZhFoto	–	Referativnyy zhurnal. Fotokinotekhnika
RZhGeod	–	Referativnyy zhurnal. Geodeziya i aeros"-yemka
RZhGeofiz	–	Referativnyy zhurnal. Geofizika
RZhInf	–	Referativnyy zhurnal. Informatics
RZhKh	–	Referativnyy zhurnal. Khimiya
RZhMekh	–	Referativnyy zhurnal. Mekhanika
RZhMetrolog	–	Referativnyy zhurnal. Metrologiya i izmeritel'naya tekhnika
RZhRadiot	–	Referativnyy zhurnal. Radiotekhnika
SovSciRev	–	Soviet science review
TiEKh	–	Teoreticheskaya i eksperimental'naya khimiya
TKiT	–	Tekhnika kino i televideniya
TMF	–	Teoreticheskaya i matematicheskaya fizika
TVT	–	Teplofizika vysokikh temperatur
UFN	–	Uspekhi fizicheskikh nauk
UFZh	–	Ukrainskiy fizicheskiy zhurnal
UMS	–	Ustalost' metallov i splavov
UNF	–	Uspekhi nauchnoy fotografii
VAN	–	Akademiya nauk SSSR. Vestnik
VAN BSSR	–	Akademiya nauk Belorusskoy SSR. Vestnik
VAN KazSSR	–	Akademiya nauk Kazakhskoy SSR. Vestnik
VBU	–	Belorusskiy universitet. Vestnik
VNDKh SSSR	–	VNDKh SSSR. Informatsionnyy byulleten'
VLU	–	Leningradskiy universitet. Vestnik. Fizika, khimiya
VMU	–	Moskovskiy universitet. Vestnik. Seriya fizika, astronomiya

ZhETF	-	Zhurnal eksperimental'noy i teoreticheskoy fiziki
ZhETF P	-	Pis'ma v Zhurnal eksperimental'noy i teoreticheskoy fiziki
ZhFKh	-	Zhurnal fizicheskoy khimii
ZhNiPFiK	-	Zhurnal nauchnoy i prikladnoy fotografii i kinematografii
ZhNKh	-	Zhurnal neorganicheskoy khimii
ZhPK	-	Zhurnal prikladnoy khimii
ZhPMTF	-	Zhurnal prikladnoy mekhaniki i tekhnicheskoy fiziki
ZhPS	-	Zhurnal prikladnoy spektroskopii
ZhTF	-	Zhurnal tekhnicheskoy fiziki
ZhVMMF	-	Zhurnal vychislitel'noy matematiki i matematicheskoy fiziki
ZL	-	Zavodskaya laboratoriya

11. AUTHOR INDEX